

UT-816
 KUCP-0113
 OHU-9808
 hep-th/9808034

Valley Views: Instantons, Large Order Behaviors, and Supersymmetry

Hideaki AOYAMA[†], Hisashi KIKUCHI^{††}, Ikuo OKOUCHI[‡],
 Masatoshi SATO^{*} and Shinya WADA[‡]

[†]*Faculty of Integrated Human Studies,
 Kyoto University, Kyoto 606-8501, Japan*
 aoyama@phys.h.kyoto-u.ac.jp

^{††}*Ohu University, Koriyama 963-8611, Japan*
 kikuchi@yukawa.kyoto-u.ac.jp

[‡]*Graduate School of Human and Environmental Studies,
 Kyoto University, Kyoto 606-8501, Japan*

dai@phys.h.kyoto-u.ac.jp, shinya@phys.h.kyoto-u.ac.jp

^{*}*Department of Physics, University of Tokyo, Tokyo 113-0033, Japan*
 msato@hep-th.phys.s.u-tokyo.ac.jp

August, 1998

Abstract

The elucidation of the properties of the instantons in the topologically trivial sector has been a long-standing puzzle. Here we claim that the properties can be summarized in terms of the geometrical structure in the configuration space, the valley. The evidence for this claim is presented in various ways. The conventional perturbation theory and the non-perturbative calculation are unified, and the ambiguity of the Borel transform of the perturbation series is removed. A ‘proof’ of Bogomolny’s “trick” is presented, which enables us to go beyond the dilute-gas approximation. The prediction of the large order behavior of the perturbation theory is confirmed by explicit calculations, in some cases to the 478-th order. A new type of supersymmetry is found as a by-product, and our result is shown to be consistent with the non-renormalization theorem. The prediction of the energy levels is confirmed with numerical solutions of the Schrödinger equation.

Contents

1	Introduction	2
2	The valley	3
2.1	The valley method	5
2.2	Valley configurations	10
2.3	Valley-instanton	14
2.4	$I\bar{I}$ valley configurations with large separations	20
3	$I\bar{I}$ valley and $\bar{I}I$ valley	24
3.1	The $\epsilon = 0$ case	25
3.2	The $\epsilon \neq 0$ case	28
3.2.1	$I\bar{I}$ valley	28
3.2.2	$\bar{I}I$ valley	30
3.3	Singularity of the Borel plane	31
3.4	Bogomolny's trick	33
4	The multi valley	34
4.1	Multi valley calculus	34
4.2	$I\bar{I}$ valley and $\bar{I}I$ valley revisited	38
5	Large order behavior of the perturbative series	40
6	\mathcal{N}-fold supersymmetry	43
6.1	Supersymmetric quantum mechanics	46
6.2	Non-renormalization theorem	53
7	Numerical verification of the prediction of the energy spectrum	58
8	Discussions	62
A	Some notes on the valley method	69
B	The determinant of the valley-instanton	70
C	The relation between the valley parameter and the separation of valley-instantons	72
D	WKB evaluation	73

1 Introduction

Elucidation of the properties of the instantons in the topologically trivial sector has been a long-standing puzzle. Although there is no doubt as to the physical importance of the instantons, it is not trivial to define them in this sector. When they are separated by infinite distance they satisfy the classical equation. But once the distance between them becomes finite there are no classical solutions. Due to the attractive force between the instanton and the anti-instanton they can easily collapse to a vacuum. Thus, it is impossible to distinguish them from the fluctuations around the vacuum. Of course, no pragmatic problem arises in the dilute-gas approximation, but the lack of a precise definition has prevented us from going beyond this approximation. The main purpose of the present article is to clarify the structure of the topologically trivial sector in theories with tunneling, and to provide a method which goes beyond the dilute-gas approximation.

From the early stages of the study of the instanton [1], it was evident that this difficulty is connected with the fact that the perturbation theory in the presence of tunneling is not Borel summable [2, 3, 4]. Both problems come from the non-separability of the tunneling and the perturbative effects. And if we change the sign of the square of the coupling constant so that the force between instantons becomes repulsive, they disappear; the instanton configuration is now free from the collapse and at the same time the perturbation series becomes Borel summable. Bogomolny [5] was the first to point out that the above “analytic continuation” of the coupling constant is the key to going beyond the dilute-gas approximation, and our work gives a precise realization of his suggestion in the context of the structures in the configuration space.

In what follows, we will present novel structures for the configuration space in the topologically trivial sector. We will perform an explicit analysis in one-dimensional quantum mechanics, with asymmetric double-well potential, but our analysis may apply to quantum field theories with weak coupling, though additional complications will be introduced in such cases.

Our starting point is a geometrical definition of the instantons in the topologically trivial sector. As was indicated by Balitsky and Yung [6], the instantons in the topologically trivial sector form valleys in the configuration space. In Section 2, following Refs.[7, 8, 9, 10], we review a method to define the valleys in the configuration space and present the construction of the valley configurations and their basic constituents, the valley-instantons. Section 3 is the core of this paper; we will give a detailed analysis of a valley that contains a pair consisting of an instanton and an anti-instanton, and show that the interplay between the perturbative effects and the tunneling effects can be summarized in a unified way in terms of the collective coordinate of the valley. The summation over the multi-instantons is carried out in Section

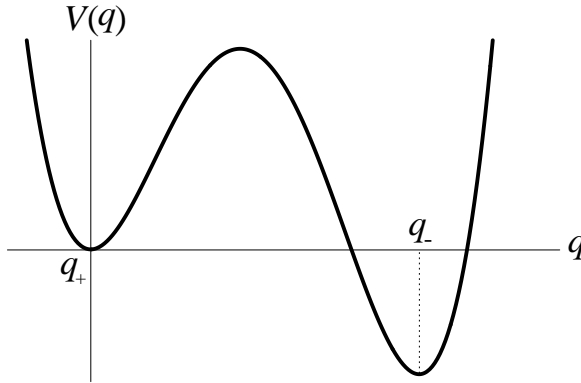


Figure 1: The asymmetric double-well potential $V(q)$ defined by Eq.(2.2) for $\epsilon = 5$ and $g = 0.1$.

4, which leads to the expression for the non-perturbative part of the energy spectrum. In Sections 5 and 7, we summarize various tests of our results. In Section 5, the prediction of the large order behavior is checked against numerical and exact calculation of the perturbative series from the 200-th to the 478-th order for a wide range of the parameters of our model. This result shows an apparent lack of Borel singularities at certain values of the parameters, which suggests the existence of some non-renormalization theorem. In Section 6, we show that the model we analyze has a new type of supersymmetry, which we dub “ \mathcal{N} -fold supersymmetry”. The non-renormalization theorem makes it possible to test the prediction of the energy spectrum. These predictions are checked against the numerical values of the energy spectrum in Section 7. We conclude with some additional remarks in Section 8. The four appendices contain some of the supporting calculations.

2 The valley

As our object of study we will take a one-dimensional quantum mechanical system with an asymmetric double-well potential. We denote the coordinate by q , and write the Euclidean action of this system as follows:

$$S[q] = \int d\tau \left[\frac{1}{2} \left(\frac{dq}{d\tau} \right)^2 + V(q) \right], \quad (2.1)$$

$$V(q) = \frac{1}{2} q^2 (1 - gq)^2 - \epsilon q. \quad (2.2)$$

This potential is plotted in Fig.1 for $\epsilon = 5$ and $g = 0.1$. For small ϵg^2 , the points $q \approx 0$ and $q \approx 1/g$ are the local minima of the potential, where $V(q) \approx 0$ and $-\epsilon$, respectively. Thus ϵ is essentially the difference between the

energies of the two minima. The parameter g plays the role of the coupling constant, since the q^3 and q^4 -terms have coefficients g and g^2 , respectively. The height of the potential barrier is approximately $V(1/2g) \approx 1/(32g^2)$, and throughout this paper we will work in the small coupling regime $g \ll 1$. In general, the existence of the two minima is limited to the range $\epsilon g^2 < \sqrt{3}/18$, to which we restrict ourselves. We will denote the coordinate of the upper and lower local minima by q_+ and q_- , respectively (see Fig.1). For the sake of definiteness, we assume that $g > 0$ and $\epsilon \geq 0$, which is convenient for calculation and entails no loss of generality.

Note that other types of quartic potential for the asymmetric double-well type can be made in the form (2.2) by a suitable linear transformation on the coordinate q and a scale change of the Euclidean time τ . Therefore, with this form of the potential we are covering a wide range of potentials. Furthermore, as we will see later, this form is essential for the argument discussing the supersymmetry.¹

Let us first describe the qualitative features of the valleys. The actual construction and calculations will be given in the subsequent sections.

For $\epsilon = 0$ this model has the instanton and anti-instanton solutions of this system, given by the following:

$$q_0^{(I)}(\tau; \tau_I) = \frac{1}{g} \frac{1}{1 + e^{-(\tau - \tau_I)}}, \quad (2.3)$$

$$q_0^{(\bar{I})}(\tau; \tau_{\bar{I}}) = \frac{1}{g} \frac{1}{1 + e^{(\tau - \tau_{\bar{I}})}}. \quad (2.4)$$

The parameter τ_I ($\tau_{\bar{I}}$) denotes the positions of the (anti-)instanton.

In the topologically trivial sector, the simplest valley in the functional space of $q(\tau)$ starts from the vacuum $q(\tau) \equiv 0$. On the outskirts of the valley, the configuration has an almost-flat region of $q \simeq 1/g$. When the width R of this region becomes infinity, the transient regions become the exact instanton and the exact anti-instanton solutions. We will call this valley the $I\bar{I}$ valley. Correspondingly, there is also an $\bar{I}I$ valley, which starts from $q(\tau) \equiv 1/g$ and develops to a pair of \bar{I} and I . For both valleys the action is a monotonically increasing function of R , approaching the sum of the instanton action and the anti-instanton action as $R \rightarrow \infty$. There are more complicated valleys, which start either from $q(\tau) \equiv 0$ or $1/g$ and develop to configurations with multiple I and \bar{I} . At the leading order (for small coupling), this part of the valley is relevant for the dilute-instanton-gas calculus.

For $\epsilon \neq 0$, the valley configurations were found to behave in a qualitatively similar manner [9, 11]. There are configurations that smoothly connect one

¹In an earlier paper [9], we have used a $(4g^3q^3 - 3g^4q^4)$ term in place of gq in the ϵ term of the potential. This was for the sake of the exact relations $q_+ = 0$ and $q_- = 1/g$. But this choice obscures the supersymmetry we present in Section 6 and is thus avoided.

minimum to the other minimum, which we call “valley-instanton” and “anti-valley-instanton”, and configurations that are similar to the pairs of these valley-instantons and anti-valley-instantons exist as solutions of the valley equation. For a one-pair configuration with distance $R(\gg 1)$ (for preview, see Fig.3), its action behaves as $S^{(I\bar{I})} \approx 2S^{(I)} - \epsilon R - (2/g^2)e^{-R}$ (Fig.4). The first term of this action comes from the valley-instanton and the anti-valley-instanton, while the second term is the “volume energy” from the region between them, where $q(\tau) = q_-$ (and $V(q_-) = -\epsilon$), and the third term is the “interaction” between the instanton and the anti-instanton. When R decreases, this configuration reaches the “bounce” solution where the action peaks, and then reduces to $q(\tau) = q_+$ for $R = 0$. At the bounce point, the valley line corresponds to the direction of the negative eigenvalue of the bounce solution. We will also call this an $I\bar{I}$ valley. There is also an $\bar{I}I$ valley (Fig.5), in which $q(\tau) = q_-$ at $R = 0$, and the action $S^{(\bar{I}I)}(R)$ is a monotonically increasing function of R for the whole range of $R = 0 \sim \infty$. Specifically, $S^{(\bar{I}I)}(R) \approx 2S^{(I)} + \epsilon R - (2/g^2)e^{-R}$ for $R \gg 1$ (Fig.6).

All these can be seen explicitly and in detail by solving the valley equation. In the rest of this section, we briefly explain the valley method used, and analytically construct the valley configurations. Furthermore, quantities needed for later calculations, such as Jacobians and determinants, are also obtained.

2.1 The valley method

We use the following equation as a precise definition of the valley[7]:

$$\int d\tau' \frac{\delta^2 S[q]}{\delta q(\tau) \delta q(\tau')} \frac{\delta S[q]}{\delta q(\tau')} = \lambda \frac{\delta S[q]}{\delta q(\tau)}, \quad (2.5)$$

This equation can be rewritten in the following form:

$$\frac{\delta}{\delta q(\tau)} \left[\frac{1}{2} \int \left(\frac{\delta S[q]}{\delta q(\tau')} \right)^2 d\tau' - \lambda S[q] \right] = 0. \quad (2.6)$$

This implies that a solution of the valley equation (2.5) extremizes the norm of the gradient vector $\int d\tau (\delta S[q]/\delta q)^2$ in the functional subspace of $q(\tau)$ with a fixed value of S , with λ playing the role of the Lagrange multiplier. This makes this equation suitable for a geometrical definition of the valley (see Fig.2).

More important is the fact that with this definition, the eigenvalue λ of the second derivative of S is removed from the loop integrations. Initially, we separate the integration along the valley line from the whole functional integration. After this step, we are left with the integrations over the directions perpendicular to the gradient “vector”, $\delta S/\delta q(\tau)$, which are the loop-integrations. This is done in the following manner.

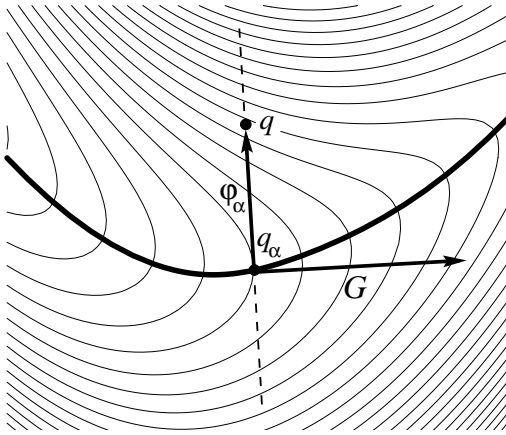


Figure 2: A schematic drawing of a valley in a two-dimensional space. The thin curved lines are the contour lines of the action. The thick line denotes the valley line. The horizontal arrow denotes the gradient vector G at a point q_α and the broken vertical line is the integration subspace for φ_α , which is perpendicular to G . Note that the vector G is not tangential to the valley line, which is a general property of the valley equation.

Firstly, we parameterize the valley by a parameter α and denote the valley configuration by $q_\alpha(\tau)$, and then take a functional integral,

$$Z = \mathcal{J} \int \mathcal{D}q e^{-S[q]}, \quad (2.7)$$

where we are adopting the natural unit, $\hbar = c = 1$. (Inserting an operator \mathcal{O} in the above does not change the following argument.) The normalization of the path-integral measure is the same as in Ref.[12]. We define the Faddeev-Popov determinant $\Delta[\varphi_\alpha]$, which is actually the Jacobian for introducing α as an integration variable, by the following:

$$\int d\alpha \delta \left(\int \varphi_\alpha(\tau) G(\tau) d\tau \right) \Delta[\varphi_\alpha] = 1, \quad (2.8)$$

where $\varphi_\alpha(\tau) \equiv q(\tau) - q_\alpha(\tau)$ are the fluctuations over which we will be doing loop-integrations, and $G(\tau)$ is the normalized gradient vector,

$$G(\tau) = \frac{\delta S}{\delta q_\alpha(\tau)} \Big/ \sqrt{\int \left(\frac{\delta S}{\delta q_\alpha(\tau')} \right)^2 d\tau'}. \quad (2.9)$$

By inserting the factor (2.8) into the functional integral (2.7), we obtain the following:

$$Z = \mathcal{J} \int d\alpha \int \mathcal{D}q \delta \left(\int \varphi_\alpha(\tau) G(\tau) d\tau \right) \Delta[\varphi_\alpha] e^{-S[q]}. \quad (2.10)$$

We expand the action $S[q]$ around $\varphi_\alpha(\tau) = 0$:

$$S[q] = S[q_\alpha] + \int \frac{\delta S[q_\alpha]}{\delta q_\alpha(\tau)} \varphi_\alpha(\tau) d\tau + \frac{1}{2} \int \frac{\delta^2 S[q_\alpha]}{\delta q_\alpha(\tau) \delta q_\alpha(\tau')} \varphi_\alpha(\tau) \varphi_\alpha(\tau') d\tau d\tau' + \dots \quad (2.11)$$

The first order term in $\varphi_\alpha(\tau)$ vanishes due to the δ -function. The integration of the second order term in $\varphi_\alpha(\tau)$ yields the determinant of the second functional derivative $D(\tau, \tau') \equiv \delta^2 S[q_\alpha]/\delta q_\alpha(\tau) \delta q_\alpha(\tau')$, *in the subspace defined by the δ -function*. At this order, the Jacobian $\Delta[\varphi_\alpha]$ is approximated as follows,

$$\Delta[\varphi_\alpha] = \int \frac{dq_\alpha(\tau)}{d\alpha} G(\tau) d\tau = \frac{\frac{dS[q_\alpha]}{d\alpha}}{\sqrt{\int d\tau \left(\frac{\delta S[q_\alpha]}{\delta q(\tau)} \right)^2}} (\equiv \Delta). \quad (2.12)$$

With this, the integral (2.10) reduces to,

$$Z = \mathcal{J} \int \frac{d\alpha}{\sqrt{2\pi \det' D}} \Delta e^{-S[q_\alpha]}. \quad (2.13)$$

at the one-loop order. In the above, \det' denotes the determinant in the subspace described above. Note the apparent reparametrization invariance of α , which should exist, as we have not specified the choice of the valley parameter α . The factor $1/\sqrt{2\pi}$ is induced by the fact that the δ -function reduces the number of the integrations over $q(\tau)$ by one.

The valley equation (2.5) dictates that the subspace $\int \varphi_\alpha(\tau) G(\tau) d\tau = 0$ does not contain the eigenvector of the eigenvalue λ . Therefore $\det' D$ is simply the product of all the eigenvalues of D less λ . This means that the valley equation (2.5) converts the eigenvalue λ completely to the collective coordinate α . This is the key property of the valley equation (2.5), since in actual applications one encounters negative, zero, or very small eigenvalues, which render the one-loop approximation useless, or at least dangerous. By choosing λ to be the undesired eigenvalue, we remove it completely from the Gaussian (and higher order) integration.

The valley equation can be made more perspicuous by introducing an auxiliary coordinate. First we will rewrite the valley equation (2.5) as follows:

$$\frac{\delta S_V[q]}{\delta q(\tau)} = 0, \quad (2.14)$$

where S_V is defined by,

$$S_V[q] = S[q] - \frac{1}{2\lambda} \int d\tau \left(\frac{\delta S[q]}{\delta q(\tau)} \right)^2. \quad (2.15)$$

The second term of the above $S_V[q]$ contains a fourth derivative term of $q(\tau)$ with respect to τ . It can be removed by introducing an auxiliary variable $F(\tau)$ as follows:

$$\begin{aligned}\bar{S}_V[q] &= S_V[q] + \frac{1}{2\lambda} \int d\tau \left(F(\tau) - \frac{\delta S[q]}{\delta q(\tau)} \right)^2 \\ &= S[q] + \frac{1}{2\lambda} \int d\tau \left(F(\tau)^2 - 2F(\tau) \frac{\delta S[q]}{\delta q(\tau)} \right).\end{aligned}\quad (2.16)$$

Taking the functional derivative of $\bar{S}_V[q]$ with respect to $q(\tau)$ and $F(\tau)$ we obtain the following equations:

$$\frac{\delta S[q]}{\delta q(\tau)} = F(\tau), \quad (2.17)$$

$$\int d\tau' \frac{\delta^2 S[q]}{\delta q(\tau) \delta q(\tau')} F(\tau') = \lambda F(\tau), \quad (2.18)$$

which are apparently equivalent to the original valley equation (2.5) upon elimination of $F(\tau)$. It is evident that any solution of the equation of motion is also a solution of the valley equation (2.18) with $F(\tau) \equiv 0$. Some of the other important properties of the valley method are noted in Appendix A.

Like any classical solution, the solution of the valley equation (2.5) may break some of the symmetries of the system. To restore them, we must introduce additional collective coordinates. The conventional collective coordinate method cannot be applied, because, in contrast to the classical solution, the existence of the zero modes of the symmetries is not guaranteed for the solution of the valley equation. We will introduce them in the manner developed in Ref.[8]. In order to achieve definiteness, we will assume that the translational symmetry is broken by the valley configuration, which is indeed the case in the model we treat in this paper.

Under translation τ_0 , the quantum fluctuation $\varphi_\alpha(\tau) \equiv q(\tau) - q_\alpha(\tau)$ transforms as

$$\begin{aligned}\varphi_\alpha(\tau) \rightarrow \varphi_\alpha^{\tau_0}(\tau) &\equiv q(\tau + \tau_0) - q_\alpha(\tau) \\ &= \varphi_\alpha(\tau + \tau_0) + q_\alpha(\tau + \tau_0) - q_\alpha(\tau).\end{aligned}\quad (2.19)$$

This transformation induces an analogue of the gauge transformation on $S[q_\alpha + \varphi_\alpha]$ [13]. The basic strategy of our collective coordinate method is to introduce the translation τ_0 into the path-integral as the “gauge orbit”. This procedure automatically guarantees the manifest invariance under the translation through the following deformation, and does not require the zero mode.

To extract the gauge orbit, we will use the Faddeev-Popov technique. In place of Eq.(2.8), we introduce the following Faddeev-Popov determinant $\Delta[\varphi_\alpha]$:

$$\int d\tau_0 \int d\alpha \delta \left(\int \varphi_\alpha^{\tau_0}(\tau) G(\tau) d\tau \right) \delta \left(\int \varphi_\alpha^{\tau_0}(\tau) \mathcal{G}(\tau) d\tau \right) \Delta[\varphi_\alpha] = 1, \quad (2.20)$$

where $\mathcal{G}(\tau)$ is a suitable function independent from τ_0 , and gives the gauge fixing condition of the translation:

$$\int \varphi_\alpha(\tau) \mathcal{G}(\tau) d\tau = 0. \quad (2.21)$$

By inserting the factor (2.20) into the functional integral, we obtain

$$\begin{aligned} Z &= \mathcal{J} \int d\tau_0 \int d\alpha \int \mathcal{D}q \delta \left(\int \varphi_\alpha^{\tau_0}(\tau) G(\tau) d\tau \right) \\ &\quad \times \delta \left(\int \varphi_\alpha^{\tau_0}(\tau) \mathcal{G}(\tau) d\tau \right) \Delta[\varphi_\alpha] e^{-S[q]}. \end{aligned} \quad (2.22)$$

As well as the usual gauge symmetry, the following relations hold.

$$\Delta[\varphi_\alpha] = \Delta[\varphi_\alpha^{\tau_0}], \quad S[q_\alpha + \varphi_\alpha^{\tau_0}] = S[q_\alpha + \varphi_\alpha]. \quad (2.23)$$

Therefore, the integration of τ_0 is trivially factored out.

$$\begin{aligned} Z &= \mathcal{J} \int d\tau_0 \int d\alpha \int \mathcal{D}\varphi_\alpha \delta \left(\int \varphi_\alpha(\tau) G(\tau) d\tau \right) \\ &\quad \times \delta \left(\int \varphi_\alpha(\tau) \mathcal{G}(\tau) d\tau \right) \Delta[\varphi_\alpha] e^{-S[q_\alpha + \varphi_\alpha]}. \end{aligned} \quad (2.24)$$

At the one-loop level, we find that the Faddeev-Popov determinant becomes as follows:

$$\Delta[\varphi_\alpha] = \left| \det \begin{pmatrix} \int \frac{\partial q_\alpha(\tau)}{\partial \tau} \mathcal{G}(\tau) d\tau & \int \frac{\partial q_\alpha(\tau)}{\partial \alpha} \mathcal{G}(\tau) d\tau \\ \int \frac{\partial q_\alpha(\tau)}{\partial \tau} G(\tau) d\tau & \int \frac{\partial q_\alpha(\tau)}{\partial \alpha} G(\tau) d\tau \end{pmatrix} \right|. \quad (2.25)$$

Because of the following equation

$$\int \frac{\partial q_\alpha(\tau)}{\partial \tau} G(\tau) d\tau = \int \frac{\partial q_\alpha(\tau)}{\partial \tau} \frac{\delta S}{\delta q_\alpha(\tau)} d\tau \left/ \sqrt{\int \left(\frac{\delta S}{\delta q_\alpha(\tau')} \right)^2 d\tau'} \right. = 0, \quad (2.26)$$

it can be simplified as

$$\Delta[\varphi_\alpha] = \left| \int \frac{\partial q_\alpha(\tau)}{\partial \tau} G(\tau) d\tau \right| \left| \int \frac{\partial q_\alpha(\tau)}{\partial \alpha} \mathcal{G}(\tau) d\tau \right|. \quad (2.27)$$

Some of the valleys may contain classical solutions, and in the neighborhood of such a solution, the valley has a quasi-zero mode which is different from λ because of the broken symmetry. To remove this dangerous mode η from the path-integral, we will designate $\mathcal{G}(\tau)$ as the normalized eigenfunction of η :

$$\int d\tau' \frac{\delta^2 S[q]}{\delta q(\tau) \delta q(\tau')} \mathcal{G}(\tau') = \eta \mathcal{G}(\tau). \quad (2.28)$$

With this gauge fixing, we obtain

$$Z = \mathcal{J} \int \int \frac{d\tau_0 d\alpha}{2\pi \sqrt{\det'' D}} \Delta[\varphi_\alpha] e^{-S[q_\alpha]}, \quad (2.29)$$

where

$$\det'' D = \frac{\det D}{\lambda \eta}. \quad (2.30)$$

2.2 Valley configurations

For the action (2.1), the valley equations (2.17) and (2.18) yield the following partial differential equations,

$$-\partial_\tau^2 q + V'(q) = F \quad (2.31)$$

$$(-\partial_\tau^2 + V''(q)) F = \lambda F. \quad (2.32)$$

From Eq.(2.31) we see that the auxiliary coordinate F acts as an external force introduced into the usual equation of motion for q . Eq.(2.32) is a self-consistent equation for F .

Since the terms in the action \bar{S}_V in (2.16) contain two time-derivatives at most, the canonical formalism can be applied. Denoting the “Lagrangian” of \bar{S}_V as L_V , the canonical momentum p_q and p_F for the coordinates q and F are given as follows,

$$p_q = \frac{\partial L_V}{\partial \dot{q}} = \dot{q} - \frac{1}{\lambda} \dot{F}, \quad (2.33)$$

$$p_F = \frac{\partial L_V}{\partial \dot{F}} = -\frac{1}{\lambda} \dot{q}. \quad (2.34)$$

This leads to the following conserved “Hamiltonian” of the system,

$$\begin{aligned} H_V &= p_q \dot{q} + p_F \dot{F} - L_V \\ &= \frac{1}{2} \dot{q}^2 - V(q) - \frac{1}{\lambda} \left(\frac{1}{2} F^2 + \dot{F} \dot{q} - F V'(q) \right). \end{aligned} \quad (2.35)$$

The conservation of this quantity can be directly confirmed by the use of the valley equations (2.31) and (2.32).

The valley Hamiltonian H_V in (2.35) is useful for numerical calculations of the valley configurations. Any $I\bar{I}$ or $\bar{I}I$ valley configuration is symmetric around the middle point between the instantons. When solving the differential equations (2.31) and (2.32) for a given λ , we choose initial values at this symmetric point so that the solutions converge as $\tau \rightarrow \infty$. This shooting method is somewhat complicated in its operation if the initial data is multi-dimensional. At the symmetric point, say $\tau = 0$, we have $\dot{q}(0) = \dot{F}(0) = 0$. The convergence conditions, $q(\infty) = q_{\pm}$, $F(\infty) = 0$, are to be satisfied choosing $q(0)$ and $F(0)$ as appropriate. Therefore at this stage the search has to be made in two-dimensional space. The valley Hamiltonian (2.35) reduces the degrees of freedom in the initial data by one, since $H_V = -V(q_{\pm})$ by the asymptotic condition for $\tau \rightarrow \infty$. Therefore we only need to choose one initial datum, say $q(0)$, to find the valley configuration. Having only one parameter to determine, this task is straightforward.

The numerical calculations were carried out for $g = 0.1$, $\epsilon = 5$, which corresponds to the potential in Fig.1. Fig.3 is the plot of $q_{\alpha}(\tau)$ and $F_{\alpha}(\tau)$ of the configurations in the $I\bar{I}$ valley. The values of the action S and the eigenvalue λ for this valley are plotted in Fig.4, where the horizontal coordinate is $\|q\| \simeq |q_{-} - q_{+}|R$ for $R \gg 1$. The configuration drawn by the broken line Fig.3 is the bounce solution, which has $F(\tau) = 0$. The action peaks at this point in the valley as seen in Fig.4. The corresponding plots for the $\bar{I}I$ valley are given in Fig.5 and Fig.6. Corresponding to the fact that there are no solutions of the equation of motion with the boundary condition $q(\pm\infty) = q_{-}$, the action behaves monotonically, as seen in Fig.6.

In Fig.3 and Fig.5, we readily see that these valleys are qualitatively similar to the valleys for the symmetric double-well case $\epsilon = 0$. Particularly, for large distances $R \gg 1$, the valley configurations are in fact made of flat inside regions of $q = q_{\mp}$ and flat outside regions where $q = q_{\pm}$. The transient regions are of fixed shape, which simply moves outward as R increases (see the curves a,b,c of Figs.3,5). It is apparent that for $R \rightarrow \infty$, each transient configuration with boundary conditions $q(-\infty) = q_{\pm}$, $q(\infty) = q_{\mp}$ becomes an independent solution of the valley equation. We call the left transient region of the $I\bar{I}$ valley, where q changes from q_{+} to q_{-} , as valley-instanton, while the other as the anti-valley-instanton, and vice versa for $\bar{I}I$ valley. The behaviour of the eigenvalue λ in Fig.4 and Fig.6 suggests that these valley-instantons have an eigenvalue of exactly zero. We note that this property is not trivial for $\epsilon \neq 0$, since in that case the valley-instanton is not a solution of the equation of motion. In fact, taking the time-derivative of Eq.(2.31), we obtain,

$$(-\partial_{\tau}^2 + V''(q)) \dot{q} = \dot{F}, \quad (2.36)$$

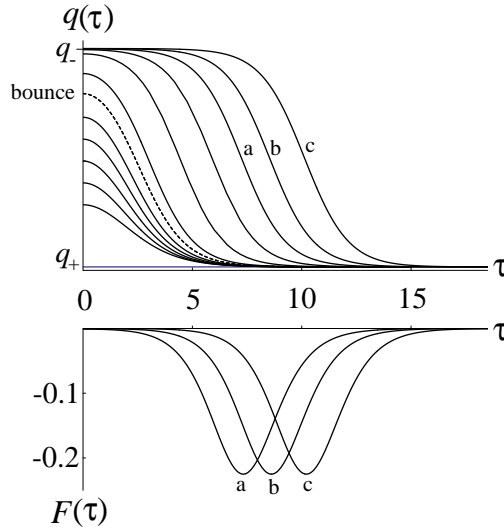


Figure 3: Configurations in $I\bar{I}$ valley. The symmetric point is chosen to be at $\tau = 0$, and only the half of the configuration, $\tau > 0$, is shown. The upper plot shows the behavior of $q(\tau)$, where the broken line denotes the bounce solution. The lower plot is $F(\tau)$. The labels a , b , and c show the correspondence between $q(\tau)$ and $F(\tau)$.

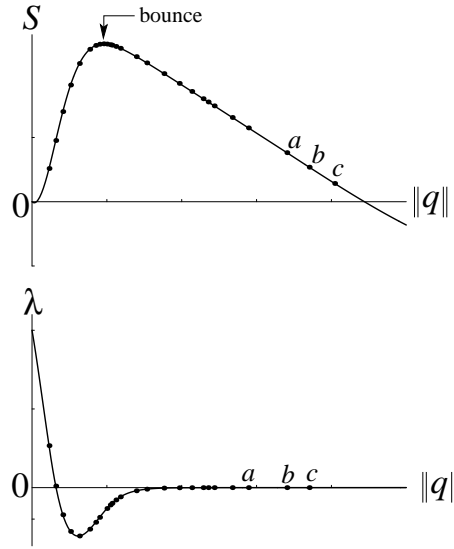


Figure 4: The action S (upper plot) and the eigenvalue λ (lower plot) of the $I\bar{I}$ valley. The labels show the action of the corresponding solutions in Fig.3. The horizontal axis is a valley parameter defined as $\alpha = \|q\| \equiv \int_0^\infty |q(\tau) - q_+| d\tau$. For $\|q\| \gg 1$, $\|q\| \simeq |q_- - q_+| R$. The peak of the action is given by the bounce solution shown in Fig.3.

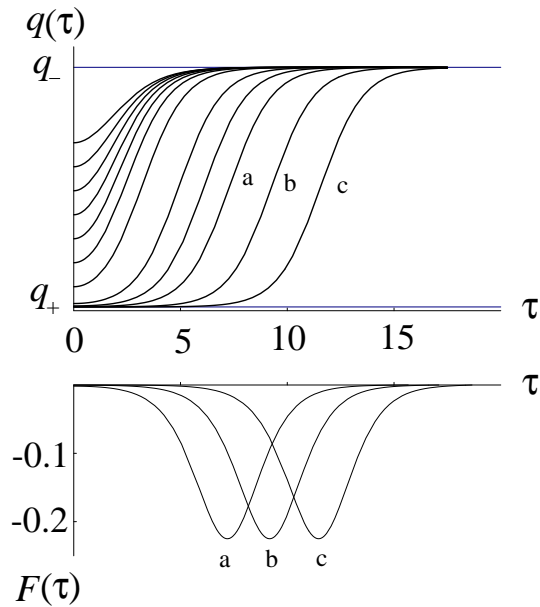


Figure 5: Configurations in \bar{II} valley.

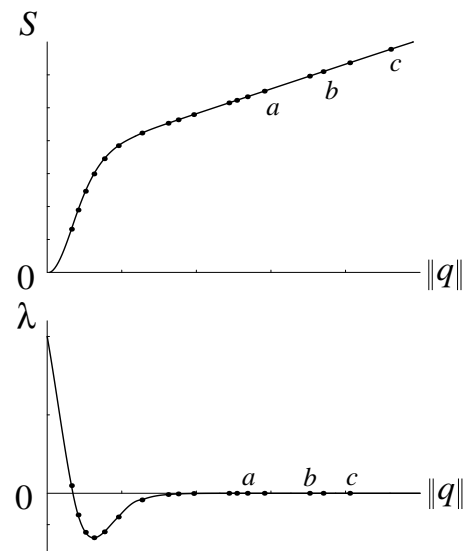


Figure 6: The action S (upper plot) and the eigenvalue λ (lower plot) of the \bar{II} valley. There are no solutions of the equation of motion under the boundary condition $q(\pm\infty) = q_-$. Therefore, the action behaves monotonically.

which shows that \dot{q} is *not* a zero mode. This is as it should be, since simple translation of the valley-instanton *does* change the action by the corresponding volume energy.

Eq.(2.36), however, can be combined with Eq.(2.32) to show that $\lambda = 0$. For this purpose, we multiply \dot{q} on Eq.(2.32), integrate over τ from $-\infty$ to ∞ , and carry out partial-integration twice to move ∂_τ^2 to act on \dot{q} . At $\tau = \pm\infty$, q of the valley-instanton is at the extrema q_\pm of the potential. Therefore the external force F goes to zero for $\tau \rightarrow \pm\infty$ (see Fig.3 and Fig.5). The surface terms of the partial integrations vanish due to this property. We thus obtain the following:

$$\int_{-\infty}^{\infty} \dot{F} F d\tau = \lambda \int_{-\infty}^{\infty} \dot{q} F d\tau. \quad (2.37)$$

The left-hand side of this equation is evidently zero according to the boundary conditions. On the right-hand side, the integral $\int_{-\infty}^{\infty} \dot{q} F d\tau$ is not zero, as is seen in Fig.3 and in Fig.5. Therefore, for the valley-instanton we find that $\lambda = 0$ and the auxiliary coordinate F is the zero mode. Note that this proof does not apply to the $I\bar{I}$ and $\bar{I}I$ configurations. This is because for those configurations the integral $\int_{-\infty}^{\infty} \dot{q} F d\tau$ is zero due to the fact that $q(\tau)$ and $F(\tau)$ are even functions around the symmetric point. And in fact, λ is not identically zero for the $I\bar{I}$ and $\bar{I}I$ valley.

Although the global features are evident from the numerical results presented in this section, we need analytic expressions of the action and other related quantities. Of special importance are the interaction terms of the actions of the $I\bar{I}$ and $\bar{I}I$ configurations. In the following we carry out an analytic construction for these configurations, using the fact that the valley-instanton possesses an exact zero eigenvalue.

2.3 Valley-instanton

The existence of the zero eigenvalue $\lambda = 0$ and the zero mode F enables us to carry out the construction of the valley-instanton. We will first carry out the analytic construction of the valley-instanton. For this purpose it is convenient to use the rescaled coordinate $\tilde{q} = gq$. The action (2.1) is written in terms of this \tilde{q} as follows:

$$S[q] = \frac{1}{g^2} \tilde{S}[\tilde{q}], \quad \tilde{S}[\tilde{q}] = \int d\tau \left[\frac{1}{2} \left(\frac{d\tilde{q}}{d\tau} \right)^2 + \tilde{V}(\tilde{q}) \right], \quad (2.38)$$

$$\tilde{V}(\tilde{q}) = \tilde{V}_0(\tilde{q}) + \epsilon g^2 \tilde{V}_1(\tilde{q}), \quad \tilde{V}_0(\tilde{q}) = \frac{1}{2} \tilde{q}^2 (1 - \tilde{q})^2, \quad \tilde{V}_1(\tilde{q}) = -\tilde{q}. \quad (2.39)$$

This implies that in the following expansion in ϵ , the actual perturbation parameter is ϵg^2 , which is natural considering that this is a dimensionless

quantity. We can also define a rescaled auxiliary coordinate $\tilde{F} = gF$ and rewrite the valley equations (2.31) and (2.32) as follows:

$$-\partial_\tau^2 \tilde{q} + \tilde{V}'(\tilde{q}) = \tilde{F} \quad (2.40)$$

$$(-\partial_\tau^2 + \tilde{V}''(\tilde{q})) \tilde{F} = 0, \quad (2.41)$$

where we used the fact that $\lambda = 0$. (In the above the prime denotes the derivative with respect to \tilde{q} .) Let us obtain the solution of this set of equations as perturbative series in ϵg^2 ,

$$\tilde{q} = \tilde{q}_0 + \epsilon g^2 \tilde{q}_1 + (\epsilon g^2)^2 \tilde{q}_2 + \dots, \quad (2.42)$$

$$\tilde{F} = \epsilon g^2 \tilde{F}_1 + (\epsilon g^2)^2 \tilde{F}_2 + \dots \quad (2.43)$$

As the zeroth order, we have only the following equation:

$$-\partial_\tau^2 \tilde{q}_0 + \tilde{V}'_0(\tilde{q}_0) = 0, \quad (2.44)$$

whose solution is the (scaled) ordinary instanton $\tilde{q}_0 = gq_0^{(I)}(\tau; 0)$. (We choose $\tau_I = 0$ for the ease of notation in this analysis. It may be reintroduced by replacing τ by $\tau - \tau_I$ at the end.)

At the first order in ϵg^2 , Eqs.(2.40) and (2.41) leads to the following:

$$(-\partial_\tau^2 + \tilde{V}''_0(\tilde{q}_0)) \tilde{q}_1 = \tilde{F}_1 - \tilde{V}'_1(\tilde{q}_0), \quad (2.45)$$

$$(-\partial_\tau^2 + \tilde{V}''_0(\tilde{q}_0)) \tilde{F}_1 = 0. \quad (2.46)$$

Eq.(2.46) dictates that \tilde{F}_1 be proportional to the zero mode of \tilde{q}_0 , which is $\dot{\tilde{q}}_0$:

$$\tilde{F}_1 = c_1 \dot{\tilde{q}}_0. \quad (2.47)$$

The proportionality constant c_1 can be fixed by the following consideration: For Eq.(2.45) to have a solution, the zero mode of the operator $-\partial_\tau^2 + \tilde{V}''_0(\tilde{q}_0)$ should not be contained in the right-hand side. Therefore the constant c_1 should be such that \tilde{F}_1 cancels the zero mode in $\tilde{V}'_1(\tilde{q}_0)$. In fact, multiplying $\dot{\tilde{q}}_0$ on both sides of Eq.(2.45), integrating over τ from $-\infty$ to ∞ and performing partial integration twice, we find that

$$\begin{aligned} 0 &= \int_{-\infty}^{\infty} \dot{\tilde{q}}_0 \tilde{F}_1 d\tau - \int_{-\infty}^{\infty} \dot{\tilde{q}}_0 \tilde{V}'_1(\tilde{q}_0) d\tau \\ &= c_1 \int_0^1 \dot{\tilde{q}}_0 d\tilde{q}_0 - \int_0^1 \tilde{V}'_1(\tilde{q}_0) d\tilde{q}_0 = \frac{1}{6} c_1 + 1, \end{aligned} \quad (2.48)$$

which fixes c_1 as $c_1 = -6$. (It is useful to note that $\dot{\tilde{q}}_0 = \tilde{q}_0(1 - \tilde{q}_0)$ in the calculation of the first term.) The expression for \tilde{q}_1 is obtained by the same

procedure as above, but integrating only from $-\infty$ to τ , which leads to the following:

$$\ddot{\tilde{q}}_0\tilde{q}_1 - \dot{\tilde{q}}_0\dot{\tilde{q}}_1 = -6\left(\frac{\dot{\tilde{q}}_0^2}{2} - \frac{\dot{\tilde{q}}_0^3}{3}\right) + \tilde{q}_0 = \tilde{V}'_0(\tilde{q}_0) = \ddot{\tilde{q}}_0. \quad (2.49)$$

The general solution of this equation is $\tilde{q}_1 = 1 + c_2\dot{\tilde{q}}_0$, where c_2 is an integration constant, which remains arbitrary at this order.

At the second order in ϵg^2 , we have the following:

$$\left(-\partial_\tau^2 + \tilde{V}''_0(\tilde{q}_0)\right)\tilde{q}_2 = \tilde{F}_2 - \frac{1}{2}\tilde{V}'''_0(\tilde{q}_0)\tilde{q}_1^2 - \tilde{V}''_1(\tilde{q}_0)\tilde{q}_1, \quad (2.50)$$

$$\left(-\partial_\tau^2 + \tilde{V}''_0(\tilde{q}_0)\right)\tilde{F}_2 = -\tilde{V}'''_0(\tilde{q}_0)\tilde{q}_1\tilde{F}_1. \quad (2.51)$$

The parameter c_2 in \tilde{q}_1 is fixed by the condition that zero mode be absent from the right-hand side of Eq.(2.51). Straightforward calculation shows that this leads to $c_2 = 0$. Proceeding in a manner similar to the first-order calculation, we find that \tilde{F}_2 satisfies the following equation:

$$\ddot{\tilde{q}}_0\tilde{F}_2 - \dot{\tilde{q}}_0\dot{\tilde{F}}_2 = -18\dot{\tilde{q}}_0^2. \quad (2.52)$$

The general solution of this equation is $\tilde{F}_2 = (18\tau + c_3)\dot{\tilde{q}}_0$, where the constant c_3 is a free parameter. It is straightforward to show that the condition for the absence of the zero mode $\dot{\tilde{q}}_0$ on the right-hand side of Eq.(2.50) fixes the parameter c_3 as $c_3 = 0$, using the fact that the integral $\int_{-\infty}^{\infty} \dot{\tilde{q}}_0^2 \tau d\tau$ vanishes since the integrand is an odd function of τ .

Summarizing the perturbative solution obtained so far, we have

$$\tilde{q}(\tau) = \tilde{q}_0(\tau) + \epsilon g^2 + O((\epsilon g^2)^2), \quad (2.53)$$

$$\tilde{F}(\tau) = -6\epsilon g^2\dot{\tilde{q}}_0(\tau) + 18(\epsilon g^2)^2\tau\dot{\tilde{q}}_0(\tau) + O((\epsilon g^2)^3). \quad (2.54)$$

The $(\epsilon g^2)^2$ term in \tilde{F} indicates that these perturbative series are valid only for $|\tau| \ll 1/\epsilon g^2$.

For $\tau \rightarrow \pm\infty$, we may solve the linearized valley equation,

$$\left(-\partial_\tau^2 + \tilde{V}''(\tilde{q}_\pm)\right)\delta\tilde{q} = \tilde{F}, \quad (2.55)$$

$$\left(-\partial_\tau^2 + \tilde{V}''(\tilde{q}_\pm)\right)\tilde{F} = 0, \quad (2.56)$$

where $\delta\tilde{q} = \tilde{q} - \tilde{q}_\pm$, The general solution of these equations are,

$$\tilde{q}(\tau) = \tilde{q}_\mp + C_\mp e^{\mp\omega_\mp\tau} + \frac{F_\mp}{2\omega_\mp}\tau e^{\mp\omega_\mp\tau}, \quad (2.57)$$

$$\tilde{F}(\tau) = F_\mp e^{\mp\omega_\mp\tau}, \quad (2.58)$$

for $\tau \rightarrow \pm\infty$, respectively. The coefficients F_{\pm}, C_{\pm} are arbitrary constants and $\omega_{\pm} \equiv \sqrt{\tilde{V}''(\tilde{q}_{\pm})}$.

For small ϵg^2 , $\tilde{q}_+ = \epsilon g^2 + O((\epsilon g^2)^2)$ and $\tilde{q}_- = 1 + \epsilon g^2 + O((\epsilon g^2)^2)$. Also, $\omega_{\pm} = 1 \mp 3\epsilon g^2 + O((\epsilon g^2)^2)$, which means that the linearized solution (2.57)–(2.58) is valid for $1 \ll |\tau|$. Therefore, we find an overlapping region $1 \ll |\tau| \ll 1/\epsilon g^2$, where both Eqs.(2.53), (2.54) and Eqs.(2.57), (2.58) are valid. In this region the exponentials in the asymptotic solutions Eq.(2.57) can be expanded in terms of $\epsilon g^2 \tau$ and be matched with Eq.(2.53)–(2.54). This matching indeed works out and fixes the constants F_{\pm}, C_{\pm} as $F_{\pm} = -6\epsilon g^2$, $C_{\pm} = \pm 1$.

In summary of the analytic construction of the valley-instanton configuration, we have the following:

$$q(\tau) = \begin{cases} \epsilon g + \frac{1}{g} e^{\omega_+ \tau} + \frac{3\epsilon g}{\omega_+} \tau e^{\omega_+ \tau} + \dots & \text{if } \tau \ll -1 ; \\ \frac{1}{g} \frac{1}{1 + e^{-\tau}} + \epsilon g + \dots & \text{if } -1/\epsilon g^2 \ll \tau \ll 1/\epsilon g^2 ; \\ \frac{1}{g} + \epsilon g - \frac{1}{g} e^{-\omega_- \tau} - \frac{3\epsilon g}{\omega_-} \tau e^{-\omega_- \tau} + \dots & \text{if } \tau \gg 1 , \end{cases} \quad (2.59)$$

$$F(\tau) = \begin{cases} -6\epsilon g e^{\omega_+ \tau} + \dots & \text{if } \tau \ll -1 ; \\ -6\epsilon g \frac{1 - 3\epsilon g^2 \tau}{(1 + e^{-\tau})(1 + e^{\tau})} + \dots & \text{if } -1/\epsilon g^2 \ll \tau \ll 1/\epsilon g^2 ; \\ -6\epsilon g e^{-\omega_- \tau} + \dots & \text{if } \tau \gg 1 . \end{cases} \quad (2.60)$$

From this solution we can evaluate the action S . First let us calculate the contribution of the solution (2.59) for $|\tau| \ll 1/\epsilon g^2$.

$$S[q_0 + \epsilon g^2 q_1] = S_0[q_0] + \epsilon g^2 S_1[q_0] + \epsilon g^2 \int \frac{\delta S_0[q_0]}{\delta q_0(\tau)} q_1(\tau) d\tau + \dots, \quad (2.61)$$

where we used unscaled quantities $q_i \equiv \tilde{q}_i/g$, etc. And S_1 is the contribution of the V_1 -term in Eq.(2.39), while S_0 denotes the rest of the terms in the action. We find that the second term vanishes. The third term is also zero due to Eq.(2.44). In the asymptotic region, $|\tau| \gg 1$, the linearized solutions should be used, which simply yields the volume energy plus the higher order terms in ϵg^2 . Therefore, the action of the configuration (2.59) restricted in region $\tau \in [-T/2, T/2]$ ($T \gg 1$) is given by $S \simeq (1/6g^2) - \epsilon T/2 + \dots$. The second term of this expression is the “volume energy” due to the

energy difference between $q = q_+$ and q_- , while the first term is the leading contribution to the valley-instanton action $S^{(I),(\bar{I})}$:

$$S^{(I),(\bar{I})} = \frac{1}{6g^2} \left[1 + O((\epsilon g^2)^2) \right]. \quad (2.62)$$

We will now turn to the evaluation of the Jacobian (2.12). The numerator is the squared norm of $F(\tau)$, the leading contribution to which comes from the integration near $\tau \sim 0$. Substituting the expression (2.60) in this region, we find that the leading contribution is,

$$\int_{-\infty}^{\infty} F^2 d\tau = 6\epsilon^2 g^2 + \dots \quad (2.63)$$

Therefore, we find that when we choose the position coordinate of the valley-instanton as the valley parameter α , the Jacobian (2.12) is given by the following:

$$\Delta = \frac{\epsilon}{\sqrt{\int_{-\infty}^{\infty} F^2 d\tau}} = \frac{1}{\sqrt{6g^2}} \left[1 + O(\epsilon g^2) \right]. \quad (2.64)$$

This leading term is the same as that of the ordinary instanton for $\epsilon = 0$.

The factor $\det' D$ can also be evaluated by the use of the fact that $\lambda = 0$. The derivation is given in Appendix B. The result for the valley-instanton located at $\tau = \tau_I$ in the range $\tau \in [-T/2, T/2]$ ($T \gg 1$) is the following (see Eq.(B.15)):

$$\frac{\det'(-\partial_{\tau}^2 + V'')}{\det(-\partial_{\tau}^2 + \omega_+^2)} = \frac{e^{(\omega_- - \omega_+)(T/2 - \tau_I)}}{2\omega_- F_+ F_-} \int_{-\infty}^{\infty} d\tau F^2(\tau). \quad (2.65)$$

Note that the exponential factor in the ratio of the determinant gives the right quantity for the zero-point energy contribution. In fact, the normalization factor \mathcal{J} of the functional integral (2.13) is given by the following:

$$\frac{\mathcal{J}}{\sqrt{\det(-\partial_{\tau}^2 + \omega_+^2)}} = e^{-\omega_+ T/2} \Upsilon_+, \quad (2.66)$$

where Υ_+ is a constant dependent on the definition of Z . For the partition function $Z = \lim_{T \rightarrow \infty} \text{Tr}(e^{-HT})$,

$$\Upsilon_+ = 1, \quad (2.67)$$

and for the amplitude $Z = \lim_{T \rightarrow \infty} \langle q_+ | e^{-HT} | q_+ \rangle$,

$$\Upsilon_+ = |\Psi(0; \omega_+)|^2, \quad (2.68)$$

where $\Psi(q; \omega)$ is the normalized Schrödinger wave function of the ground state for the harmonic oscillator of frequency ω and therefore $\Psi(0; \omega) = (\omega/\pi)^{1/4}$. Thus we find that

$$\frac{\mathcal{J}}{\sqrt{\det'(-\partial_\tau^2 + V'')}} = \frac{\Upsilon_+}{\sqrt{\kappa^{(I)}}} \exp \left\{ -\frac{\omega_+}{2} \left(\frac{T}{2} + \tau_I \right) - \frac{\omega_-}{2} \left(\frac{T}{2} - \tau_I \right) \right\}, \quad (2.69)$$

where

$$\kappa^{(I)} \equiv \frac{1}{2\omega_- F_+ F_-} \int_{-\infty}^{\infty} F^2 d\tau. \quad (2.70)$$

For the anti-valley-instanton, $\det' D$ is evaluated in a similar manner, but slightly modified due to the difference of the boundary condition at $\tau = \pm\infty$. Eqs.(2.65), (2.66) and (2.69) become as follows,

$$\frac{\det'(-\partial_\tau^2 + V'')}{\det(-\partial_\tau^2 + \omega_-^2)} = \frac{e^{(\omega_+ - \omega_-)(T/2 - \tau_I)}}{2\omega_+ F_+ F_-} \int_{-\infty}^{\infty} d\tau F^2(\tau), \quad (2.71)$$

$$\frac{\mathcal{J}}{\sqrt{\det(-\partial_\tau^2 + \omega_-^2)}} = e^{-\omega_- T/2} \Upsilon_-, \quad (2.72)$$

$$\frac{\mathcal{J}}{\sqrt{\det'(-\partial_\tau^2 + V'')}} = \frac{\Upsilon_-}{\sqrt{\kappa^{(\bar{I})}}} \exp \left\{ -\frac{\omega_-}{2} \left(\frac{T}{2} + \tau_I \right) - \frac{\omega_+}{2} \left(\frac{T}{2} - \tau_I \right) \right\}. \quad (2.73)$$

Here

$$\kappa^{(\bar{I})} \equiv \frac{1}{2\omega_+ F_+ F_-} \int_{-\infty}^{\infty} F^2 d\tau, \quad (2.74)$$

and for $Z = \lim_{T \rightarrow \infty} \text{Tr}(e^{-HT})$, Υ_- is

$$\Upsilon_- = 1, \quad (2.75)$$

and for $Z = \lim_{T \rightarrow \infty} \langle q_- | e^{-HT} | q_- \rangle$

$$\Upsilon_- = |\Psi(0; \omega_-)|^2. \quad (2.76)$$

The results (2.69) and (2.73) properly represent the zero-point energies $\omega_{\pm}/2$ at $q = q_{\pm}$. At the leading order in ϵg^2 , we find that $\omega_+ = \omega_- = 1$ and

$$\kappa^{(I)} = \kappa^{(\bar{I})} = \kappa \equiv \frac{1}{12}, \quad (2.77)$$

thus the difference between the results (2.69) and (2.73) disappears.

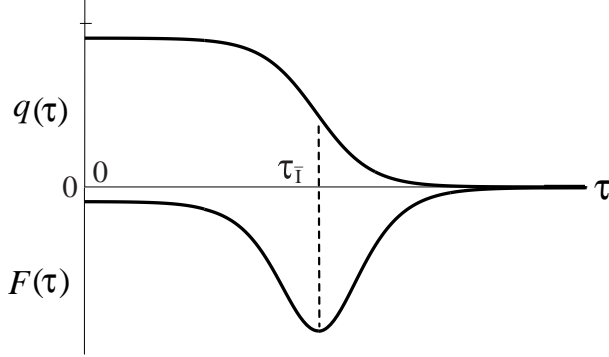


Figure 7: The $I\bar{I}$ valley configuration with a large separation. The symmetric point is chosen to be at $\tau = 0$, so that $\tau_I = -\tau_{\bar{I}}$.

2.4 $I\bar{I}$ valley configurations with large separations

The rescaled valley equations can be solved for the $I\bar{I}$ valley configurations in much the same manner as above. The calculation is especially straightforward for the leading terms in the ϵg^2 -expansion, which we will carry out in the following.²

For this purpose, we will neglect the \tilde{V}_1 term in Eq.(2.39). Furthermore, we will confine ourselves to the outskirts of the valley, where the eigenvalue $\lambda \ll 1$. This allows us to solve the valley equation in a perturbation by λ :

$$\tilde{q}(\tau) = \tilde{q}_0(\tau) + \lambda \tilde{q}_1(\tau) + \dots, \quad (2.78)$$

$$\tilde{F}(\tau) = \lambda \tilde{F}_1(\tau) + \lambda^2 \tilde{F}_2(\tau) + \dots \quad (2.79)$$

We will nominate the symmetric point of the configuration as $\tau = 0$, and solve the equation for the region $\tau \geq 0$ (see Fig.7). Therefore we choose $\tilde{q}_0(\tau)$ as the ordinary anti-instanton solution at $\tau = \tau_{\bar{I}} (\gg 1)$; $\tilde{q}_0(\tau) = g q_0^{(\bar{I})}(\tau; \tau_{\bar{I}})$. The parameter $\tau_{\bar{I}}$ will be related to λ through the boundary conditions,

$$\dot{\tilde{q}}(0) = \dot{\tilde{F}}(0) = 0, \quad (2.80)$$

$$\tilde{q}(\infty) = \tilde{F}(\infty) = 0, \quad (2.81)$$

for $\lambda \rightarrow 0$ as $\tau_{\bar{I}} \rightarrow \infty$. The equations we obtain at each order of λ are as follows:

$$O(\lambda^0) : -\partial_\tau^2 \tilde{q}_0 + \tilde{V}_0'(\tilde{q}_0) = 0, \quad (2.82)$$

$$O(\lambda^1) : \left(-\partial_\tau^2 + \tilde{V}_0''(\tilde{q}_0) \right) \tilde{q}_1 = \tilde{F}_1, \quad (2.83)$$

$$\left(-\partial_\tau^2 + \tilde{V}_0''(\tilde{q}_0) \right) \tilde{F}_1 = 0, \quad (2.84)$$

$$O(\lambda^2) : \left(-\partial_\tau^2 + \tilde{V}_0''(\tilde{q}_0) \right) \tilde{F}_2 + \tilde{V}_0'''(\tilde{q}_0) \tilde{q}_1 \tilde{F}_1 = \tilde{F}_1. \quad (2.85)$$

²This interaction term coincides with the one obtained in Ref.[5]. However our derivation is based on the valley method.

The first equation (2.82) is satisfied by the anti-instanton solution. In the following we first solve Eq.(2.84) for \tilde{F}_1 , then Eq.(2.83) for \tilde{q}_1 , and subsequently Eq.(2.85) for \tilde{F}_2 , satisfying the boundary conditions (2.81) at $\tau = \infty$. At the conclusion of the process we require the boundary conditions (2.80) at $\tau = 0$, which read;

$$\dot{\tilde{q}}_0(0) + \lambda \dot{\tilde{q}}_1(0) = 0, \quad (2.86)$$

$$\dot{\tilde{F}}_1(0) + \lambda \dot{\tilde{F}}_2(0) = 0. \quad (2.87)$$

The solution of Eq.(2.84) is simply given by the translation mode of the anti-instanton $\dot{\tilde{q}}_0(\tau) (\equiv -\psi_1(\tau))$:

$$\tilde{F}_1(\tau) = c_1 \psi_1(\tau). \quad (2.88)$$

This evidently satisfies $\tilde{F}_1(\infty) = 0$. The constant c_1 is to be determined by the boundary condition at $\tau = 0$ later.

In order to solve Eq.(2.83), it is convenient to define a Green function,

$$\bar{G}(\tau, \tau') \equiv \frac{1}{2} (\psi_1(\tau)\psi_2(\tau')\theta(\tau - \tau') + \psi_1(\tau')\psi_2(\tau)\theta(\tau' - \tau)), \quad (2.89)$$

where $\psi_2(\tau)$ is the other zero mode solution of Eq.(2.84), which is chosen so that the Wronskian is,

$$W = \psi_1 \dot{\psi}_2 - \dot{\psi}_1 \psi_2 = 2, \quad (2.90)$$

and therefore has the following asymptotic behaviour:

$$\psi_2(\tau) \simeq \begin{cases} e^{\tau - \tau_I} & \text{for } \tau - \tau_I \gg 1; \\ -e^{-(\tau - \tau_I)} & \text{for } \tau - \tau_I \ll -1. \end{cases} \quad (2.91)$$

The solution of Eq.(2.83) is then written as follows,

$$\tilde{q}_1(\tau) = \int_0^\infty d\tau' \bar{G}(\tau, \tau') \tilde{F}_1(\tau'). \quad (2.92)$$

It is straightforward to show that $\tilde{q}_1(\infty) = 0$. Further,

$$\dot{\tilde{q}}_1(0) = \frac{c_1}{2} \dot{\psi}_2(0) \int_0^\infty \psi_1(\tau)^2 d\tau \simeq \frac{c_1 e^{\tau_I}}{12}. \quad (2.93)$$

From this, we find that the boundary condition (2.86) leads to,

$$c_1 = \frac{12}{\lambda g} e^{-2\tau_I}. \quad (2.94)$$

Eq.(2.85) can be solved as follows:

$$\tilde{F}_2(\tau) = \int_0^\infty d\tau' \bar{G}(\tau, \tau') B(\tau') \tilde{F}_1(\tau'), \quad (2.95)$$

where $B(\tau) \equiv (1 - \tilde{V}_0'''(\tilde{q}_0)\tilde{q}_1)$. Just as before, this satisfies $\tilde{F}_2(\infty) = 0$. At $\tau = 0$, we find that

$$\dot{\tilde{F}}_2(0) = \frac{c_1}{2}\dot{\psi}_2(0)B, \quad (2.96)$$

where

$$B \equiv \int_0^\infty B(\tau)\psi_1^2(\tau)d\tau, \quad (2.97)$$

is the quantity of $O(1)$. From this, we find that the boundary condition (2.87) leads to

$$\lambda = -\frac{2}{B}e^{-2\tau_I}. \quad (2.98)$$

The factor B is evaluated to be $1/12$ in Appendix C.

Next we will evaluate the contribution of the region $\tau \in [0, \infty]$ to the action as follows:

$$\begin{aligned} S[q] &= S[q_0] + \frac{\delta S[q_0]}{\delta q_0}(\lambda q_1 + \dots) + \frac{1}{2}\frac{\delta^2 S[q_0]}{\delta q_0^2}(\lambda q_1 + \dots)^2 + \dots \\ &= S[q_0] + \frac{\lambda^2}{2}\int_0^\infty q_1 F_1 d\tau - \frac{\lambda}{2}\dot{q}_0(0)q_1(0) + \dots \end{aligned} \quad (2.99)$$

where we used the fact that the linear term in $\lambda q_1 + \dots$ vanishes due to the equation of motion and the last term is the sum of the surface terms. The first term on the left side is given by the following:

$$S[q_0] = \frac{1}{g^2} \left(\frac{1}{6} - \frac{1}{2}e^{-2\tau_I} \right). \quad (2.100)$$

The second term is of order of $\lambda^2 \sim e^{-4\tau_I}$, and is of next-to-leading order. The last term is evaluated as follows,

$$-\frac{\lambda}{2}\dot{q}_0(0)q_1(0) = -\frac{\lambda}{2} \left(-\frac{1}{g}e^{-\tau_I} \right) \frac{c_1}{2}\psi_2(0) \int_0^\infty \psi_1(\tau)^2 d\tau \simeq -\frac{e^{-2\tau_I}}{2g^2}. \quad (2.101)$$

Combining all contributions, we find that at the leading order of ϵg^2 ,

$$S^{(I\bar{I})} = 2S^{(I)} - \epsilon R + S_{\text{int}}^{(I\bar{I})}, \quad (2.102)$$

where $S_{\text{int}}^{(I\bar{I})}$ is the interaction term,

$$S_{\text{int}}^{(I\bar{I})} = -\frac{2}{g^2}e^{-R}. \quad (2.103)$$

We have denoted the distance between I and \bar{I} by $R = |\tau_I - \tau_{\bar{I}}| = 2\tau_{\bar{I}}$. In the same way, the $\bar{I}I$ configuration with a large separation R between the anti-valley-instanton and the valley-instanton is given by the following at the leading order of ϵg^2 :

$$S^{(\bar{I}I)} = 2S^{(I)} + \epsilon R + S_{\text{int}}^{(\bar{I}I)}, \quad (2.104)$$

where $S_{\text{int}}^{(\bar{I}I)}$ is the interaction term,

$$S_{\text{int}}^{(\bar{I}I)} = -\frac{2}{g^2} e^{-R}. \quad (2.105)$$

Finally, let us evaluate $\Delta[\varphi_R]$ in Eq.(2.27) and $\det'' D$ in Eq.(2.30). (Here we denote φ_α as φ_R .) We choose the eigenfunction of the second lowest eigenvalue of $D(\tau, \tau')$ as the gauge fixing function $\mathcal{G}(\tau)$. This choice enables us to be completely free from the difficulties that come from the quasi zero mode. The configuration on the $I\bar{I}$ valley constructed above is

$$q_R^{(I\bar{I})}(\tau) \underset{\epsilon g^2 \rightarrow 0}{\overset{R \rightarrow \infty}{=}} \theta(-\tau) q_0^{(I)}(\tau; \tau_I) + \theta(\tau) q_0^{(\bar{I})}(\tau; \tau_{\bar{I}}), \quad (2.106)$$

$$F^{(I\bar{I})}(\tau) \underset{\epsilon g^2 \rightarrow 0}{\overset{R \rightarrow \infty}{=}} \theta(-\tau) \lambda \dot{q}_0^{(I)}(\tau; \tau_I) - \theta(\tau) \lambda \dot{q}_0^{(\bar{I})}(\tau; \tau_{\bar{I}}), \quad (2.107)$$

where $\tau_{\bar{I}} = -\tau_I$ and λ is given by Eq.(2.98). Therefore, we find

$$\int \frac{\partial q_R^{(I\bar{I})}(\tau)}{\partial R} G(\tau) d\tau \underset{\epsilon g^2 \rightarrow 0}{\overset{R \rightarrow \infty}{=}} \frac{1}{\sqrt{12g^2}}. \quad (2.108)$$

The gauge fixing function behaves as follows:

$$(2.109)$$

$$\mathcal{G}(\tau) \underset{\epsilon g^2 \rightarrow 0}{\overset{R \rightarrow \infty}{=}} \frac{\theta(-\tau) \dot{q}_0^{(I)}(\tau; \tau_I) + \theta(\tau) \dot{q}_0^{(\bar{I})}(\tau; \tau_{\bar{I}})}{\sqrt{\int (\theta(-\tau) \dot{q}_0^{(I)}(\tau; \tau_I) + \theta(\tau) \dot{q}_0^{(\bar{I})}(\tau; \tau_{\bar{I}}))^2 d\tau}}. \quad (2.110)$$

Consequently, we find

$$\int \frac{\partial q_R^{(I\bar{I})}(\tau)}{\partial \tau} \mathcal{G}(\tau) d\tau \underset{\epsilon g^2 \rightarrow 0}{\overset{R \rightarrow \infty}{=}} \sqrt{\frac{1}{3g^2}}. \quad (2.111)$$

Combining Eq.(2.108) and Eq.(2.111), $\Delta[\varphi_R]$ is evaluated as

$$\Delta[\varphi_R] \underset{\epsilon g^2 \rightarrow 0}{\overset{R \rightarrow \infty}{=}} \frac{1}{6g^2}. \quad (2.112)$$

Note that the factorization property at $R \rightarrow \infty$ holds: The above $\Delta[\varphi_R]$ coincides with the product of the Jacobian (2.64) of the valley-instanton and that of the anti-valley-instanton.

The one-loop determinant can be evaluated from the following equation:

$$\frac{\mathcal{J}}{\sqrt{\det''(-\partial_\tau^2 + V_{I\bar{I}}'')}} = \frac{\mathcal{J}}{\sqrt{\det(-\partial_\tau^2 + \omega_+^2)}} \sqrt{\frac{\det(-\partial_\tau^2 + \omega_+)}{\det''(-\partial_\tau^2 + V_{I\bar{I}}'')}}, \quad (2.113)$$

where $V_{I\bar{I}} = V(q_R^{(I\bar{I})})$. Under the above choice of $\mathcal{G}(\tau)$, the following relation holds:

$$\frac{\det''(-\partial_\tau^2 + V_{I\bar{I}}'')}{\det(-\partial_\tau^2 + \omega_+^2)} \xrightarrow{R \rightarrow \infty} \frac{\det'(-\partial_\tau^2 + V_I'')}{\det(-\partial_\tau^2 + \omega_+^2)} \cdot \frac{\det'(-\partial_\tau^2 + V_{\bar{I}}'')}{\det(-\partial_\tau^2 + \omega_-^2)}, \quad (2.114)$$

where $V_I (V_{\bar{I}})$ is the potential of the (anti-)valley-instanton background. From the valley-instanton results (2.65) and (2.66), we find

$$\frac{\mathcal{J}}{2\pi\sqrt{\det''(-\partial_\tau^2 + V_{I\bar{I}}'')}} \Delta[\varphi_R] \xrightarrow[\epsilon g^2 \rightarrow 0]{R \rightarrow \infty} \Upsilon \times \frac{e^{-T/2}}{\pi g^2}, \quad (2.115)$$

where $\Upsilon \equiv \lim_{\epsilon g^2 \rightarrow 0} \Upsilon_\pm$.

For the $I\bar{I}$ valley, we find the following in the similar manner:

$$\Delta[\varphi_R] \xrightarrow[\epsilon g^2 \rightarrow 0]{R \rightarrow \infty} \frac{1}{6g^2}. \quad (2.116)$$

$$\frac{\mathcal{J}}{2\pi\sqrt{\det''(-\partial_\tau^2 + V_{I\bar{I}}'')}} \Delta[\varphi_R] \xrightarrow[\epsilon g^2 \rightarrow 0]{R \rightarrow \infty} \Upsilon \times \frac{e^{-T/2}}{\pi g^2}. \quad (2.117)$$

3 $I\bar{I}$ valley and $\bar{I}I$ valley

Consider the transition amplitudes between one of the local minima of the potential and itself:

$$Z = \begin{cases} \lim_{T \rightarrow \infty} \langle q_+ | e^{-HT} | q_+ \rangle, \\ \lim_{T \rightarrow \infty} \langle q_- | e^{-HT} | q_- \rangle. \end{cases} \quad (3.1)$$

In general, all configurations made of the same number of I and \bar{I} are relevant for the amplitude, but we will first evaluate this against the background of the $I\bar{I}$ and $\bar{I}I$ valleys. Due to the restriction of the background, only a few states in the Hilbert space can be treated in an appropriate way, but the essence of the physics in the topologically trivial sector already appears in this background. The general configurations will be taken into account in Section 4.1. Due to the boundary condition, the $I\bar{I}$ valley is relevant for the former amplitude of Eq.(3.1), and the $\bar{I}I$ valley for the latter one.

As was shown in Section 2.1, except for the collective coordinates of the valleys, the path integral in the background of these valleys can be performed with Gaussian integrals. Then we obtain

$$\begin{aligned} Z &= \lim_{T \rightarrow \infty} \mathcal{J} \int \int \frac{d\tau_0 dR}{2\pi\sqrt{\det'' D}} \Delta[\varphi_R] e^{-S(R)} \\ &= \lim_{T \rightarrow \infty} |\Psi(0)|^2 \times \frac{e^{-T/2}}{\pi g^2} \int_0^T dR (T - R) e^{-\tilde{S}(R)/g^2}, \end{aligned} \quad (3.2)$$

where R is the collective coordinate of the valley corresponding to the relative distance between the valley-instanton and the anti-valley-instanton,³ and we have abbreviated $\Psi(0; \omega)$ with $\omega = 1$ as $\Psi(0)$. (Namely, $\Psi(0) = (1/\pi)^{1/4}$.) The factor before the integration of R comes from Eqs.(2.115) and (2.117). Here we have also performed the integration of the collective coordinate of the translational symmetry. Since the configurations in the valleys must be one of the minima of the potential at $\tau = \pm T/2$, a non-trivial factor $(T - R)$ results from the integration. As was shown in the previous section, the action of the valley behaves as follows:

$$\tilde{S}(R) = \begin{cases} \sigma R^2 & \text{at } R \rightarrow 0 ; \\ \frac{1}{3} - 2e^{-R} - \epsilon g^2 R & \text{at } R \rightarrow \infty, \end{cases} \quad (3.3)$$

for the $I\bar{I}$ valley, and

$$\tilde{S}(R) = \begin{cases} \sigma R^2 & \text{at } R \rightarrow 0 ; \\ \frac{1}{3} - 2e^{-R} + \epsilon g^2 R & \text{at } R \rightarrow \infty, \end{cases} \quad (3.4)$$

for the $\bar{I}I$ valley. Here σ is a constant which will be determined later.

For both of the valleys, the configuration at $R = 0$ is the vacuum and at $R \sim \infty$ the well-separated valley-instanton–anti-valley-instanton pair. These configurations are smoothly connected along the valleys. In the following, we will show that these geometrical structures in the configuration space lead to the nontrivial structure of the quantum physics in the topological trivial sector.

3.1 The $\epsilon = 0$ case

First, let us consider the case of $\epsilon = 0$. We will now carry out the Borel transformation of the path-integral, which was first suggested in Ref.[15] and later developed on the basis of the valley method [16]. Changing the integration variable R to $t = \tilde{S}(R)$, the transition amplitude becomes

$$Z = \lim_{x \rightarrow 1/3} |\Psi(0)|^2 \times \frac{e^{-T/2}}{\pi g^2} \int_{C_V} dt F(t) e^{-t/g^2}, \quad (3.5)$$

³Strictly speaking, only when $R \gg 1$, R coincides with the relative distance between the valley-instanton and anti-valley-instanton. For other values of R , we define R so as to satisfy Eqs.(3.2)-(3.4).

where $x = \tilde{S}(T) = 1/3 - 2e^{-T}$, $C_V = [0, x]$. From Eq.(3.3), it is found that $F(t)$ behaves as follows:

$$F(t) = \begin{cases} \frac{T}{\sqrt{4\sigma t}} & \text{for } t \rightarrow 0; \\ \frac{1}{1/3 - t} \ln \left(\frac{1/3 - t}{1/3 - x} \right) & \text{for } t \rightarrow 1/3. \end{cases} \quad (3.6)$$

To obtain the full form of $F(t)$, a detailed analysis of the valley is needed. Instead, we will simply assume that the form of $F(t)$ is as follows:

$$F(t) = \frac{f(t)}{\sqrt{4\sigma t(1/3 - t)}} \ln \left(\frac{1/3 - t}{1/3 - x} \right), \quad (3.7)$$

where $f(t)$ is a function that satisfies

$$f(0) = -\frac{T}{3 \ln(1 - 3x)}, \quad f(1/3) = \sqrt{\frac{4\sigma}{3}}. \quad (3.8)$$

The integral (3.5) contains both the perturbative contribution at $t \sim 0$ and the non-perturbative one at $t \sim 1/3$. To separate the perturbative and non-perturbative contributions, we can deform the contour C_V to the sum of C_P and C_{NP} as is shown in Fig.8. Then the amplitude becomes

$$\begin{aligned} Z &= \lim_{x \rightarrow 1/3} |\Psi(0)|^2 \times \frac{e^{-T/2}}{\pi g^2} \int_{C_P} dt F(t) e^{-t/g^2} \\ &\quad + \lim_{x \rightarrow 1/3} |\Psi(0)|^2 \times \frac{e^{-T/2}}{\pi g^2} \int_{C_{NP}} dt F(t) e^{-t/g^2}. \end{aligned} \quad (3.9)$$

Note that there is a significant resemblance between the first term on the right-hand side and the formal Borel summation of the perturbation series. *Therefore, we identify the first term of Eq.(3.9) as the formal Borel-summation of the perturbative series, and the second term as the non-perturbative contribution.* As we shall see, this decomposition naturally explains the interplay between them. For simplicity, we denote the first term as Z_P and the second as Z_{NP} .

According to the above assumption, the first term of Eq.(3.9) is given by the ordinary perturbation theory. Schematically, it is given by

$$Z_P = \lim_{T \rightarrow \infty} |\Psi(0)|^2 \times e^{-T/2} \left(1 + P_0(g^2) + P_1(g^2)T + P_2(g^2)T^2 + \dots \right), \quad (3.10)$$

where $P_i(g^2)$ ($i = 0, 1, 2, \dots$) are polynomials starting with g^2 -terms. In order to avoid contradicting the assumption, the parameter σ is determined as

$$\sigma = \frac{1}{4\pi g^2 T^2}. \quad (3.11)$$

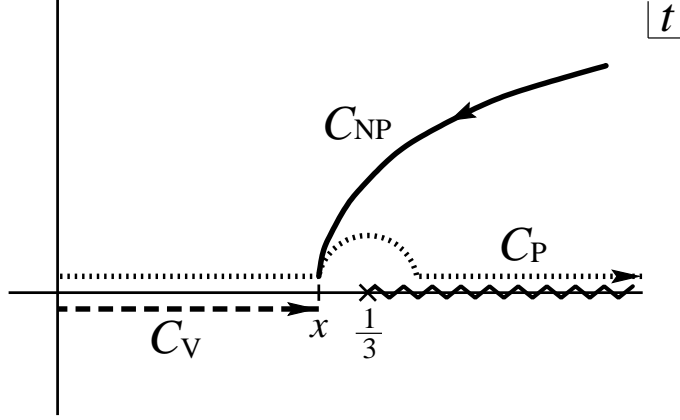


Figure 8: Deformation of the contour C_V to the sum of C_P and C_{NP} .

The second term of Eq.(3.9) can be evaluated as follows,

$$\begin{aligned}
Z_{NP} &= \lim_{x \rightarrow 1/3} |\Psi(0)|^2 \times \frac{e^{-T/2}}{\pi g^2} \int_{\infty e^{i\chi}}^x dt F(t) e^{-t/g^2} \\
&= \lim_{x \rightarrow 1/3} |\Psi(0)|^2 \times \frac{e^{-T/2-1/3g^2}}{\pi g^2} \\
&\quad \times \int_{x-1/3}^{\infty e^{i\chi}} ds \frac{f(1/3+s)}{\sqrt{4\sigma(1/3+s)s}} \ln\left(\frac{-s}{1/3-x}\right) e^{-s/g^2} \\
&= \lim_{x \rightarrow 1/3} |\Psi(0)|^2 \times \frac{e^{-T/2-1/3g^2}}{\pi g^2} \int_{x-1/3}^{\infty e^{i\chi}} ds \frac{1}{s} \ln\left(\frac{-s}{1/3-x}\right) e^{-s/g^2} + \dots \\
&= \lim_{T \rightarrow \infty} |\Psi(0)|^2 \times \frac{e^{-T/2-1/3g^2}}{\pi g^2} \left[\frac{T^2}{2} - T \left\{ \gamma + \ln\left(-\frac{2}{g^2}\right) \right\} \right. \\
&\quad \left. + \frac{\Gamma''(1)}{2} + \gamma \ln\left(-\frac{2}{g^2}\right) + \frac{1}{2} \left\{ \ln\left(-\frac{2}{g^2}\right) \right\}^2 + \dots \right], \tag{3.12}
\end{aligned}$$

where $s = t - 1/3$, and χ is the angle of the path C_{NP} at infinity. In the above we have retained only the leading contribution in g^2 . Therefore, we obtain the following equation.

$$\begin{aligned}
Z &= Z_P + Z_{NP} \\
&= \lim_{T \rightarrow \infty} \sum_{\varsigma=\pm 1} \frac{|\Psi(0)|^2}{2} \left[1 + P_0(g^2) \right. \\
&\quad \left. + \alpha^2 \left\{ \frac{\Gamma''(1)}{2} + \gamma \ln\left(-\frac{2}{g^2}\right) + \frac{1}{2} \left\{ \ln\left(-\frac{2}{g^2}\right) \right\}^2 + \dots \right\} \right]
\end{aligned}$$

$$\begin{aligned} & \times e^{-T/2} \left[1 + T \left\{ \bar{P}_1(g^2) + \varsigma \alpha - \alpha^2 \left\{ \gamma + \ln \left(-\frac{2}{g^2} \right) + \dots \right\} \right\} \right. \\ & \left. + \frac{T^2}{2} \left\{ \bar{P}_2(g^2) + \alpha^2 \{1 + \dots\} \right\} + \dots \right], \end{aligned} \quad (3.13)$$

where $\alpha = e^{-1/6g^2}/\sqrt{\pi g^2}$ and $\bar{P}_i(g^2) = P_i(g^2)/(1 + P_0(g^2))$ ($i = 1, 2$).

To obtain the non-perturbative corrections, we can compare this with the following:

$$\begin{aligned} Z &= \lim_{T \rightarrow \infty} \langle q_+ | e^{-HT} | q_+ \rangle \\ &= \lim_{T \rightarrow \infty} \sum_{\varsigma=\pm 1} |\Psi_\varsigma(q_+)|^2 e^{-E_\varsigma(\epsilon=0, N_+=0)T} + \dots, \end{aligned} \quad (3.14)$$

where $E_\varsigma(\epsilon = 0, N_+ = 0), \varsigma = \pm 1$ are the energies of the first two lowest states and $\Psi_\varsigma(q_+)$ are the values of the normalized wave functions of the states at $q = q_+$. These states are perturbatively degenerated as,

$$E_\varsigma(\epsilon = 0, N_+ = 0) = \frac{1}{2} + O(g^2), \quad (3.15)$$

and the degeneracy is resolved by the tunneling effect. The non-perturbative corrections for these energies are thus found as

$$E_{\varsigma, \text{NP}}(\epsilon = 0, N_+ = 0) = \varsigma \alpha + \alpha^2 \left\{ \gamma + \ln \left(-\frac{2}{g^2} \right) \right\}, \quad (3.16)$$

where $\varsigma = \pm 1$. In addition, we obtain the non-perturbative correction for the values of the wave functions at $q = q_+$:

$$\begin{aligned} & |\Psi_\varsigma(q_+)|_{\text{NP}}^2 \\ &= \frac{\alpha^2}{2} |\Psi(0)|^2 \left\{ \frac{\Gamma''(1)}{2} + \gamma \ln \left(-\frac{2}{g^2} \right) + \frac{1}{2} \left\{ \ln \left(-\frac{2}{g^2} \right) \right\}^2 \right\}. \end{aligned} \quad (3.17)$$

Note that there are imaginary terms in Eqs.(3.16) and (3.17). As will be explained in Section 3.3, this is because that the perturbative corrections for them are non-Borel-summable.

3.2 The $\epsilon \neq 0$ case

3.2.1 $I\bar{I}$ valley

As was seen in Fig.4, the action of the $I\bar{I}$ valley $\tilde{S}(R)$ is not an invertible function of R . Then, if we change the integral variable R to $t = \tilde{S}(R)$ in Eq.(3.2), there arises an apparent singularity. To avoid this, we add $\epsilon g^2 \tilde{S}_1(R)$

$$\epsilon g^2 \tilde{S}_1 = \epsilon g^2 \int d\tau \tilde{q}_R(\tau) \quad (3.18)$$

from the action and define the new integral variable t as

$$t = \tilde{S}(R) + \epsilon g^2 \tilde{S}_1(R) = \tilde{S}_0(R). \quad (3.19)$$

Here $\tilde{q}_R(\tau)$ is the $I\bar{I}$ valley with R . The function $\tilde{S}_0(R)$ is invertible, so this causes no apparent singularity. When $\epsilon \rightarrow 0$, this definition of t smoothly coincides with that in the case of $\epsilon = 0$, since $\epsilon g^2 \tilde{S}_1(R)$ is zero when $\epsilon = 0$.

The remaining analysis is an extension of the case of $\epsilon = 0$. Using t , the transition amplitude is rewritten as

$$Z = \lim_{x \rightarrow 1/3} |\Psi(0)|^2 \times \frac{e^{-T/2}}{\pi g^2} \int_{C_V} dt F(t) e^{-t/g^2}, \quad (3.20)$$

where $x = \tilde{S}_0(T) = 1/3 - 2e^{-T}$ and $C_V = [0, x]$. As $\tilde{S}_0(R)$ behaves as

$$\tilde{S}_0(R) = \begin{cases} \sigma R^2 & \text{for } R \rightarrow 0; \\ \frac{1}{3} - 2e^{-R} & \text{for } R \rightarrow \infty, \end{cases} \quad (3.21)$$

then $F(t)$ satisfies

$$F(t) = \begin{cases} \frac{T}{\sqrt{4\sigma t}} & \text{for } t \rightarrow 0; \\ \frac{1}{1/3 - t} \left(\frac{1/3 - t}{2} \right)^{-\epsilon} \ln \left(\frac{1/3 - t}{1/3 - x} \right) & \text{for } t \rightarrow 1/3. \end{cases} \quad (3.22)$$

We assume the form of $F(t)$ to be

$$F(t) = \frac{f(t)}{\sqrt{4\sigma t}(1/3 - t)} \left(\frac{1/3 - t}{2} \right)^{-\epsilon} \ln \left(\frac{1/3 - t}{1/3 - x} \right), \quad (3.23)$$

where $f(t)$ is a function which satisfies

$$f(0) = -\frac{6^{-\epsilon} T}{3 \ln(1 - 3x)}, \quad f(1/3) = \sqrt{4\sigma/3}. \quad (3.24)$$

We can identify the perturbative contribution and non-perturbative contribution in the same manner of the case of $\epsilon = 0$, and we find the non-perturbative contribution to be as follows.

• $\epsilon \notin \mathbf{Z}$

$$\begin{aligned} Z_{\text{NP}} &= \lim_{T \rightarrow \infty} |\Psi(0)|^2 \times \frac{e^{-T/2-1/3g^2}}{\pi g^2} \left[\left(-\frac{2}{g^2} \right)^\epsilon \Gamma(-\epsilon) T \right. \\ &\quad - \left(-\frac{2}{g^2} \right)^\epsilon \left\{ \ln \left(-\frac{2}{g^2} \right) \Gamma(-\epsilon) - \Gamma'(-\epsilon) \right\} \\ &\quad \left. + \sum_{N_-=0}^{\infty} \left(\frac{2}{g^2} \right)^{N_-} \frac{e^{-(N_- - \epsilon)T}}{N_-!(N_- - \epsilon)^2} \right]. \end{aligned} \quad (3.25)$$

- $\epsilon = \mathcal{N} \geq 0, \mathcal{N} \in \mathbf{Z}$

$$\begin{aligned}
Z_{\text{NP}} &= \lim_{T \rightarrow \infty} |\Psi(0)|^2 \times \frac{e^{-T/2-1/3g^2}}{\pi g^2} \left[\left(\frac{2}{g^2} \right)^{\mathcal{N}} \frac{1}{\mathcal{N}!} \frac{T^2}{2} \right. \\
&\quad - \left(\frac{2}{g^2} \right)^{\mathcal{N}} \left\{ \ln \left(-\frac{2}{g^2} \right) - \psi(\mathcal{N}+1) \right\} \frac{T}{\mathcal{N}!} \\
&\quad + \left(\frac{2}{g^2} \right)^{\mathcal{N}} \frac{1}{\mathcal{N}!} \left\{ \frac{1}{2} \left\{ \ln \left(-\frac{2}{g^2} \right) \right\}^2 - \psi(\mathcal{N}+1) \ln \left(-\frac{2}{g^2} \right) \right. \\
&\quad \left. + \frac{\Gamma''(1)}{2} - \gamma \sum_{k=1}^{\mathcal{N}} \frac{1}{k} + \sum_{k=1, l=1, k \geq l}^{\mathcal{N}} \frac{1}{k l} \right\} \\
&\quad \left. + \sum_{N_- = 0, N_- \neq \mathcal{N}}^{\infty} \left(\frac{2}{g^2} \right)^{N_-} \frac{e^{-(N_- - \mathcal{N})T}}{N_-! (N_- - \mathcal{N})^2} \right], \tag{3.26}
\end{aligned}$$

where $\psi(z) \equiv d \log \Gamma(z) / dz$ is the psi function.

The result (3.25) leads to the following for the non-perturbative contribution to the perturbative ground state at $q = q_+$,

$$E_{\text{NP}}^{(+)}(\epsilon, N_+ = 0) = -\alpha^2 \left(-\frac{2}{g^2} \right)^\epsilon \Gamma(-\epsilon). \tag{3.27}$$

Furthermore, the non-perturbative contribution to the normalized wave function of this state is found to be the following

$$\begin{aligned}
|\Psi(q_+)|_{\text{NP}}^2 &= -\alpha^2 |\Psi(0)|^2 \left(-\frac{2}{g^2} \right)^\epsilon \\
&\quad \times \left\{ \ln \left(-\frac{2}{g^2} \right) \Gamma(-\epsilon) - \Gamma'(-\epsilon) \right\}. \tag{3.28}
\end{aligned}$$

The case where $\epsilon = \mathcal{N} \geq 0, \mathcal{N} \in \mathbf{Z}$ requires further discussion, which will be given in the next section.

3.2.2 $\bar{I}I$ valley

The evaluation of the amplitude in the background of the $\bar{I}I$ valley can be performed in the same manner as that of the $I\bar{I}$ valley. The non-perturbative part of the amplitude is the following:

$$\begin{aligned}
Z_{\text{NP}} &= \lim_{T \rightarrow \infty} |\Psi(0)|^2 \times \frac{e^{(\epsilon-1/2)T-1/3g^2}}{\pi g^2} \left[\left(-\frac{2}{g^2} \right)^{-\epsilon} \Gamma(\epsilon) T \right. \\
&\quad \left. - \left(-\frac{2}{g^2} \right)^{-\epsilon} \left\{ \ln \left(-\frac{2}{g^2} \right) \Gamma(\epsilon) - \Gamma'(\epsilon) \right\} \right]
\end{aligned}$$

$$+ \sum_{N_+=0}^{\infty} \left(\frac{2}{g^2} \right)^{N_+} \frac{e^{-(N_++\epsilon)T}}{N_+!(N_++\epsilon)^2} \Big]. \quad (3.29)$$

From the above equation, we find the following non-perturbative contributions for the perturbative ground state at $q = q_-$:

$$E_{\text{NP}}^{(-)}(\epsilon, N_- = 0) = -\alpha^2 \left(-\frac{2}{g^2} \right)^{-\epsilon} \Gamma(\epsilon), \quad (3.30)$$

$$\begin{aligned} |\Psi(q_-)|_{\text{NP}}^2 &= -\alpha^2 |\Psi(0)|^2 \left(-\frac{2}{g^2} \right)^{-\epsilon} \\ &\quad \times \left\{ \ln \left(-\frac{2}{g^2} \right) \Gamma(\epsilon) - \Gamma'(\epsilon) \right\}. \end{aligned} \quad (3.31)$$

3.3 Singularity of the Borel plane

An immediate consequence of our decomposition of the perturbative and non-perturbative contribution is

$$\text{Im}Z_{\text{P}} + \text{Im}Z_{\text{NP}} = 0. \quad (3.32)$$

This is because $Z = Z_{\text{P}} + Z_{\text{NP}}$ is real. Thus, this simple equation explains why the imaginary part of the formal Borel summation of the perturbation series is canceled by that of the non-perturbative contribution. At the same time, it also shows that the nonzero imaginary part of the non-perturbative contribution is a necessary and sufficient condition for the non-Borel-summability of the perturbative expansion.

Furthermore, assuming that $f(t)$ in Eqs.(3.7) and (3.23) has the following form:

$$f(t) = \tilde{f}(t, g^2/t), \quad (3.33)$$

where $\tilde{f}(t, s)$ is an analytic function of t for small s , we can predict the large order behavior of the perturbative contribution. To this end, we examine the analyticity of $Z_{\text{P}}(g^2)$ in the complex g^2 -plane. Let θ denote the phase of g^2 , $g^2 = |g^2|e^{i\theta}$. When the phase of g^2 changes to 2π , the contour of $Z_{\text{P}}(g^2)$ changes as Fig.9. Thus we obtain

$$Z_{\text{P}}(g^2 e^{2\pi i}) = Z_{\text{P}}(g^2) + \lim_{x \rightarrow 1/3} |\Psi(0)|^2 \times \frac{e^{-T/2}}{\pi g^2} \int_C dt F(t) e^{-t/g^2}, \quad (3.34)$$

where the contour C is given in Fig.10. Therefore, $Z_{\text{P}}(g^2)$ has a cut on the real axis in the complex g^2 -plane. This is the only singularity near the origin.

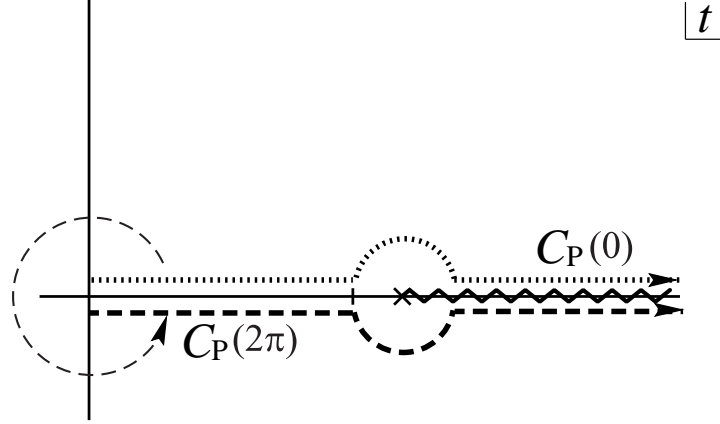


Figure 9: The change of the contour $C_P(\theta)$ of $Z_P(|g^2|e^{i\theta})$ as θ is changed from zero to 2π .

Thus the dispersion relation becomes

$$\begin{aligned}
Z_P(g^2) &= \frac{1}{2\pi i} \oint_{C_{g^2}} dz \frac{Z_P(z)}{z - g^2} \\
&= \frac{1}{\pi} \int_0^\infty dz \frac{\text{Im}Z_P(z)}{z - g^2} + \dots \\
&= -\frac{1}{\pi} \int_0^\infty dz \frac{\text{Im}Z_{\text{NP}}(z)}{z - g^2} + \dots \\
&= -\frac{1}{\pi} \sum_{n=0}^\infty \int_0^\infty dz \frac{\text{Im}Z_{\text{NP}}(z)}{z^{n+1}} g^{2n} + \dots,
\end{aligned} \tag{3.35}$$

where C_{g^2} is the contour that circles around $z = g^2$, and we have neglected the contribution from the singularity far from the origin. Thus, the following large order behavior of $Z_P(g^2)$ is predicted:

$$\begin{aligned}
Z_P(g^2) &= \sum_{m=1}^\infty c_m g^{2m}, \\
c_m &\stackrel{m \rightarrow \infty}{=} -\frac{1}{\pi} \int_0^\infty dg^2 \frac{\text{Im}Z_{\text{NP}}(g^2)}{g^{2m+2}}.
\end{aligned} \tag{3.36}$$

Rewriting this in terms of the energies and the wave functions, we find the perturbative contribution to the energy E_P and to the wave function $|\Psi(q_\pm)|_P^2$ as follows,

$$\begin{aligned}
E_P(g^2) &= \sum_{m=0}^\infty e_m g^{2m}, \\
e_m &\stackrel{m \rightarrow \infty}{=} -\frac{1}{\pi} \int_0^\infty dg^2 \frac{\text{Im}E_{\text{NP}}(g^2)}{g^{2m+2}}.
\end{aligned} \tag{3.37}$$

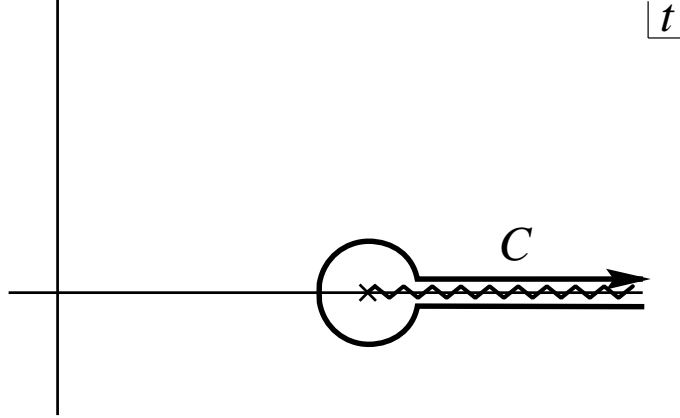


Figure 10: The contour of integral

and

$$\begin{aligned}
 |\Psi(q_{\pm})|_{\text{P}}^2 &= \sum_{m=0}^{\infty} w_m g^{2m}, \\
 w_m &\stackrel{m \rightarrow \infty}{=} -\frac{1}{\pi} \int_0^{\infty} dg^2 \frac{\text{Im}|\Psi(q_{\pm})|_{\text{NP}}^2}{g^{2m+2}}.
 \end{aligned} \tag{3.38}$$

Detailed tests of these predictions are performed in Section 5.

3.4 Bogomolny's trick

In the early eighties, Bogomolny [5] suggested a procedure to calculate the tunneling effect beyond the dilute-gas approximation. He suggested that by the formal analytic continuation of the coupling constant which changes the force between instantons from attractive to repulsive, the instantons in the topologically trivial sector become meaningful and their contributions can be separated from the perturbation theory. The same trick was used by Zinn-Justin [14] to obtain the energy levels of the excited states. Our identification of the non-perturbative contribution is a precise realization of Bogomolny's suggestion, and it provides an explicit justification for this trick.

To see this, let us examine $Z_{\text{NP}}(g^2)$ in the complex g^2 -plane. As is shown in Fig.11, if we perform the analytic continuation of $Z_{\text{NP}}(|g^2|e^{i\theta})$ from $\theta = 0$ to $\theta = \pi$, the contour for $Z_{\text{NP}}(|g^2|e^{i\theta})$ changes from $C_{\text{NP}}(0)$ to $C_{\text{NP}}(\pi)$. And in the weak coupling limit the integral of $C_{\text{NP}}(\pi)$ can be well-approximated by that of C_V , because the dominant contribution of the integral comes from $t \sim x$. Therefore, in the case of $g^2 = |g^2|e^{i\pi}$ when the interaction between instantons is repulsive, $Z_{\text{NP}}(|g^2|e^{i\pi})$ coincides approximately with what Bogomolny suggested as a method of evaluation:

$$Z_{\text{NP}}(|g^2|e^{i\pi}) = Z(|g^2|e^{i\pi}). \tag{3.39}$$

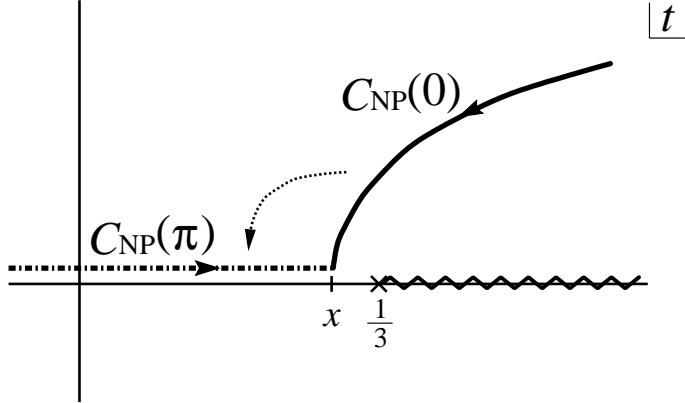


Figure 11: The change of the contour $C_{NP}(\theta)$ of $Z_{NP}(|g^2|e^{i\theta})$ as θ is changed from zero to π .

Note that the coincidence $Z_{NP}(g^2) = Z(g^2)$ does not hold for $\theta = 0$; while $Z_{NP}(g^2)$ could be complex, $Z(g^2)$ never possesses the imaginary part in this case. This is because a so-called Stokes phenomena occurs for $Z(g^2)$; the terms in $Z(g^2)$ which are negligible for $\theta = \pi$ become relevant for $\theta = 0$. Since the imaginary part of $Z_{NP}(g^2)$ is necessary to cancel the ambiguity of the Borel transform of the perturbation theory, the formal analytic continuation of $Z(g^2)$ which Bogomolny originally suggested should be replaced with the *real* analytic continuation of $Z_{NP}(g^2)$.

One can easily find that $Z_{NP}(g^2)$ has the same asymptotic expansion for $\theta = 0$ and $\theta = \pi$. Therefore, the asymptotic expansion of $Z_{NP}(g^2)$ with $\theta = 0$ can be obtained by the analytic continuation of the asymptotic expansion of $Z(g^2)$ with $\theta = \pi$. We will use this in the next section.

4 The multi valley

4.1 Multi valley calculus

In this section we will evaluate the partition function $Z = \lim_{T \rightarrow \infty} \text{Tr}(e^{-HT})$, by summing over those configurations made of several valley-instantons, by utilizing the knowledge of the valley-instantons and the interactions among them in Section 2, and applying the analytic continuation discussed in Section 3.4. This enables us to evaluate non-perturbative contributions to excited states as well as the ground state.

We will take a valley made of n -pairs of the valley-instanton and the anti-valley-instanton with periodic boundary condition. Since we perform the calculation for $g^2 = |g^2|e^{i\pi} < 0$, the force between the valley-instanton and the anti-valley-instanton becomes repulsive. Therefore, the configura-

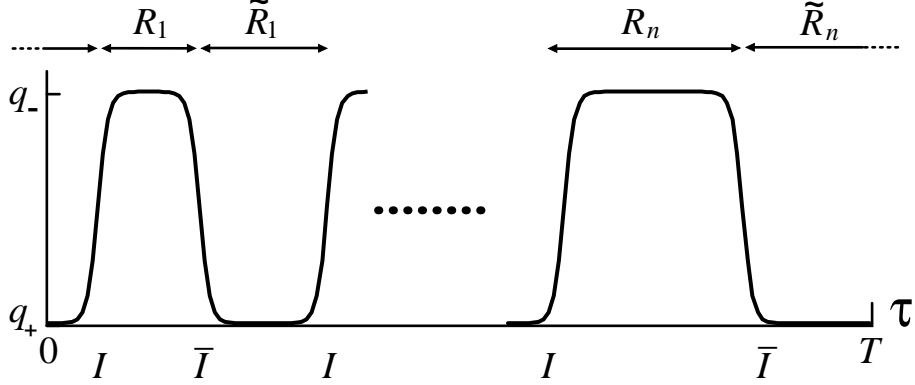


Figure 12: The collective coordinates R_i and \tilde{R}_i for n -pair configuration of valley-instanton and anti-valley-instanton.

tions with large separations between valley-instantons dominate. From the calculation of the action for one pair in Section 2, we find that the action of this n -pair configuration is given by the following:

$$S = \frac{n}{3g^2} - \epsilon \sum_{i=1}^n R_i - \frac{2}{g^2} \sum_{i=1}^n e^{-R_i} - \frac{2}{g^2} \sum_{i=1}^n e^{-\tilde{R}_i}, \quad (4.1)$$

where R_i is the distance between the i -th valley-instanton and the i -th anti-valley-instanton and \tilde{R}_i is the distance between the i -th anti-valley-instanton and the $(i+1)$ -th valley-instanton (mod n). (See Fig.12.) The expression (4.1) is valid when all the valley-instanton and the anti-valley-instantons are well-separated, that is, when $R_i, \tilde{R}_i \gg 1$.

We will write the sum of the contributions of the n -pairs of valley-instantons to the partition function Z for $n = 1 \sim \infty$ as follows,

$$Z_{\text{NP}} = \lim_{T \rightarrow \infty} \sum_{n=1}^{\infty} \alpha^{2n} J_n, \quad (4.2)$$

where the constant α contains the contributions of the Jacobian (2.64) and the R -independent part of the determinant (2.77), and is at the leading order in ϵg^2 ,

$$\alpha = \frac{\Delta}{\sqrt{2\pi\kappa}} e^{-S^{(I)}} = \frac{e^{-1/6g^2}}{g\pi^{1/2}}. \quad (4.3)$$

The term J_n is defined as follows:

$$\begin{aligned} J_n &= \frac{T}{n} \int_0^{\infty} \prod_{i=1}^n dR_i d\tilde{R}_i \delta \left(\sum_{i=1}^n (R_i + \tilde{R}_i) - T \right) \\ &\times \exp \left(\left(\epsilon - \frac{1}{2} \right) \sum_{i=1}^n R_i - \frac{1}{2} \sum_{i=1}^n \tilde{R}_i + \frac{2}{g^2} \sum_{i=1}^n e^{-R_i} + \frac{2}{g^2} \sum_{i=1}^n e^{-\tilde{R}_i} \right). \end{aligned} \quad (4.4)$$

Eq.(4.2) can be evaluated in a manner similar to that performed by Zinn-Justin for the ordinary instanton case [14]. First, we rewrite the δ -function as follows:

$$\delta \left(\sum_{i=1}^n (R_i + \tilde{R}_i) - T \right) = \frac{1}{2\pi i} \int_{-i\infty-\eta}^{i\infty-\eta} ds \exp \left(-sT + s \sum_{i=1}^n (R_i + \tilde{R}_i) \right), \quad (4.5)$$

where η is a positive real number. This allows factorization of the integrals over R_i and \tilde{R}_i in the following manner.

$$J_n = \frac{1}{2\pi i} \int_{-i\infty-\eta}^{i\infty-\eta} ds K_+(s)^n K_-(s)^n, \quad (4.6)$$

where $K_{\pm}(s)$ are,

$$\begin{aligned} K_{\pm}(s) &\equiv \int_0^{\infty} dR \exp \left(s_{\pm}R + \frac{2}{g^2} e^{-R} \right) \\ &= \left(-\frac{2}{g^2} \right)^{s_{\pm}} \Gamma(-s_{\pm}), \end{aligned} \quad (4.7)$$

$$s_+ \equiv s - \frac{1}{2}, \quad s_- \equiv s + \epsilon - \frac{1}{2}. \quad (4.8)$$

This leads to the following expression.

$$\begin{aligned} Z_{\text{NP}} &= \frac{T}{2\pi i} \int_{-i\infty-\eta}^{i\infty-\eta} ds e^{-Ts} \sum_{n=1}^{\infty} \frac{(\alpha^2 K_+(s) K_-(s))^n}{n} \\ &= -\frac{T}{2\pi i} \int_{-i\infty-\eta}^{i\infty-\eta} ds e^{-Ts} \ln(1 - \alpha^2 K_+(s) K_-(s)). \end{aligned} \quad (4.9)$$

By partial integration we find that

$$Z_{\text{NP}} = -\frac{1}{2\pi i} \int_{-i\infty-\eta}^{i\infty-\eta} ds e^{-Ts} \frac{\phi'(s)}{\phi(s)}, \quad (4.10)$$

where

$$\phi(s) \equiv 1 - \alpha^2 K_+(s) K_-(s). \quad (4.11)$$

From Eq.(4.7), we see that $\phi(s)$ has both poles and zeros in s . Denoting the poles by $s = E_0(N)$ and the zeros by $E(N)$, we find that

$$Z_{\text{NP}} = \sum_N e^{-E(N)T} - \sum_N e^{-E_0(N)T}. \quad (4.12)$$

The poles of $\phi(s)$ are given by the poles of the Γ -functions, $s = E_0^{(\pm)}(\epsilon, N_{\pm})$ defined as follows,

$$E_0^{(+)}(\epsilon, N_+) = \frac{1}{2} + N_+, \quad (4.13)$$

$$E_0^{(-)}(\epsilon, N_-) = -\epsilon + \frac{1}{2} + N_-, \quad (4.14)$$

which are the perturbative zeroth order energies of the N_{\pm} -th excited states around $q = q_{\pm}$, respectively. The subtraction in Eq.(4.12) corresponds to the fact that our Z_{NP} does not contain this zeroth order term (and in fact vanishes for $g = 0$). Therefore the full partition function has only the first term of Eq.(4.12). This means that the non-perturbative contributions to the energy spectrum are given by the zeros of $\phi(s)$:

$$\phi(s) = 0, \quad (4.15)$$

This equation is identical to the result obtained by the WKB approximation (this derivation is given in Appendix D).

Let us solve Eq.(4.15) in a perturbation of $\alpha \ll 1$. In the case when the poles of the Γ -functions of K_+ and K_- do not coincide, the solutions $s = E_0^{(\pm)}(\epsilon, N_{\pm}) + E_{\text{NP}}^{(\pm)}(\epsilon, N_{\pm})$ are found by a series expansion in α^2 :

$$E_{\text{NP}}^{(\pm)}(\epsilon, N_{\pm}) = \alpha^2 \frac{(-1)^{N_{\pm}+1}}{N_{\pm}!} \left(-\frac{2}{g^2} \right)^{\pm\epsilon+2N_{\pm}} \Gamma(\mp\epsilon - N_{\pm}) + O(\alpha^4). \quad (4.16)$$

The result (4.16) may diverge depending on ϵ and N_{\pm} . In fact, the poles occur when the argument of the Γ -functions is zero or an negative integer. This happens when the zeroth order energies of the states around q_+ and q_- are degenerate, which is allowed when $\epsilon = \mathcal{N}$ ($\mathcal{N} \in \mathbf{Z}$). In fact, these divergences in $E_{\text{NP}}^{(\pm)}(\epsilon, N_{\pm})$ are caused by the confluence of the corresponding poles of the Γ functions in K_+ and K_- . In cases where this happens, we need to use a different expansion scheme in α , $E(N) = E_0(N) + \alpha\rho_1 + \alpha^2\rho_2 + O(\alpha^3)$. The zeroth order term $E(N)$ is chosen so that the arguments of the Γ functions in K_{\pm} are zero or a negative integer $-N_{\pm}$ at the same time, which means

$$E_0(N_{\pm}) = \frac{1}{2} + N_{\pm} = -\epsilon + \frac{1}{2} + N_{\pm}. \quad (4.17)$$

This situation is illustrated in Fig.13. Straightforward calculation yields the following non-perturbative correction $E_{\varsigma, \text{NP}}(\epsilon, N_+)$ to the energy levels:

$$E_{\varsigma, \text{NP}}(\epsilon, N_+) = \varsigma \alpha \sqrt{\frac{1}{N_+! N_-!} \left(\frac{2}{g^2} \right)^{N_+ + N_-}} + \frac{\alpha^2}{2} \frac{1}{N_+! N_-!} \left(\frac{2}{g^2} \right)^{N_+ + N_-} \left[2 \ln \left(-\frac{2}{g^2} \right) - \psi(N_+ + 1) - \psi(N_- + 1) \right], \quad (4.18)$$

where $\varsigma = \pm 1$ and $N_- = N_+ + \epsilon = N_+ + \mathcal{N}$. The plus and the minus signs in the expression (4.18) correspond to two (approximate) linear combinations of the perturbative states in the left and right well with the same zeroth order energy. This situation is analogous to the lifting of the degeneracy by the

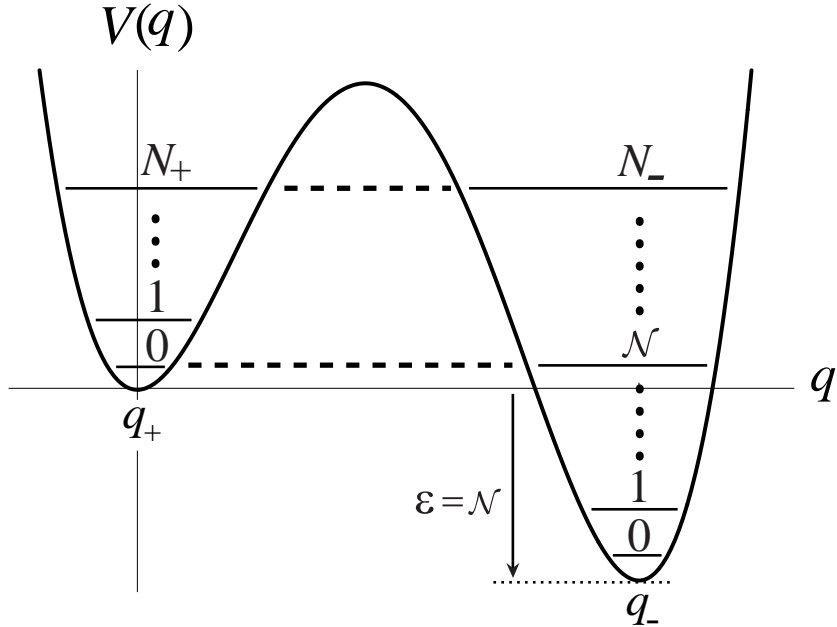


Figure 13: The potential $V(q)$ and the zeroth order eigenstates when Eq.(4.17) is satisfied.

instanton contribution for the symmetric double-well potential. (In fact, in the limit $\epsilon \rightarrow 0$ the ordinary instanton result for the energy splitting between the ground state and the first excited state is recovered.)

The non-perturbative contributions to the energy eigenvalue obtained here contain both a real part and an imaginary part. As discussed in the previous section the imaginary part is related to the large order behaviour of the perturbative series. We will confirm this in the following section by directly calculating the perturbative coefficients and comparing them with the prediction of the valley method. The real part of the energy needs further consideration: Normally the non-perturbative contribution is obscured by the perturbative contribution. The quantities which receive only a non-perturbative contribution provide a meaningful test of the non-perturbative effect, while other quantities do not provide such a test. We will discuss such a non-renormalization theorem in Section 6, and then using that result we will test the real part of the energy expression in Section 7.

4.2 $II\bar{I}$ valley and $\bar{I}I$ valley revisited

Before proceeding to the various tests of the result in Section 4.1, it is instructive to go back to the $II\bar{I}$ and $\bar{I}I$ valleys and compare the result of Section 3 with that of Section 4.1. If we compare Eq.(3.16) with Eq.(4.18), and

Eqs.(3.27) and (3.30) with Eq.(4.16), it will be seen that there is a complete agreement between them.

In Section 3, we did not evaluate the non-perturbative contribution to the perturbative ground state at $q = q_+$ in the case of $\epsilon = \mathcal{N} > 0$, $\mathcal{N} \in \mathbf{Z}$. The reason is that in this case the ground state is degenerate with the perturbative \mathcal{N} -th excited state at $q = q_-$, thus the mixing of the states should be taken into account. Without knowledge of the mixing, the non-perturbative correction to the energy levels cannot be uniquely determined.⁴

We, however, find that the result (3.26) is consistent with the result (4.18) if the non-perturbative contribution of the perturbative ground state at $q = q_+$ satisfies the following relations:

$$E_{\varsigma, \text{NP}}(\epsilon, N_+ = 0) = \varsigma \alpha \sqrt{\frac{1}{\mathcal{N}!} \left(\frac{2}{g^2}\right)^{\mathcal{N}}} + \frac{\alpha^2}{2} \frac{1}{\mathcal{N}!} \left(\frac{2}{g^2}\right)^{\mathcal{N}} \left[2 \ln \left(-\frac{2}{g^2}\right) - \psi(1) - \psi(\mathcal{N} + 1) \right], \quad (4.19)$$

$$|\Psi_{\varsigma}(q_+)|_{\text{NP}}^2 = \varsigma \alpha \frac{|\Psi(0)|^2}{4} \sqrt{\frac{1}{\mathcal{N}!} \left(\frac{2}{g^2}\right)^{\mathcal{N}}} (\psi(1) - \psi(\mathcal{N} + 1)) + \alpha^2 \frac{|\Psi(0)|^2}{2} \left(\frac{2}{g^2}\right)^{\mathcal{N}} \frac{1}{\mathcal{N}!} \left[-\ln \left(-\frac{2}{g^2}\right) \psi(\mathcal{N} + 1) - \sum_{k=1}^{\mathcal{N}} \frac{\gamma}{k} + \sum_{k \geq l}^{\mathcal{N}} \frac{1}{kl} + \frac{\Gamma''(1)}{2} + \frac{1}{2} \left\{ \ln \left(-\frac{2}{g^2}\right) \right\}^2 \right] \quad (4.20)$$

where $\varsigma = \pm 1$. We also note that the above non-perturbative corrections for the energy and the wave function are reproduced by the following 2×2 effective Hamiltonian:

$$H_{\text{NP}} = \begin{pmatrix} W & Y \\ Y & X \end{pmatrix}, \quad (4.21)$$

where

$$W = \alpha^2 \frac{1}{\mathcal{N}!} \left(\frac{2}{g^2}\right)^{\mathcal{N}} \left\{ \ln \left(-\frac{2}{g^2}\right) - \psi(\mathcal{N} + 1) \right\}, \quad (4.22)$$

$$X = \alpha^2 \frac{1}{\mathcal{N}!} \left(\frac{2}{g^2}\right)^{\mathcal{N}} \left\{ \ln \left(-\frac{2}{g^2}\right) - \psi(1) \right\}, \quad (4.23)$$

$$Y = \alpha \sqrt{\frac{1}{\mathcal{N}!} \left(\frac{2}{g^2}\right)^{\mathcal{N}}}. \quad (4.24)$$

⁴In the case of $\mathcal{N}=0$, \mathbf{Z}_2 symmetry exists in the system, which makes it possible to determine the mixing. This is why we can obtain Eqs.(3.16) and (3.17).

The (1,1) component W is interpreted as the matrix element between the perturbative ground state at $q = q_+$ and itself, and the (2,2) component X as that between the perturbative \mathcal{N} -th excited state at $q = q_-$ and itself. The off-diagonal component Y is the matrix element between the ground state and the \mathcal{N} -th excited state. This result supports Eqs.(4.19) and (4.20).

Finally, we would like to comment on the non-perturbative corrections for the normalized wave function of the ground state, Eqs.(3.17), (3.28), (3.31) and (4.20). These corrections cannot be evaluated by the calculation in Section 4.1, where we have considered $Z = \lim_{T \rightarrow \infty} \text{Tr}(e^{-HT})$, since no information concerning the wave function is contained in this partition function. (See Eq.(4.12).) According to the argument of Section 3.3, we can predict that the perturbation series in g^2 for the normalized wave function of the ground state should be non-Borel-summable.

5 Large order behavior of the perturbative series

The expressions of the non-perturbative contribution to the energy levels (4.16) and (4.18) contain imaginary parts starting at the order α^2 , and are given by the following for the non-degenerate case:

$$\text{Im} \left(E_{\text{NP}}^{(\pm)}(\epsilon, N) \right) = -\alpha^2 \frac{1}{N!} \left(\frac{2}{g^2} \right)^{\pm\epsilon+2N} \frac{\pi}{\Gamma(1 \pm \epsilon + N)}, \quad (5.1)$$

where we have omitted the subscripts \pm of N for brevity. For the degenerate case $\epsilon = \mathcal{N}$, we have

$$\text{Im} (E_{\varsigma, \text{NP}}(\mathcal{N}, N)) = -\alpha^2 \frac{\pi}{N!(N+\mathcal{N})!} \left(\frac{2}{g^2} \right)^{2N+\mathcal{N}}. \quad (5.2)$$

We note that the result (5.1) reduces to (5.2) for $\epsilon = \mathcal{N}$:

$$\text{Im} \left(E_{\text{NP}}^{(+)}(\mathcal{N}, N) \right) = \text{Im} \left(E_{\text{NP}}^{(-)}(\mathcal{N}, N + \mathcal{N}) \right) = \text{Im} (E_{\varsigma, \text{NP}}(\mathcal{N}, N)). \quad (5.3)$$

The imaginary part of the energy is continuous in ϵ at $\epsilon = \mathcal{N}$.

We recall the relation between the imaginary part of the non-perturbative contribution and the large order behaviour of the perturbative series explained in Section 3.4. The following relation holds:

$$E_{\text{P}}^{(\pm)}(\epsilon, N, m) = -\frac{1}{\pi} \int_0^\infty dg^2 \frac{\text{Im}(E_{\text{NP}}^{(\pm)}(\epsilon, N))}{g^{2m+2}} \quad (5.4)$$

for the perturbative coefficients of the energy levels defined by

$$E_P^{(\pm)}(\epsilon, N) = \sum_{m=0}^{\infty} E_P^{(\pm)}(\epsilon, N, m) g^{2m}. \quad (5.5)$$

Substituting the result (5.1) into Eq.(5.4), we obtain the following for the perturbative coefficient $E_P^{(\pm)}(\epsilon, N, m)$,

$$\begin{aligned} E_P^{(\pm)}(\epsilon, N, m) &= A^{(\pm)}(\epsilon, N) 3^m \Gamma(\pm \epsilon + 2N + m + 1) \\ &\times \left[1 + O\left(\frac{1}{m}\right) \right], \end{aligned} \quad (5.6)$$

where the coefficient $A^{(\pm)}(\epsilon, N)$ is defined as follows,

$$A^{(\pm)}(\epsilon, N) \equiv -\frac{3}{\pi} \frac{6^{\pm \epsilon + 2N}}{N! \Gamma(\pm \epsilon + 1 + N)}. \quad (5.7)$$

We note that the higher order corrections of $O(\epsilon g^2)$ and $O(g^2)$ that we have ignored in Eq.(5.1) contribute only to the $O(1/m)$ correction, or more specifically the $O(1/(\pm \epsilon + 2N + m))$ correction in the result (5.6).⁵

The expression for $E_P^{(-)}(\epsilon, 1)$ coincides with the expression obtained in Ref.[18, 19]. In order to confirm our prediction, we have independently carried out the numerical and exact calculation of the perturbative coefficients $E_P^{(\pm)}(\epsilon, N, m)$ for much wider parameter ranges and to much higher orders, using the methods described in Ref.[20, 18, 19]. Specifically, the method given in Ref.[18] works for any excited state by replacing the zeroth order wave function by the n -th order harmonic oscillator wave function, and is fastest in *exact* computer calculations. We have calculated the following five categories of the perturbative coefficients to the 200-th order:

- (a) $N = 0$ $(-)$ level (the perturbative ground state at $q = q_-$) for $\epsilon = 0$ to 10 with $\Delta\epsilon = 0.2$ interval. Floating point calculation.
- (b) $N = 0$ $(+)$ level (the perturbative ground state at $q = q_+$) for $\epsilon = 0$ to 20 with $\Delta\epsilon = 0.2$. Floating point calculation.
- (c) $N = 1, 2, 3$ $(-)$ levels for $\epsilon = 0$ to 10.5 with $\Delta\epsilon = 0.5$. Exact calculation,
- (d) $N = 1, 2, 3$ $(+)$ levels for $\epsilon = 0$ to 20 with $\Delta\epsilon = 1.5$. Exact calculation,
- (e) $N = 4, 5, 6$ $(-)$ levels for $\epsilon = 2.5$. Floating point calculation.

⁵An attempt to calculate this type of correction is given in Ref.[17].

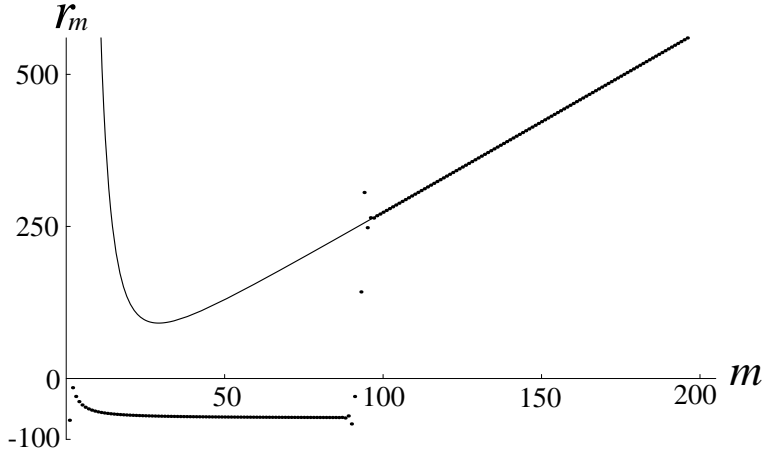


Figure 14: The plot of the ratio of successive perturbative coefficients r_m (dots) and the fitted curve (solid line) for the ground state at $\epsilon = 9.8$. The fitting was done for $m = 150 \sim 200$.

In the above, ‘‘exact’’ calculation indicates an algebraic calculation carried out in Mathematica.

We can compare these results with Eqs.(5.6) and (5.7) with the following procedures. First, in order to check the leading m -dependent terms in Eq.(5.6), we take their ratio.

$$\frac{E_P^{(\pm)}(\epsilon, N, m)}{E_P^{(\pm)}(\epsilon, N, m-1)} = 3(\pm\epsilon + 2N + m). \quad (5.8)$$

We use the result of the corresponding perturbative coefficients \hat{E}_m for $m = 150$ to 200 , and fit them as follows:

$$r_m = \frac{\hat{E}_m}{\hat{E}_{m-1}} = a_0 + a_1 m + \frac{a_2}{m} + \frac{a_3}{m^2} + \frac{a_4}{m^3}, \quad (5.9)$$

for all the categories (a)–(e). A plot of r_m for the ground state for $\epsilon = 9.8$ is given in Fig.14 as a sample. The fit works to good accuracy for values from $m = 150$ to 200 as can be seen in this figure. The same is true for all the cases in the above five categories (a)–(e) we have examined so far. The resulting coefficients are compared with their theoretical predictions:

$$a_0 = 3(\pm\epsilon + 2N), \quad a_1 = 3. \quad (5.10)$$

In all the cases, the theoretical prediction (5.10) is confirmed with good accuracy, the maximum error being 2 %.

Next, we examine $A^{(\pm)}(\epsilon, N)$ defined by Eq.(5.6). For this purpose we use the following quantity b_m :

$$b_m = (\pm\epsilon + 2N + m + 2)d_{m+1} - (\pm\epsilon + N + m + 1)d_m, \quad (5.11)$$

where

$$d_m \equiv \frac{\hat{E}_m}{3^m \Gamma(\pm\epsilon + 2N + m)}. \quad (5.12)$$

This quantity is defined so that it is free from the correction term of order $1/(\epsilon + 2N + m + 1)$ to \hat{E}_m . (This is not particularly crucial, since the order of our calculation is high.) Thus the numerical fit can be performed with the following formula:

$$b_m = c_0 + \frac{c_2}{m^2} + \cdots + \frac{c_8}{m^8}, \quad (5.13)$$

and is compared with the theoretical prediction:

$$c_0 = A^{(\pm)}(\epsilon, N). \quad (5.14)$$

The result for case (a) is plotted in Fig.15. The difference between Eq.(5.7) and the calculated value is at most 0.1 %, which happens at $\epsilon = 9.8$. For case (b), plotted in Fig.16, the error is at most 15 % (at $\epsilon = 20$). Cases (c) and (d) are plotted in Fig.17. The maximum error is 65 % for the case of $A^{(+)}(20.5, 3)$. Since this error is somewhat large, we have carried out a yet higher order calculation for this case. The error decreases to 32 % at the 364-th order, and to 17 % at the 478-th order, in both cases using the last 50 coefficients. This consistent decrease of the error for increasing m is in excellent agreement with our large order predictions. For the case (e) the maximum error is 0.15 %.

The reader may note that $A^{(-)}(\epsilon, 0)$ is zero for any positive integer ϵ as seen in Fig.15. Similar zeros in $A^{(-)}(\epsilon, N)$ are also seen in Fig.17. This is due to a new type of supersymmetry for these values of ϵ . We will elaborate upon this in the next section.

6 \mathcal{N} -fold supersymmetry

In the previous section, we have seen that the Borel singularity of perturbation theory apparently disappears for the first \mathcal{N} excited states at $q = q_-$ for $\epsilon = \mathcal{N}$ ($\mathcal{N} = 1, 2, 3, \dots$). Hereafter we will call these states isolated states, since these states do not have degenerate partners at $q = q_+$ (see Fig.13). In Table 1, we have listed the perturbative coefficients for several low-lying states for $\mathcal{N} = 1$. The perturbative correction for the ground state is not only Borel summable but in fact identically zero at every order. We also notice that the perturbation calculation cannot lift the degeneracy that exists at

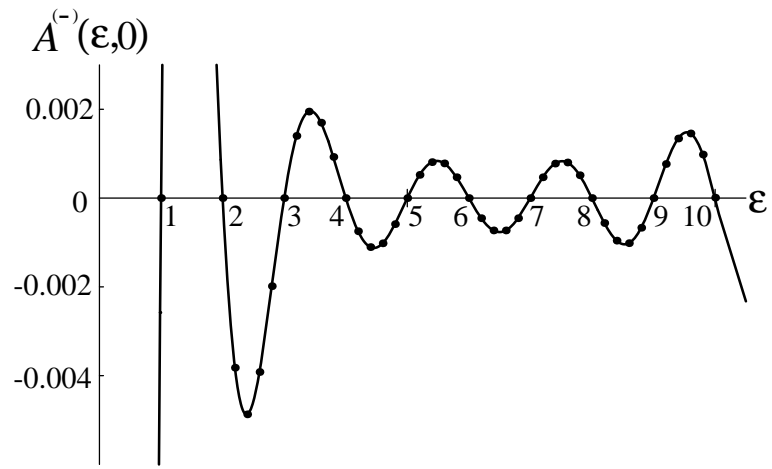


Figure 15: The comparison of the fitting to the perturbative coefficients (indicated by dots) and the theoretical prediction (solid line) of $A^{(-)}(\epsilon, 0)$.

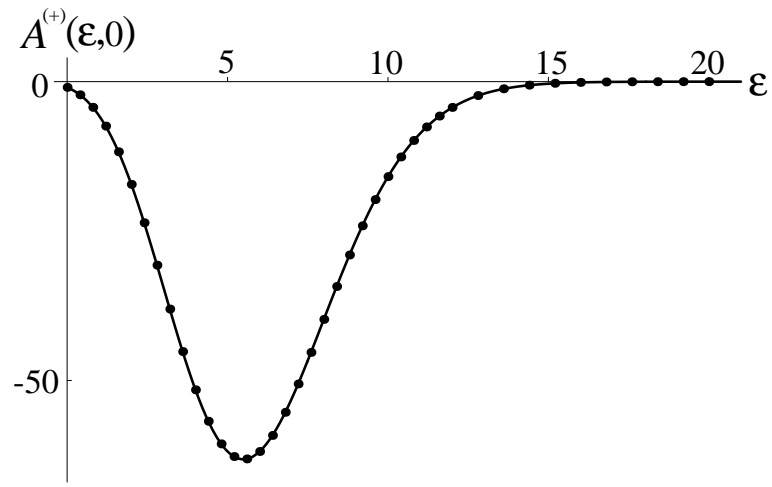


Figure 16: The comparison of the fitting to the perturbative coefficients (indicated by dots) and the theoretical prediction (solid line) of $A^{(+)}(\epsilon, 0)$.

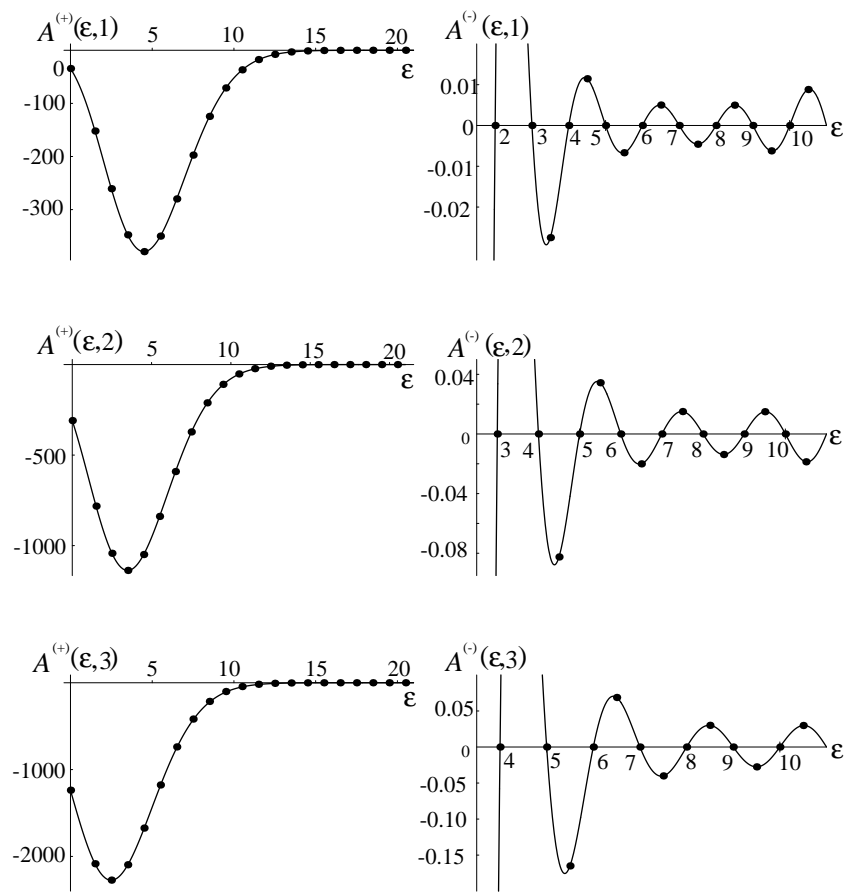


Figure 17: The comparison of the fitting to the perturbative coefficients (indicated by dots) and the theoretical prediction (solid line) of $A^{(\pm)}(\epsilon, N)$ for $N = 1 \sim 3$.

the zeroth order in g : $E_P^{(-)}(1, N, m)$ and $E_P^{(+)}(1, N - 1, m)$ are identical for all m . Interestingly similar features prevail in the results of the other values of \mathcal{N} . The results for $\mathcal{N} = 2, 3$ show similar characteristics as seen in Table 2 and 3.

The degeneracy reminds us of the non-renormalization theorem of supersymmetric theories. This holds that quantum correction at any finite order of perturbation theory cannot induce supersymmetry breaking if it is unbroken at the tree level, and the present model can actually be cast into a supersymmetric quantum mechanics at $\mathcal{N} = 1$ [21]. The degeneracy between the perturbative coefficients, $E_P^{(-)}(1, N, m)$ and $E_P^{(+)}(1, N - 1, m)$, is then understood as that between the bosonic and fermionic levels of the perturbatively unbroken supersymmetry. In this section we will show that this explanation also applies to other \mathcal{N} . We will reveal a new symmetry of the model that reduces to the ordinary supersymmetry at $\mathcal{N} = 1$ and can be understood as one of its possible extensions. We dub it \mathcal{N} -fold supersymmetry.

Considerations based on this symmetry will further reveal that the perturbative series of the isolated levels is convergent with a finite convergence radius. The perturbative series of these levels has a much stronger property than expected by the lack of the Borel singularity. To begin with, we briefly review the supersymmetric quantum mechanics, focusing upon the specific realization of the non-renormalization theorem.

6.1 Supersymmetric quantum mechanics

We will start by clarifying the supersymmetry that underlies our model at $\mathcal{N} = 1$. To see this, let us define the supercharges [21] by

$$Q^\dagger \equiv D\psi^\dagger, \quad Q = D^\dagger\psi, \quad (6.1)$$

where

$$D = p - iW(q), \quad D^\dagger = p + iW(q), \quad (6.2)$$

$p = -i(d/dq)$ is the canonical momentum of q , and $W(q)$ is defined by

$$W(q) = q(1 - gq). \quad (6.3)$$

In the definitions (6.1), ψ and ψ^\dagger are the annihilation and creation operators for a fermionic degree of freedom. They satisfy $\{\psi^\dagger, \psi\} = 1$ and $\psi^{\dagger 2} = \psi^2 = 0$. As a result, Q^2 and $Q^{\dagger 2}$ vanish:

$$Q^2 = Q^{\dagger 2} = 0. \quad (6.4)$$

The supersymmetric Hamiltonian \mathbf{H} is given by

$$\mathbf{H} = \frac{1}{2} \{Q^\dagger, Q\} = \frac{1}{2} (p^2 + W^2(q)) + W'(q) \left(\psi^\dagger\psi - \frac{1}{2} \right). \quad (6.5)$$

m	$E_P^{(-)}(0)$	$E_P^{(-)}(1), E_P^{(+)}(0)$	$E_P^{(-)}(2), E_P^{(+)}(1)$	$E_P^{(-)}(3), E_P^{(+)}(2)$	$E_P^{(-)}(4), E_P^{(+)}(3)$
0	0.5	1.5	2.5	3.5	4.5
1	0	-3	-1.2×10^1	-2.7×10^1	-4.8×10^1
2	0	-1.95×10^1	-1.41×10^2	-4.665×10^2	-1.098×10^3
3	0	-2.70×10^2	-3.330×10^3	-1.5930×10^4	-4.9320×10^4
4	0	-5.1791×10^3	-1.0474×10^5	-7.1373×10^5	-2.8885×10^6
5	0	-1.2110×10^5	-3.8959×10^6	-3.7318×10^7	-1.9624×10^8
6	0	-3.2594×10^6	-1.6258×10^8	-2.1630×10^9	-1.4695×10^{10}
7	0	-9.7888×10^7	-7.3976×10^9	-1.3523×10^{11}	-1.1804×10^{12}
8	0	-3.2201×10^9	-3.6075×10^{11}	-8.9708×10^{12}	-1.0008×10^{14}
9	0	-1.1464×10^{11}	-1.8643×10^{13}	-6.2466×10^{14}	-8.8621×10^{15}
10	0	-4.3816×10^{12}	-1.0131×10^{15}	-4.5323×10^{16}	-8.1376×10^{17}
11	0	-1.7875×10^{14}	-5.7580×10^{16}	-3.4085×10^{18}	-7.7085×10^{19}
12	0	-7.7506×10^{15}	-3.4088×10^{18}	-2.6465×10^{20}	-7.5041×10^{21}
13	0	-3.5604×10^{17}	-2.0961×10^{20}	-2.1154×10^{22}	-7.4855×10^{23}
14	0	-1.7282×10^{19}	-1.3358×10^{22}	-1.7367×10^{24}	-7.6343×10^{25}
15	0	-8.8443×10^{20}	-8.8090×10^{23}	-1.4620×10^{26}	-7.9464×10^{27}
16	0	-4.7629×10^{22}	-6.0040×10^{25}	-1.2602×10^{28}	-8.4300×10^{29}
17	0	-2.6943×10^{24}	-4.2259×10^{27}	-1.1113×10^{30}	-9.1043×10^{31}
18	0	-1.5983×10^{26}	-3.0695×10^{29}	-1.0016×10^{32}	-1.0001×10^{34}
19	0	-9.9264×10^{27}	-2.2997×10^{31}	-9.2230×10^{33}	-1.1167×10^{36}
20	0	-6.4447×10^{29}	-1.7765×10^{33}	-8.6724×10^{35}	-1.2667×10^{38}

Table 1: The perturbative coefficients of the energy levels $E_P^{(\pm)}(1, N, m)$ defined in Eq.(5.5). In the first row $E_P^{(\pm)}(N)$ is a shorthand denotation for $E_P^{(\pm)}(1, N, m)$.

m	$E_{\text{P}}^{(-)}(0)$	$E_{\text{P}}^{(-)}(1)$	$E_{\text{P}}^{(-)}(2), E_{\text{P}}^{(+)}(0)$	$E_{\text{P}}^{(-)}(3), E_{\text{P}}^{(+)}(1)$	$E_{\text{P}}^{(-)}(4), E_{\text{P}}^{(+)}(2)$
0	0.5	1.5	2.5	3.5	4.5
1	0	0	-6	-1.8×10^1	-3.6×10^1
2	0	0	-5.1×10^1	-2.55×10^2	-7.14×10^2
3	0	0	-9.09×10^2	-7.227×10^3	-2.7954×10^4
4	0	0	-2.2136×10^4	-2.7102×10^5	-1.4323×10^6
5	0	0	-6.4877×10^5	-1.1942×10^7	-8.5387×10^7
6	0	0	-2.1620×10^7	-5.8676×10^8	-5.6267×10^9
7	0	0	-7.9445×10^8	-3.1262×10^{10}	-3.9879×10^{11}
8	0	0	-3.1605×10^{10}	-1.7757×10^{12}	-2.9907×10^{13}
9	0	0	-1.3451×10^{12}	-1.0635×10^{14}	-2.3481×10^{15}
10	0	0	-6.0762×10^{13}	-6.6658×10^{15}	-1.9161×10^{17}
11	0	0	-2.8970×10^{15}	-4.3483×10^{17}	-1.6165×10^{19}
12	0	0	-1.4520×10^{17}	-2.9405×10^{19}	-1.4046×10^{21}
13	0	0	-7.6282×10^{18}	-2.0554×10^{21}	-1.2533×10^{23}
14	0	0	-4.1917×10^{20}	-1.4817×10^{23}	-1.1458×10^{25}
15	0	0	-2.4051×10^{22}	-1.0998×10^{25}	-1.0714×10^{27}
16	0	0	-1.4391×10^{24}	-8.3939×10^{26}	-1.0233×10^{29}
17	0	0	-8.9697×10^{25}	-6.5820×10^{28}	-9.9710×10^{30}
18	0	0	-5.8182×10^{27}	-5.2988×10^{30}	-9.9051×10^{32}
19	0	0	-3.9242×10^{29}	-4.3774×10^{32}	-1.0025×10^{35}
20	0	0	-2.7497×10^{31}	-3.7096×10^{34}	-1.0331×10^{37}

Table 2: The perturbative coefficients of the energy levels $E_{\text{P}}^{(\pm)}(2, N, m)$.

m	$E_{\text{P}}^{(-)}(0)$	$E_{\text{P}}^{(-)}(1)$	$E_{\text{P}}^{(-)}(2)$	$E_{\text{P}}^{(-)}(3), E_{\text{P}}^{(+)}(0)$	$E_{\text{P}}^{(-)}(4), E_{\text{P}}^{(+)}(1)$
0	0.5	1.5	2.5	3.5	4.5
1	-1	2	-1	-1.0×10^1	-2.5×10^1
2	1.5	0	-1.5	-1.05×10^2	-4.125×10^2
3	-4	8	-4	-2.290×10^3	-1.36×10^4
4	1.3125×10^1	0	-1.3125×10^1	-6.7676×10^4	-5.9131×10^5
5	4.8×10^1	9.6×10^1	-4.8×10^1	-2.3888×10^6	-3.009×10^7
6	1.8769×10^2	0	-1.8769×10^2	-9.5181×10^7	-1.7008×10^9
7	-7.68×10^2	1.536×10^3	-7.68×10^2	-4.1525×10^9	-1.0385×10^{11}
8	3.2477×10^3	0	-3.2477×10^3	-1.9476×10^{11}	-6.7357×10^{12}
9	-1.4080×10^4	2.8160×10^4	-1.4080×10^4	-9.7049×10^{12}	-4.5906×10^{14}
10	6.2247×10^4	0	-6.2247×10^4	-5.0965×10^{14}	-3.263×10^{16}
11	-2.7955×10^5	5.5910×10^5	-2.7955×10^5	-2.8048×10^{16}	-2.4059×10^{18}
12	1.2718×10^6	0	-1.2718×10^6	-1.6112×10^{18}	-1.8330×10^{20}
13	-5.8491×10^6	1.1698×10^7	-5.8491×10^6	-9.6315×10^{19}	-1.4386×10^{22}
14	2.7148×10^7	0	-2.7148×10^7	-5.9791×10^{21}	-1.1606×10^{24}
15	-1.2701×10^8	2.5402×10^8	-1.2701×10^8	-3.8483×10^{23}	-9.6071×10^{25}
16	5.9828×10^8	0	-5.9828×10^8	-2.5649×10^{25}	-8.1491×10^{27}
17	-2.8353×10^9	5.6706×10^9	-2.8353×10^9	-1.7687×10^{27}	-7.0762×10^{29}
18	1.3508×10^{10}	0	-1.3508×10^{10}	-1.2610×10^{29}	-6.2853×10^{31}
19	-6.4664×10^{10}	1.2933×10^{11}	-6.4664×10^{10}	-9.2892×10^{30}	-5.7075×10^{33}
20	3.1087×10^{11}	0	-3.1087×10^{11}	-7.0678×10^{32}	-5.2964×10^{35}

Table 3: The perturbative coefficients of the energy levels $E_{\text{P}}^{(\pm)}(3, N, m)$.

All the states are labeled by the quantum number of the fermion number operator $N_f = \psi^\dagger \psi$. The operator Q^\dagger transforms a bosonic state $|b\rangle$ (with $N_f = 0$) to a fermionic one $|f\rangle$ (with $N_f = 1$), and Q does vice versa. By construction, Q and Q^\dagger commute with \mathbf{H}

$$[\mathbf{H}, Q] = [\mathbf{H}, Q^\dagger] = 0. \quad (6.6)$$

Therefore, the Hamiltonian is invariant under the transformations generated by the supercharges.

The relation between this supersymmetric Hamiltonian and our Hamiltonian becomes obvious if we introduce a matrix representation of ψ

$$\psi^\dagger = \begin{pmatrix} 0 & 1 \\ 0 & 0 \end{pmatrix}, \quad \psi = \begin{pmatrix} 0 & 0 \\ 1 & 0 \end{pmatrix}. \quad (6.7)$$

In this representation, the bosonic state $|b\rangle$ and the fermionic one $|f\rangle$ are written as

$$|b\rangle = \begin{pmatrix} 0 \\ \Psi^{(-)} \end{pmatrix}, \quad |f\rangle = \begin{pmatrix} \Psi^{(+)} \\ 0 \end{pmatrix}, \quad (6.8)$$

and the supersymmetric Hamiltonian is decomposed into two components:

$$\mathbf{H} = \begin{pmatrix} H_+ & 0 \\ 0 & H_- \end{pmatrix}. \quad (6.9)$$

Here we denote the fermionic component by H_+ and the bosonic by H_- which are given by

$$H_- = \frac{1}{2} D^\dagger D, \quad H_+ = \frac{1}{2} D D^\dagger, \quad (6.10)$$

or more explicitly

$$H_\pm = -\frac{1}{2} \frac{d^2}{dq^2} + \frac{1}{2} q^2 (1 - gq)^2 \mp (gq - \frac{1}{2}). \quad (6.11)$$

One can readily check $H_+ - 1/2$ is indeed the Hamiltonian of our model with $\mathcal{N} = 1$, i.e., the one derived from the action (2.1)-(2.2) with $\epsilon = 1$. The Hamiltonian $H_- - 1/2$ becomes $H_+ - 1/2$ as a result of the mirror transformation with respect to the $q = 1/2g$ axis. Therefore, the dynamics of our model with $\mathcal{N} = 1$ are same as that of the supersymmetric Hamiltonian \mathbf{H} .

In considering the eigenvalues of \mathbf{H} , we will work on the decomposed form of the equation, i.e.,

$$H_\pm \Psi^{(\pm)} = E^{(\pm)} \Psi^{(\pm)}. \quad (6.12)$$

The perturbative energy levels $E_p^{(\pm)}$ calculated in the previous section were those of the well-local states in the left well of $H_+ - 1/2$ and of the states

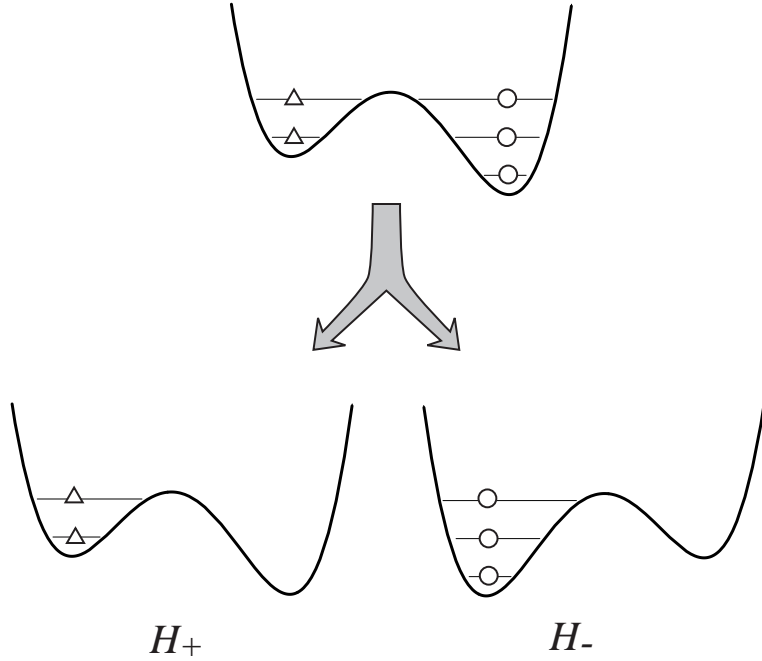


Figure 18: The correspondence between the states in the left and right wells of the potential (2.2) with $\epsilon = 1$ and the states in the left wells of $H_{\pm} - 1/2$.

in the right well. It is convenient to identify the latter states with the well-local ones in the left well at $q \sim 0$ of $H_- - 1/2$ (see Fig.18). These states correspond to “bosonic” states, while the well-local states in the left well of $H_+ - 1/2$ correspond to “fermionic” states.

At $g = 0$, \mathbf{H} reduces to that of the supersymmetric harmonic oscillator. The eigenvalues $E^{(\pm)}$ and eigenfunctions $\Psi^{(\pm)}$ can be solved immediately. They are labeled by an integer $N (= 0, 1, 2, \dots)$ representing the level of excitation. The solution for $\Psi^{(\pm)}$ is

$$\Psi_N^{(\pm)}(q) = H_N(q) e^{-q^2/2} \quad (6.13)$$

by the use of the N -th Hermite polynomial $H_N(q) \equiv (-1)^N e^{q^2} \frac{d^N}{dq^N} e^{-q^2}$; the corresponding eigenvalues are $E_N^{(-)} = N$ and $E_N^{(+)} = N + 1$. The ground state $\Psi_0^{(-)}$ is of zero-point energy and the supersymmetry is not broken. The degeneracy between the fermionic and bosonic spectra due to the unbroken supersymmetry is manifest in the pairs of $E_{N+1}^{(-)}$ and $E_N^{(+)}$.

Now let us examine a case where g is a nonzero quantity. When one applies perturbation theory to Eq.(6.12) by expanding the wave functions and the eigenvalues in g , one gets

$$E_N^{(\pm)} = -\frac{1}{2} + \sum_{m=0}^{\infty} E_P^{(\pm)}(1, N, m) g^{2m}, \quad (6.14)$$

where $E_P^{(\pm)}(1, N, m)$ is exactly what we have calculated in the previous section, Eq.(5.5). If we recall the identification of the state in the right well of $H^{(+)}$ and the one in the left of $H^{(-)}$, it will be seen that the perturbative coefficients of $E_N^{(-)}$ are given by those of $E_P^{(-)}(1, N)$ calculated in the previous section. The disappearance of the correction to $E_0^{(-)}$ and the persistence of the degeneracy between $E_{N+1}^{(-)}$ and $E_N^{(+)}$ are now seen in the context of the unbroken supersymmetry of \mathbf{H} in perturbation.

A direct demonstration of the non-renormalization theorem can be obtained for the present case, by considering the function obtained from $D\Psi_G = 0$,

$$\Psi_G(q) = \exp\left(-\int_0^q dq' W(q')\right) = \exp\left(-\frac{q^2}{2} + g\frac{q^3}{3}\right). \quad (6.15)$$

Since this function starts with $\Psi_0^{(-)}(q)$ in the expansion in g and obviously satisfies $H_- \Psi_G = 0$, it mimics the zero-energy state of H_- , whose existence is the indicator of unbroken supersymmetry.

The function Ψ_G is not normalizable, and cannot, therefore, be accepted as the physical zero-energy state. Thus, the supersymmetry is dynamically broken at any non zero values of g [21]. The perturbation theory, however, cannot detect it, for the unnormalizability does not appear at any finite order in g in the expansion of Ψ_G . (There can be no zero-energy state in H_+ either, for the spectrum of H_+ is necessarily the same as that of H_- .)

Since the perturbation cannot break the supersymmetry, the degeneracy of the excitations must persist in the perturbation. Thanks to the simplicity of the quantum mechanics, we can check this directly. The explicit contents of the supersymmetry relation (6.6) are the two equations

$$DH_- = H_+ D, \quad (6.16)$$

$$D^\dagger H_+ = H_- D^\dagger. \quad (6.17)$$

We will focus on Eq.(6.16) in the following discussion. This holds that if $\Psi^{(-)}$ is an eigenfunction of H_- with the eigenvalue $E^{(-)}$ then $D\Psi^{(-)}$ is that of H_+ with the same eigenvalue. The operators D and D^\dagger are written as

$$D = (-i)e^{(gq^3/3)}ae^{-(gq^3/3)}, \quad D^\dagger = ie^{-(gq^3/3)}a^\dagger e^{(gq^3/3)}, \quad (6.18)$$

where

$$a \equiv \frac{d}{dq} + q \quad (6.19)$$

is the annihilation operator in the harmonic oscillator up to an unimportant factor $\sqrt{2}$, $[a, a^\dagger] = 2$. The operator D has a as the leading term in its expansion in g ; $D = a + O(g)$. Thus if the state $\Psi^{(-)}$ is for the $(N+1)$ -th excitation and starts with $H_{N+1}(q)e^{-q^2/2}$ in the perturbative expansion,

$D\Psi^{(-)}$ starts with $H_N(q)e^{-q^2/2}$ and represents the N -th excitation of H_+ . This observation suggests the degeneracy in the perturbative energy levels.

To be more specific we can rewrite the two Hamiltonians as

$$H_+ = (1/2)e^{(gq^3/3)} a(a^\dagger - 2gq^2) e^{-(gq^3/3)}, \quad (6.20)$$

$$H_- = (1/2)e^{(gq^3/3)} (a^\dagger - 2gq^2)a e^{-(gq^3/3)}. \quad (6.21)$$

In conducting the perturbative analysis of $E_{N+1}^{(-)}$ we need not necessarily expand $\Psi_{N+1}^{(-)}$ in g directly. Since the asymptotic expansion is unique, we may adopt another convenient expansion scheme for the eigenfunction as long as it is well-defined. Looking at Eqs.(6.18), (6.20), and (6.21) we can expand $\Phi^{(-)} \equiv e^{-(gq^3/3)}\Psi^{(-)}$ in g ,

$$\Phi_{N+1}^{(-)}(q) = H_{N+1}(q)e^{-q^2/2} + \sum_{m=1}^{\infty} g^m \Phi_{N+1}^{(m)}(q). \quad (6.22)$$

The eigenvalue equation for $E_{N+1}^{(-)}$ now reads

$$\frac{1}{2} (a^\dagger - 2gq^2) a \Phi_{N+1}^{(-)} = E_{N+1}^{(-)} \Phi_{N+1}^{(-)}. \quad (6.23)$$

By multiplying a on both sides of Eq.(6.23), we obtain the following:

$$\frac{1}{2} a (a^\dagger - 2gq^2) [a \Phi_{N+1}^{(-)}] = E_{N+1}^{(-)} [a \Phi_{N+1}^{(-)}]. \quad (6.24)$$

The function $[a \Phi_{N+1}^{(-)}]$ starts with $H_N(q)e^{-(q^2/2)}$ when expanded in g . Eq.(6.24) shows that $\Psi^{(+)} \equiv e^{(gq^3/3)}[a \Phi_{N+1}^{(-)}]$ has the same perturbative series as $E_{N+1}^{(-)}$ to the eigenvalue in H_+ . This proves that the $(N+1)$ -th excitation of H_- and the N -th of H_+ have the same perturbative series.

We can now turn to the other values of \mathcal{N} . The first 20 coefficients of $E_P^{(\pm)}$ for $\mathcal{N} = 2$ are listed in Table 2 and those for $\mathcal{N} = 3$ are listed in Table 3. The vanishing coefficients at $\mathcal{N} = 2$ for the two isolated states draw our attention first.⁶ The perturbative degeneracy remains, but this time between $E_P^{(-)}(\mathcal{N}, N + \mathcal{N}, m)$ and $E_P^{(+)}(\mathcal{N}, N, m)$. In the next section, we will present the general proofs of these properties of the perturbative coefficients.

6.2 Non-renormalization theorem

We will start with the degeneracy, and define a pair of two Hamiltonians $H_{\pm}(\mathcal{N})$ with \mathcal{N} as a parameter,

$$H_{\pm}(\mathcal{N}) \equiv -\frac{1}{2} \frac{d^2}{dq^2} + \frac{1}{2} q^2 (1 - gq)^2 \mp \mathcal{N} \left(gq - \frac{1}{2} \right). \quad (6.25)$$

⁶Supersymmetry provides an explanation for the vanishing coefficients for only the first excited state [18].

The Hamiltonians $H_{\pm}(\mathcal{N})$ are related to the action (2.1)-(2.2) again with $\epsilon = \mathcal{N}$. We denote the wave function and the eigenvalue of the N -th excited state in the left well of $H_{\pm}(\mathcal{N})$ by $\Psi_N^{(\pm)}$ and $E_N^{(\pm)}$, as in the case of the previous subsection. The degeneracy between the $N + \mathcal{N}$ -th excited level at the right well and the N -th at the left in Table 2 and 3 is realized between the eigenvalues $E^{(\pm)}$ of the left wells of $H_{\pm}(\mathcal{N})$. The Hamiltonians are also rewritten as

$$H_+(\mathcal{N}) = \frac{1}{2}DD^\dagger - (\mathcal{N} - 1) \left(gq - \frac{1}{2} \right), \quad (6.26)$$

$$H_-(\mathcal{N}) = \frac{1}{2}D^\dagger D + (\mathcal{N} - 1) \left(gq - \frac{1}{2} \right). \quad (6.27)$$

As in the supersymmetric case, these two Hamiltonians transform to each other by mirror transformation and thus describe the same quantum mechanics.

The point of the explanation concerning the degeneracy in $\mathcal{N} = 1$ was Eq.(6.16), and the fact that the operator D reduces the level of excitation by 1. What we have now is degeneracy between $E_{N+\mathcal{N}}^{(-)}$ and $E_N^{(+)}$. Correspondingly, we find $H_{\pm}(\mathcal{N})$ satisfies

$$D^{\mathcal{N}} H_-(\mathcal{N}) = H_+(\mathcal{N}) D^{\mathcal{N}}, \quad (6.28)$$

$$D^{\dagger \mathcal{N}} H_+(\mathcal{N}) = H_-(\mathcal{N}) D^{\dagger \mathcal{N}}. \quad (6.29)$$

The proof is as follows. We first note that the equation

$$H_+(\mathcal{N}) D = D H_+(\mathcal{N} - 2) - i(\mathcal{N} - 1)g, \quad (6.30)$$

is proved from Eqs.(6.2) and (6.26). We examine Eq.(6.28). The other will be proved in a similar way. We start with $H_+(\mathcal{N}) D^{\mathcal{N}}$ and move each D to the left using Eq.(6.30). After moving all D 's we obtain

$$H_+(\mathcal{N}) D^{\mathcal{N}} = D^{\mathcal{N}} H_+(\mathcal{N} - 2\mathcal{N}) - ig D^{\mathcal{N}-1} \sum_{k=0}^{\mathcal{N}-1} (\mathcal{N} - 1 - 2k). \quad (6.31)$$

The terms in the summation over k on the right-hand side cancel each other and $H_+(-\mathcal{N}) = H_-(-\mathcal{N})$. This proves Eq.(6.28).

Once we have obtained Eq.(6.28), the perturbative degeneracy is proved in a similar manner to the ordinary supersymmetric case. In terms of a and a^\dagger ,

$$H_{\pm}(\mathcal{N}) = e^{(gq^3/3)} h_{\pm} e^{-(gq^3/3)}, \quad (6.32)$$

where

$$h_+ = (1/2)a(a^\dagger - 2gq^2) - (\mathcal{N} - 1) \left(gq - \frac{1}{2} \right), \quad (6.33)$$

$$h_- = (1/2)(a^\dagger - 2gq^2)a + (\mathcal{N} - 1) \left(gq - \frac{1}{2} \right). \quad (6.34)$$

Substituting Eqs.(6.18) and (6.32) into Eq.(6.28) leads

$$a^N h_- = h_+ a^N. \quad (6.35)$$

This establishes that the perturbative series of the $(N + \mathcal{N})$ -th level in h_- is the same as that of the N -th level in h_+ . In turn it establishes the perturbative degeneracy between $E_{N+\mathcal{N}}^{(-)}$ and $E_N^{(+)}$. The wave function $\Psi_N^{(-)}$ of the $(N + \mathcal{N})$ -th state of $H^{(-)}(\mathcal{N})$ is related to the wave function $\Psi_N^{(+)}$ of the N -th excited state of $H^{(+)}(\mathcal{N})$:

$$D^{\mathcal{N}} \Psi_{N+\mathcal{N}}^{(-)} = \Psi_N^{(+)}. \quad (6.36)$$

On the contrary, the isolated states should satisfy

$$D^{\mathcal{N}} \Psi_N^{(-)} = 0 \quad (N = 0, 1, 2, \dots, \mathcal{N} - 1), \quad (6.37)$$

which is the analogue of the ground state condition of the supersymmetric case. Since $D^{\mathcal{N}}$ is rewritten as

$$D^{\mathcal{N}} = e^{-(q^2/2)+(gq^3/3)} \left(-i \frac{d}{dq} \right)^{\mathcal{N}} e^{(q^2/2)-(gq^3/3)}, \quad (6.38)$$

the solutions for Eq.(6.37) have the form

$$\Psi_N^{(-)} = f(q) \exp \left(-\frac{q^2}{2} + g \frac{q^3}{3} \right), \quad (6.39)$$

where $f(q)$ is a polynomial of q of order $\mathcal{N} - 1$ at most. Again the unnormalizability of $\Psi_N^{(-)}$ disappears once it is expanded in g , as in the case of $\mathcal{N} = 1$. Plugging Eq.(6.39) into

$$H_-(\mathcal{N}) \Psi_N^{(-)} = E \Psi_N^{(-)}, \quad (6.40)$$

we obtain

$$f'' + 2(gq^2 - q)f' + [-2g(\mathcal{N} - 1)q + 2E + \mathcal{N} - 1]f = 0. \quad (6.41)$$

Let us write the polynomial f explicitly as

$$f(q) = \sum_{n=0}^{\mathcal{N}-1} a_n q^n. \quad (6.42)$$

Only polynomials of the order of $(\mathcal{N} - 1)$ at most can be a consistent solution for (6.41): Otherwise the terms $2g[q^2f' - (\mathcal{N} - 1)qf]$ in (6.41) forces $f(q)$ to have much higher powers.⁷

⁷We note that the equation (6.41) is rewritten in the form $[-(1/2)(J^-)^2 - gJ^+ + J^0]f = Ef$ where $J^- = d/dq$, $J^0 = q(d/dq) - (1/2)(\mathcal{N} - 1)$, and $J^+ = q^2(d/dq) - (\mathcal{N} - 1)q$ are the $SL(2, \mathbb{Q})$ generators for the \mathcal{N} -dimensional representation. This is the eigenvalue problem equation of the quantum top, known in connection with the quasi-exactly-solvable problem [22]. This also accounts for the fact that the solution f is obtained in polynomials of the order $\mathcal{N} - 1$.

It is convenient to write the resulting equation for a_n in a matrix form

$$\mathbf{M}_{\mathcal{N}}(E) \cdot \mathbf{a} = 0, \quad (6.43)$$

where $\mathbf{a}^T = (a_0, a_1, \dots, a_{\mathcal{N}-1})$. The (i, j) -element of $\mathbf{M}_{\mathcal{N}}(E)$ is given by

$$\mathbf{M}_{\mathcal{N}}(E)_{ij} = 2g(i-\mathcal{N})\delta_{i,j+1} + (2E+\mathcal{N}-1-2i)\delta_{i,j} + (i+2)(i+1)\delta_{i,j-2}, \quad (6.44)$$

where i and j run from 0 to $\mathcal{N}-1$. The matrix $\mathbf{M}_{\mathcal{N}}(E)$ has the explicit form

$$\mathbf{M}_{\mathcal{N}}(E) \equiv$$

$$\begin{pmatrix} 2E+\mathcal{N}-1 & 0 & 2 & 0 & \dots \\ 2g(1-\mathcal{N}) & 2E+\mathcal{N}-3 & 0 & 6 & \dots \\ 0 & 2g(2-\mathcal{N}) & 2E+\mathcal{N}-5 & 0 & \dots \\ 0 & 0 & 2g(3-\mathcal{N}) & 2E+\mathcal{N}-7 & \ddots \\ & & \vdots & & \end{pmatrix} \quad (6.45)$$

at the upper left corner and

$$\mathbf{M}_{\mathcal{N}}(E) \equiv$$

$$\begin{pmatrix} \ddots & & \vdots & \\ 2E-\mathcal{N}+7 & 0 & (\mathcal{N}-2)(\mathcal{N}-3) & 0 \\ -6g & 2E-\mathcal{N}+5 & 0 & (\mathcal{N}-1)(\mathcal{N}-2) \\ \dots & 0 & -4g & 2E-\mathcal{N}+3 \\ 0 & 0 & -2g & 2E-\mathcal{N}+1 \end{pmatrix} \quad (6.46)$$

at the lower right.

The condition that there exists a non-trivial solution for \mathbf{a} is

$$\det \mathbf{M}_{\mathcal{N}}(E) = 0. \quad (6.47)$$

Writing this condition explicitly for several lowest values of \mathcal{N} , we obtain

$$\begin{aligned} \mathcal{N} = 1 : \quad & E = 0, \\ \mathcal{N} = 2 : \quad & \left(E - \frac{1}{2}\right) \left(E + \frac{1}{2}\right) = 0, \\ \mathcal{N} = 3 : \quad & E(E-1)(E+1) + 2g^2 = 0, \\ \mathcal{N} = 4 : \quad & \left(E - \frac{3}{2}\right) \left(E - \frac{1}{2}\right) \left(E + \frac{1}{2}\right) \left(E + \frac{3}{2}\right) + 12Eg^2 = 0, \\ \mathcal{N} = 5 : \quad & E(E-2)(E-1)(E+1)(E+2) + 6(7E^2 - 52)g^2 = 0. \end{aligned} \quad (6.48)$$

These algebraic equations for E of the order \mathcal{N} determine the perturbative eigenvalues of the \mathcal{N} isolated states. The solutions are consistent with those we expect as the energy levels in perturbation theory. They reproduce the energy levels of the first \mathcal{N} lowest states of the harmonic oscillator at $g = 0$, which are $E = -(\mathcal{N}/2) + (1/2), -(\mathcal{N}/2) + (3/2), \dots, (\mathcal{N}/2) - (1/2)$. The perturbative corrections are identically zero at any g^2 for $\mathcal{N} = 2$ as well as $\mathcal{N} = 1$. We have also checked that the equation at other values of \mathcal{N} ($\mathcal{N} \geq 3$) correctly regenerates the perturbative coefficients obtained in the previous section once it is solved in powers of g^2 .

The very existence of the algebraic equation (6.47) for E tells us that the perturbative series for the isolated energy levels are *convergent*, not simply Borel summable.

Finally, we will combine the relations (6.28) and (6.29) into a compact form, which suggests the name “ \mathcal{N} -fold supersymmetry”, and will present an interesting relation between the Hamiltonians $H_{\pm}(\mathcal{N})$ and a new Hamiltonian that will be introduced naturally as a direct extension of the supersymmetric Hamiltonian.

We will define the \mathcal{N} -fold supercharge in 2×2 matrix notation by

$$Q_{\mathcal{N}}^{\dagger} = \begin{pmatrix} 0 & D^{\mathcal{N}} \\ 0 & 0 \end{pmatrix}, \quad Q_{\mathcal{N}} = \begin{pmatrix} 0 & 0 \\ (D^{\dagger})^{\mathcal{N}} & 0 \end{pmatrix}. \quad (6.49)$$

These obviously satisfy

$$Q_{\mathcal{N}}^2 = Q_{\mathcal{N}}^{\dagger 2} = 0, \quad (6.50)$$

and induce transformations between the “bosonic” state $|\mathcal{B}\rangle$ and the “fermionic” state $|\mathcal{F}\rangle$:

$$|\mathcal{B}\rangle \equiv \begin{pmatrix} 0 \\ \Psi^{(-)} \end{pmatrix}, \quad |\mathcal{F}\rangle \equiv \begin{pmatrix} \Psi^{(+)} \\ 0 \end{pmatrix}. \quad (6.51)$$

The relations (6.28) and (6.29) now become compact as

$$[H_{\mathcal{N}}, Q_{\mathcal{N}}] = [H_{\mathcal{N}}, Q_{\mathcal{N}}^{\dagger}] = 0 \quad (6.52)$$

where $H_{\mathcal{N}}$ is defined by

$$H_{\mathcal{N}} = \begin{pmatrix} H_{+}(\mathcal{N}) & 0 \\ 0 & H_{-}(\mathcal{N}) \end{pmatrix}, \quad (6.53)$$

in terms of the Hamiltonians $H_{\pm}(\mathcal{N})$ in Eq.(6.25). The supersymmetric Hamiltonian is constructed from the supercharges Q and Q^{\dagger} :

$$\mathbf{H}_{\mathcal{N}} = \frac{1}{2} \{Q_{\mathcal{N}}, Q_{\mathcal{N}}^{\dagger}\} = \frac{1}{2} \begin{pmatrix} D^{\mathcal{N}} D^{\dagger \mathcal{N}} & 0 \\ 0 & D^{\dagger \mathcal{N}} D^{\mathcal{N}} \end{pmatrix}, \quad (6.54)$$

which we call the \mathcal{N} -fold supersymmetric Hamiltonian. The Hamiltonian $\mathbf{H}_{\mathcal{N}}$ commutes with $Q_{\mathcal{N}}$ and $Q_{\mathcal{N}}^{\dagger}$. We can define the states

$$|\mathcal{B}_0\rangle \equiv \begin{pmatrix} 0 \\ \Psi_N^{(-)} \end{pmatrix}, \quad N = 0, 1, \dots, \mathcal{N} - 1, \quad (6.55)$$

using the perturbative isolated states $\Psi_N^{(-)}$ of $H_{-}(\mathcal{N})$. These states satisfy

$$\mathbf{H}_{\mathcal{N}}|\mathcal{B}_0\rangle = 0, \quad (6.56)$$

and play the role of the \mathcal{N} vacua of $\mathbf{H}_{\mathcal{N}}$. The symmetry generated by $Q_{\mathcal{N}}$ and $Q_{\mathcal{N}}^{\dagger}$ is \mathcal{N} -fold of the ordinary supersymmetry in the sense of the number of perturbative vacua and the change in the level of excitation.

By the definition of $\mathbf{H}_{\mathcal{N}}$ and Eq.(6.52), it is obvious that

$$[\mathbf{H}_{\mathcal{N}}, H_{\mathcal{N}}] = 0. \quad (6.57)$$

Therefore $\mathbf{H}_{\mathcal{N}}$ is a function of $H_{\mathcal{N}}$. By counting the highest orders of d/dq in both operators, we find that $\mathbf{H}_{\mathcal{N}}$ must be a polynomial of $H_{\mathcal{N}}$ of order \mathcal{N} . Since the perturbative isolated states satisfy Eqs.(6.47) and (6.56), we conjecture that

$$\mathbf{H}_{\mathcal{N}} = \frac{1}{2} \det \mathbf{M}_{\mathcal{N}}(H_{\mathcal{N}}). \quad (6.58)$$

In the above, we have fixed the overall constant by comparing the highest powers of d/dq on both sides. We have checked this conjecture explicitly by hand to the value $\mathcal{N} = 3$, and algebraically on a computer to $\mathcal{N} = 10$.

The non-renormalization theorem in the \mathcal{N} -fold supersymmetric quantum mechanics guarantees the absence of any perturbative correction to the energy of the ground states in $\mathbf{H}_{\mathcal{N}}$ and the persistence of the degeneracy in perturbation theory.

7 Numerical verification of the prediction of the energy spectrum

In this section we will numerically verify the prediction with regard to the energy spectrum made from the valley method. The result (4.16) obtained in Section 4 is for the case of no perturbative degeneracy, or even for the isolated states in the presence of degeneracy. The result (4.18) is for the perturbatively degenerate states. In principle we can use these to check the validity of the valley method by a comparison with exact numerical energy levels. There is, however, a great difficulty for general values of ϵ . The valley result represents only the non-perturbative part and needs to be combined

with the perturbative predictions. This is important for numerical studies, since the perturbative part has in general a much larger numerical value than does the non-perturbative. The problem is that we know only the leading Borel singularity of the perturbation series. After canceling it with the imaginary part of the non-perturbative contribution we obtained, we are still left with non-leading Borel singularities in the perturbation theory. This prohibits us from making numerical predictions for the energy levels.

The model with $\epsilon = \mathcal{N}$ has a great advantage in this respect. For the isolated states we can obtain the perturbative contribution exactly by solving Eq.(6.47). Remember that the equation generates all the perturbative coefficients and, thus, it contains complete information on the perturbative contribution. Correspondingly, the valley prediction for these states derived from Eq.(4.16) is free from any imaginary element. Regarding the perturbatively degenerate states, their energy splittings have no perturbative corrections because of the \mathcal{N} -fold supersymmetry.

In this section we will carry out the numerical calculation for the energy spectra in the case of $\mathcal{N} = 0, 1, 2, 3$, and compare them with the valley predictions. We label its energy levels by a single integer k , E_k ($k = 0, 1, 2, \dots$), counting from bottom. That is, the energy of the ground state, the first excited state, and so on, are denoted by E_0, E_1, \dots , respectively. They thus include the isolated states localized at the lower right well. We will first make the correspondence with the result in the previous sections and identify the quantities on which we will perform the comparison.

For \mathcal{N} isolated states, $k = 0, 1, \dots, \mathcal{N} - 1$, we use $E_k^{(P)}$ for denoting the perturbative contribution to the energy, which is the solution of Eq.(6.47). In fact they are zero at $\mathcal{N} = 1$ and just $-1/2$ or $1/2$ at $\mathcal{N} = 2$. In the case of $\mathcal{N} = 3$, the equation reads

$$E(E - 1)(E + 1) + 2g^2 = 0. \quad (7.1)$$

This equation has three real roots up to $g^2 = \sqrt{3}/9$ and each of them represents $E_k^{(P)}$. We will first solve the equation numerically at various values of g , and then we will define the non-perturbative correction by

$$\Delta E_k \equiv E_k - E_k^{(P)}. \quad (7.2)$$

We can compare this with the valley prediction

$$\Delta E_k^{(V)} = \alpha^2 \frac{(-1)^{k+1}}{k!} \Gamma(\mathcal{N} - k) \left(-\frac{2}{g^2}\right)^{-\mathcal{N}+2k}, \quad (7.3)$$

which is derived from Eq.(4.16) by the insertions $\epsilon = \mathcal{N}$ and $N_- = k$.

For the perturbatively degenerate energy levels, $k = \mathcal{N}, \mathcal{N} + 1, \dots$, we will consider the energy splitting defined by the following equation:

$$\Delta E_{k k+1} \equiv E_{k+1} - E_k. \quad (7.4)$$

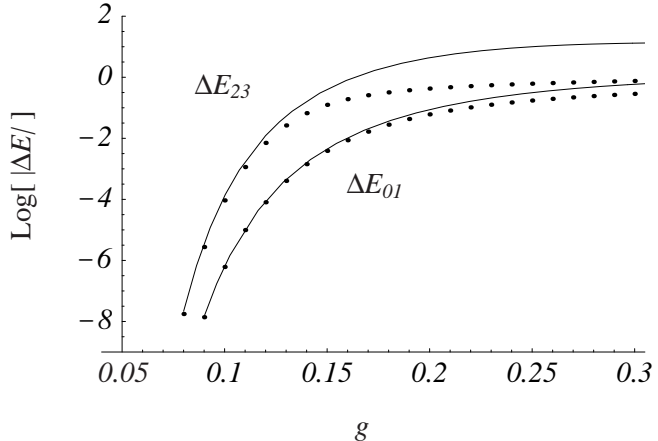


Figure 19: The comparison in absolute values on the logarithmic scale between the instanton prediction and the exact numerical result for the energy splitting at $\mathcal{N} = 0$. The solid lines stand for the instanton predictions, while the dots show the corresponding exact numerical results.

The valley prediction in relation to this splitting is

$$\Delta E_{k k+1}^{(V)} = 2\alpha \sqrt{\frac{1}{[(k - \mathcal{N})/2]![(k + \mathcal{N})/2]!}} \left(\frac{2}{g^2}\right)^k, \quad (7.5)$$

as derived from Eq.(4.18) by the insertion of $N_{\pm} = (k \mp \mathcal{N})/2$.

The result of the comparison is plotted in Figs.19-22. The valley prediction monotonically approaches to the exact values as g decreases for all levels. This fact clearly shows that the results (4.16) and (4.18) obtained on the basis of the valley method are indeed the leading terms of the non-perturbative correction to the energy spectrum.

There are various sources of corrections to the leading term that could account for the discrepancy in the figures. First is the fact that the potential (2.2) ceases to have two minima at g larger than $\sqrt{\sqrt{3}/(18\mathcal{N})}$, that are $g > 0.31$ at $\mathcal{N} = 1$, 0.22 at 2, and 0.18 at 3, respectively. For those values of g , the valley-instanton is no longer a solution of the valley equation and the valley prediction becomes unreliable. Thus it is natural for the valley prediction to have a relatively large discrepancy at these values as above. Even for the smaller g , there must be higher-order corrections from fluctuations in the valley background. The inclusion of those corrections will generate an $O(g^2)$ correction relative to the leading term.

In Tables 4-6, we list the specific values of ΔE_k , $\Delta E_{k k+1}$, $\Delta E_k^{(V)}$, $\Delta E_{k k+1}^{(V)}$, and the relative discrepancy δ between them,

$$\delta \equiv \left| \frac{\Delta E^{(V)} - \Delta E}{\Delta E} \right|. \quad (7.6)$$

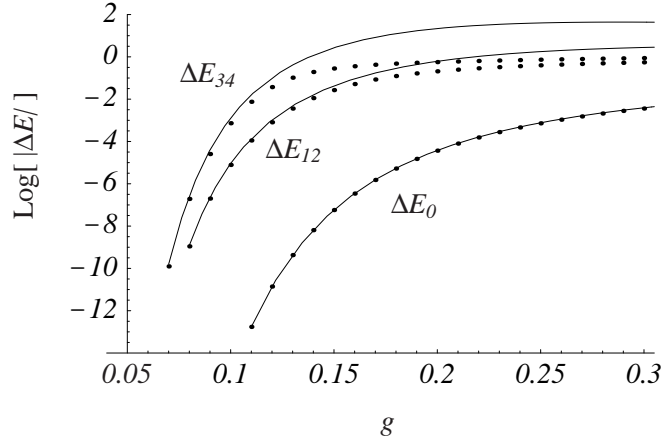


Figure 20: The comparison between the valley prediction and the exact numerical result for the non-perturbative corrections to the isolated energy level and splitting at $\mathcal{N} = 1$. The solid lines stand for the valley prediction, while the dots show the corresponding exact numerical result.

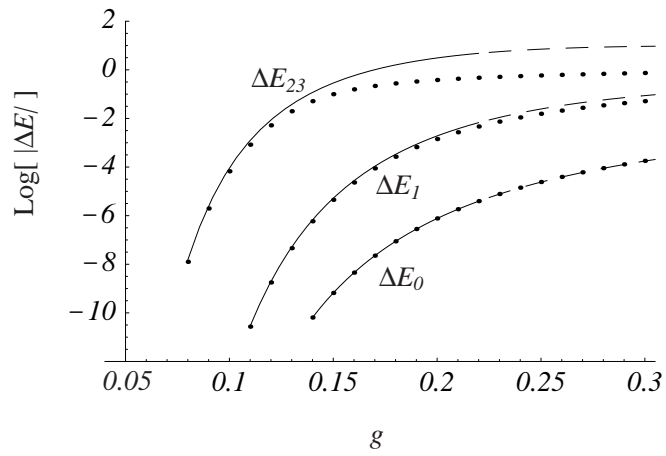


Figure 21: The comparison between the valley prediction and the exact numerical result at $\mathcal{N} = 2$. We use dashed lines to represent the valley prediction at g larger than 0.22, as the valley prediction has no justification for those values, as explained in the text.

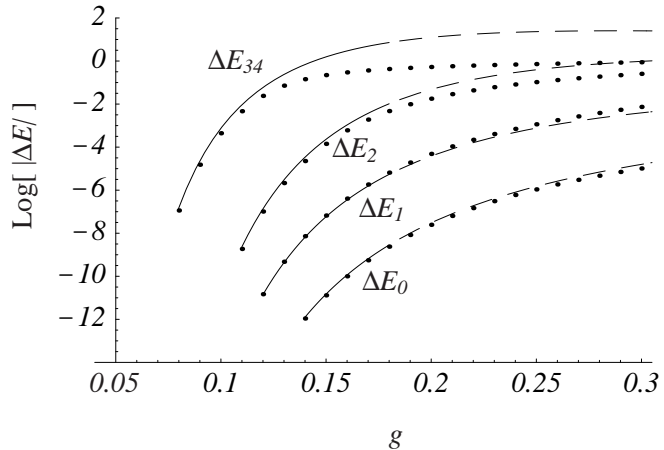


Figure 22: The comparison between the valley prediction and the exact numerical result at $\mathcal{N} = 3$. We use dashed lines to represent the valley prediction at g larger than 0.18, as the valley prediction has no justification for those values, as explained in the text. The critical value of g for the equation (7.1) to cease to have real solutions is well beyond the scope of this figure.

Because of the accumulation of round-off error in the calculation of the energy, it is difficult to carry out the numerical calculation for smaller g than shown in the figures and tables. The discrepancy is not necessarily small, even at the lowest g . Nevertheless the discrepancy decreases as g decreases and the behavior of the decrease seems consistent with the expected dependence on g^2 . The legitimacy of our valley prediction as the leading term of the non-perturbative contribution is solid.

The excellence of the agreement of the valley prediction and the exact result for the ground state energy in both $\mathcal{N} = 1$ and 2 is very striking. This may indicate a new sort of non-renormalization theorem, even in the non-perturbative sector.

Finally, we note that these non-zero values of ΔE are the quantitative measure of the dynamical breaking of the \mathcal{N} -fold supersymmetry.

8 Discussions

1. First we would like to outline the results of this paper. We have examined the geometrical structure of the configuration space of the path integral, and shown that in one-dimensional quantum mechanics:
 - (a) There are valleys in the configuration space which connect the vacuum and the instanton-like configuration. (Section 2)

g	ΔE_0	$\Delta E_0^{(V)}$	δ
0.12	1.389×10^{-11}	1.408×10^{-11}	0.0137
0.14	6.431×10^{-9}	6.544×10^{-9}	0.0176
0.16	3.442×10^{-7}	3.523×10^{-7}	0.0236
0.18	5.255×10^{-6}	5.417×10^{-6}	0.0309
0.20	3.680×10^{-5}	3.826×10^{-5}	0.0395
0.22	1.548×10^{-4}	1.624×10^{-4}	0.0495
0.24	4.604×10^{-4}	4.881×10^{-4}	0.0603
0.26	1.073×10^{-3}	1.149×10^{-3}	0.0710
0.28	2.098×10^{-3}	2.266×10^{-3}	0.0805
0.30	3.603×10^{-3}	3.920×10^{-3}	0.0879
g	ΔE_{12}	$\Delta E_{12}^{(V)}$	δ
0.08	1.103×10^{-9}	1.222×10^{-9}	0.108
0.10	7.801×10^{-6}	9.220×10^{-6}	0.182
0.12	8.066×10^{-4}	1.042×10^{-3}	0.292
0.14	1.123×10^{-2}	1.651×10^{-2}	0.470
0.16	5.175×10^{-2}	9.275×10^{-2}	0.792
0.18	1.238×10^{-1}	2.873×10^{-1}	1.32
0.20	2.070×10^{-1}	6.185×10^{-1}	1.99
0.22	2.880×10^{-1}	1.053	2.66
0.24	3.627×10^{-1}	1.534	3.23
0.26	4.308×10^{-1}	2.006	3.66
0.28	4.930×10^{-1}	2.429	3.93
0.30	5.504×10^{-1}	2.783	4.06
g	ΔE_{34}	$\Delta E_{34}^{(V)}$	δ
0.07	1.246×10^{-10}	1.589×10^{-10}	0.275
0.09	2.550×10^{-5}	3.985×10^{-5}	0.563
0.11	7.517×10^{-3}	1.607×10^{-2}	1.14
0.13	1.037×10^{-1}	4.118×10^{-1}	2.97
0.15	2.814×10^{-1}	2.705	8.61
0.17	4.238×10^{-1}	8.455	18.9
0.19	5.241×10^{-1}	17.12	31.7
0.21	6.027×10^{-1}	26.50	43.0
0.23	6.709×10^{-1}	34.54	50.5
0.25	7.334×10^{-1}	40.14	53.7

Table 4: The values of non-perturbative part of the energy spectrum at $\mathcal{N} = 1$; ΔE is from the exact numerical calculation, $\Delta E^{(V)}$ the valley prediction, and δ is their relative discrepancy $\delta = |(\Delta E^{(V)} - \Delta E)/\Delta E|$.

g	ΔE_0	$\Delta E_0^{(V)}$	δ
0.14	-6.438×10^{-11}	-6.413×10^{-11}	0.00387
0.16	-4.530×10^{-9}	-4.510×10^{-9}	0.00445
0.18	-8.825×10^{-8}	-8.776×10^{-8}	0.00569
0.20	-7.706×10^{-7}	-7.651×10^{-7}	0.00713
0.22	-3.967×10^{-6}	-3.932×10^{-6}	0.00877
0.24	-1.421×10^{-5}	-1.406×10^{-5}	0.0106
0.26	-3.933×10^{-5}	-3.884×10^{-5}	0.0126
0.28	-9.018×10^{-5}	-8.884×10^{-5}	0.0148
0.30	-1.795×10^{-4}	-1.764×10^{-4}	0.0170
g	ΔE_1	$\Delta E_1^{(V)}$	δ
0.12	1.788×10^{-9}	1.956×10^{-9}	0.0942
0.14	5.883×10^{-7}	6.678×10^{-7}	0.135
0.16	2.317×10^{-5}	2.753×10^{-5}	0.188
0.18	2.659×10^{-4}	3.344×10^{-4}	0.258
0.20	1.423×10^{-3}	1.913×10^{-3}	0.344
0.22	4.658×10^{-3}	6.714×10^{-3}	0.441
g	ΔE_{23}	$\Delta E_{23}^{(V)}$	δ
0.08	1.260×10^{-8}	1.527×10^{-8}	0.212
0.10	6.689×10^{-5}	9.220×10^{-5}	0.378
0.12	5.211×10^{-3}	8.687×10^{-3}	0.667
0.14	5.139×10^{-2}	1.179×10^{-1}	1.29
0.16	1.576×10^{-1}	5.797×10^{-1}	2.68
0.18	2.765×10^{-1}	1.596	4.77
0.20	3.826×10^{-1}	3.093	7.08

Table 5: The values of non-perturbative part of the energy spectrum at $\mathcal{N} = 2$. Since the numerical agreement of $\Delta E_0^{(V)}$ with the exact value is excellent, we think it permissible to write them up to $g = 0.3$, although the valley-instanton ceases to be a solution of the valley equation at $g \geq 0.2$.

g	ΔE_0	$\Delta E_0^{(V)}$	δ
0.15	1.305×10^{-11}	1.483×10^{-11}	0.137
0.16	1.002×10^{-10}	1.155×10^{-10}	0.152
0.17	5.553×10^{-10}	6.508×10^{-10}	0.172
0.18	2.383×10^{-9}	2.843×10^{-9}	0.193
g	ΔE_1	$\Delta E_1^{(V)}$	δ
0.13	-4.738×10^{-10}	-4.324×10^{-10}	0.0874
0.14	-7.289×10^{-9}	-6.544×10^{-9}	0.102
0.15	-6.639×10^{-8}	-5.859×10^{-8}	0.117
0.16	-4.068×10^{-7}	-3.523×10^{-7}	0.134
0.17	-1.836×10^{-6}	-1.558×10^{-6}	0.151
0.18	-6.527×10^{-6}	-5.417×10^{-6}	0.170
g	ΔE_2	$\Delta E_2^{(V)}$	δ
0.11	1.868×10^{-9}	2.362×10^{-9}	0.265
0.12	1.019×10^{-7}	1.358×10^{-7}	0.333
0.13	2.144×10^{-6}	3.028×10^{-6}	0.412
0.14	2.257×10^{-5}	3.407×10^{-5}	0.510
0.15	1.420×10^{-4}	2.315×10^{-4}	0.630
0.16	6.040×10^{-4}	1.075×10^{-3}	0.780
0.17	1.900×10^{-3}	3.731×10^{-3}	0.964
0.18	4.732×10^{-3}	1.032×10^{-2}	1.18
g	ΔE_{34}	$\Delta E_{34}^{(V)}$	δ
0.08	1.140×10^{-7}	1.559×10^{-7}	0.367
0.09	1.524×10^{-5}	2.301×10^{-5}	0.509
0.10	4.415×10^{-4}	7.528×10^{-4}	0.705
0.11	4.657×10^{-3}	9.275×10^{-3}	0.991
0.12	2.402×10^{-2}	5.910×10^{-2}	1.46
0.13	7.170×10^{-2}	2.378×10^{-1}	2.32
0.14	0.143×10^{-1}	6.878×10^{-1}	3.81

Table 6: The values of non-perturbative part of the energy spectrum at $\mathcal{N} = 3$.

- (b) The perturbative and non-perturbative contributions in the path integral can be separated in terms of the valley. (Section 3)
- (c) In the separation, the imaginary part of the non-perturbative contribution and the Borel singularity of the perturbative contribution cancels trivially. (Section 3)
- (d) Bogomolny's trick is proved to be sound, thus enabling us to go beyond the dilute-gas approximation. (Section 3.4 and Section 4.1)
- (e) Based on the above separation, the large order behavior of the perturbation series is predicted. The prediction reproduces the perturbation theory excellently. (Section 3.3 and Section 5)
- (f) A new type of supersymmetry in quantum mechanics is found. Non-renormalization theorems of the \mathcal{N} -fold supersymmetry hold. (Section 6)
- (g) The energy spectrum calculated by our valley calculus reproduces those derived directly from the Schrödinger equation. (Section 7)

2. The asymmetric double-well potential was also treated by Balitsky and Yung [23]. Their calculation, however, utilized a complex solution, which requires the deformation of the path-integral in the infinite dimensional configuration space. This procedure is difficult to justify, and furthermore it obscures the analytic continuation in the complex g^2 -plane. On the other hand, our analysis involves only the real configurations, and the analytic continuation is well-defined in the finite dimensional collective coordinate space.

3. To parameterize the valley, we have used R , which corresponds to the relative distance between I and \bar{I} . But as was denoted in the footnote to Section 3, the definition of R is not simple. The simplest variable to parameterize the valley is the eigenvalue λ in the valley equation (2.5). In further research on valleys, one might use λ rather than R .

4. Our analyses have been done in the topologically trivial sector, but the extension to the topologically non-trivial sector is straightforward. For example, we can construct a valley in the one instanton sector which consists of the $n + 1$ instantons and the n anti-instantons. The valley equation is the same as in the topological trivial sector, and the only change is the boundary condition of q at $\tau = \pm\infty$.

5. In Section 3.3, we have predicted the large order behavior of the perturbative series for the square of the absolute value of the normalized wave function at $q = q_{\pm}$ (see Eq.(3.38)). We have not tested this prediction, but we note that the prediction is consistent with the result in

Section 6. In Section 6, we have shown that if $\epsilon = \mathcal{N}$ the perturbative ground state (or more generally first \mathcal{N} perturbative excited states) at $q = q_-$ can be constructed exactly. The state is normalizable at any finite order of the perturbation of g , but if we sum up the contributions at all orders, the state becomes unnormalizable. This unnormalizability indicates the non-Borel-summability of the the perturbative series for the square of the absolute value of the *normalized* wave function at $q = q_-$.

6. In Section 7, we have found in Figs.20-22 that for the first $(\mathcal{N} - 1)$ -th energy levels our valley calculus agrees excellently with the numerical calculation. In spite of the fact that we have only taken into account the lowest order corrections in the background of the valley, and neglected the higher order corrections, the agreement is better than expected. This may suggest another non-renormalization theorem for the higher order corrections on the valley calculus. Indeed, for the instanton calculus in the supersymmetric QCD, similar types of the non-renormalization theorem are known to hold [24].
7. The techniques of this paper may be applied to the model in quantum field theory. In quantum field theory, there are three types of singularities in the Borel plane, which are known as the IR renormalon, UV renormalon, and the instanton singularities [4, 15]. The former two singularities are outside the scope of this paper, but the instanton singularity is manageable by a straightforward extension of our method. A promising application of our method is to processes with huge numbers of particles. The number of Feynman diagrams of these processes is large and the instanton type singularity is closely related with this fact [25, 15].
8. One of the interesting processes with high multiplicities is the electroweak baryon and lepton number violating process at high energy scattering [26, 27]. The process is the tunneling effect, and the height of the tunneling barrier is $O(10)$ TeV. The amplitude of the process at that energy is naively expected to be enhanced, and the process inevitably contains a huge number of particles (massive gauge and Higgs bosons) [28, 29, 30]. A plausible calculation does not yet exist.

Based on the optical theorem, Porrati and later Khoze and Ringwald proposed a method to treat a huge number of particles [31, 32]. The problem with their method is that the optical theorem itself does not distinguish the baryon number violating process (tunneling effect) and the baryon number preserving one (the perturbative effect). The extension of our method to the electroweak theory might make it possible to

separate them, although the detailed analysis of the geometrical structure of the theory is needed. The valley instanton in the electroweak theory has already been constructed in Ref.[33].

More detailed arguments about this subject are given in Ref.[34].

9. The extension of our method to string theory is an interesting possibility. Unfortunately, it is difficult at present because of the lack of a satisfactory non-perturbative formulation of string theory (e.g. string field theory). But the consideration of the large order behavior of string theory [35] and the existence of the solitonic object [36] suggests that a geometrical structure similar to that of our model exists in the configuration space of the non-perturbative formulation of the string theory.

Acknowledgment

M. Sato wishes to acknowledge suggestions by T. Eguchi and thank K. Fujikawa, M. Kato and H. Kawamura for discussions. H. Aoyama's work was supported in part by the Grant-in-Aid for Scientific Research 10120218 and 10640259. H. Kikuchi's work was supported in part by the Grant-in-Aid for Scientific Research 09226232. M. Sato and S. Wada were supported in part by Grants-in-Aid for JSPS fellows. Numerical computation in this work was in part supported by the computing facility at the Yukawa Institute for Theoretical Physics, Kyoto University. We would like to thank J. Constable, Faculty of Integrated Human Studies, Kyoto University, for careful reading of the manuscript.

A Some notes on the valley method

In this appendix we will note some of the important properties of the valley method, which have not been explicitly described in previous references.

Firstly, we note its relation to the ordinary collective coordinate method. In our context, this corresponds to the cases when there are non-trivial solutions of equations of motion. That is, cases where $F(\tau) \equiv 0$. These cases can be treated by a limiting procedure and the valley method reduces to the usual collective coordinate method. This is done in the following manner: When $F(\tau) = 0$, both the numerator and the denominator of the Jacobian $\Delta[\varphi_\alpha]$ of Eq.(2.12) are zero. This quantity can be obtained by introducing a small perturbation to the action that renders $F(\tau) \neq 0$ and making the perturbation vanish at the end. Let us take $S[q] \rightarrow S[q] + \rho W[q]$. Since the eigenvalue λ is zero $\rho \neq 0$, λ is of order ρ and the valley solutions are expanded as $q = q_0 + \rho q_1 + \dots$, $F = \rho F_1 + \dots$. The ρ -expansion of Eq.(2.17) and Eq.(2.18) yields the following:

$$\frac{\delta S[q_0]}{\delta q_0(\tau)} = 0, \quad (\text{A.1})$$

$$\int d\tau' \frac{\delta^2 S[q_0]}{\delta q_0(\tau) \delta q_0(\tau')} F_1(\tau') = 0. \quad (\text{A.2})$$

The first equation is the original equation of motion. The second gives $F_1 \propto \dot{q}_0$, which proportional constant is to be determined at the higher-order equations. The gradient vector $G(\tau)$ is independent from this proportional constant:

$$G(\tau) = \frac{F_1(\tau)}{\sqrt{\int F_1^2 d\tau'}} = \frac{\dot{q}_0(\tau)}{\sqrt{\int \dot{q}_0^2 d\tau'}}, \quad (\text{A.3})$$

By choosing the valley parameter α as the translation coordinate of $q_0(\tau)$, the Jacobian is found to be the following:

$$\Delta[q_\alpha] = \int \dot{q}_0(\tau) G(\tau) d\tau = \sqrt{\int \dot{q}_0^2 d\tau'}. \quad (\text{A.4})$$

This is the Jacobian of the ordinary collective coordinate method [12].

The second is the extension to the multi-dimensional valley, which will be needed when there are multiple dangerous eigenvalues. The definition of the D -dimensional valley is as follows:

$$\frac{\delta S[q]}{\delta q(\tau)} = \sum_{i=1}^D F_i(\tau), \quad (\text{A.5})$$

$$\int d\tau' \frac{\delta^2 S[q]}{\delta q(\tau) \delta q(\tau')} F_i(\tau') = \lambda_i F_i(\tau) \quad (i = 1, \dots, D), \quad (\text{A.6})$$

The Gaussian integration is performed in the subspace defined by $\int \phi(\tau)G_i(\tau)d\tau = 0$ for $i = 1, \dots, D$ [7], where G_j is the normalized function of F_i . The Jacobian of the collective coordinate volume element $\prod_i da_i$ is given by the determinant of

$$C_{ij} \equiv \int d\tau' \frac{\partial q(\tau')}{\partial \alpha_i} G_j(\tau'), \quad (\text{A.7})$$

where the valley is parametrized by the D collective coordinates α_i .

B The determinant of the valley-instanton

In this appendix we will calculate the determinant for a valley-instanton, utilizing the fact that it has a zero eigenvalue, as is proven in Section 2.2. We will consider the valley-instanton located at $\tau = \tau_I$ in the region $\tau \in [-T/2, T/2]$, and calculate the normalized determinant, using the following formula [12] for $\omega_{\pm}(T/2 \pm \tau_I) \gg 1$.

$$\frac{\det'(-\partial_{\tau}^2 + V'')}{\det(-\partial_{\tau}^2 + \omega_+^2)} = \frac{\psi(T/2)}{\lambda\psi_0(T/2)}, \quad (\text{B.1})$$

where the eigenvalues are determined with the use of the Dirichlet boundary conditions at $\pm T/2$. The eigenvalue λ is the one that appears in the valley equations and goes to zero in the limit $T \rightarrow \infty$. The functions $\psi(\tau), \psi_0(\tau)$ are the solutions of following differential equations:

$$(-\partial_{\tau}^2 + V''(q))\psi(\tau) = 0, \quad (\text{B.2})$$

$$(-\partial_{\tau}^2 + \omega_+^2)\psi_0(\tau) = 0, \quad (\text{B.3})$$

with boundary conditions, $\psi(-T/2) = \psi_0(-T/2) = 0$ and $\dot{\psi}(-T/2) = \dot{\psi}_0(-T/2) = 1$.

The function ψ is given by the following:

$$\psi_0(\tau) = \frac{1}{2\omega_+} \left(e^{\omega_+(\tau+T/2)} - e^{-\omega_+(\tau+T/2)} \right), \quad (\text{B.4})$$

which yields $\psi_0(T/2) \sim e^{\omega_+ T} / (2\omega_+)$.

For the construction of the function $\psi(\tau)$, we can utilize the auxiliary coordinate $F(\tau)$, which is the eigenfunction with zero eigenvalue,

$$(-\partial_{\tau}^2 + V''(q))F = 0. \quad (\text{B.5})$$

with converging boundary conditions at $\tau = \pm\infty$. It has the following asymptotic behavior:

$$F(\tau) \sim F_{\mp} e^{\mp\omega_+(\tau-\tau_I)}, \quad (\text{B.6})$$

for $\tau \rightarrow \pm T/2$ as was shown in Section 2.2. We denote the other independent solution of Eq.(B.5) by $\bar{F}(\tau)$, in which we choose to have the following Wronskian:

$$W = F(\tau)\dot{\bar{F}}(\tau) - \dot{F}(\tau)\bar{F}(\tau) = 2\omega_+\omega_-.$$
 (B.7)

This implies that the asymptotic behavior of $\bar{F}(\tau)$ for $\tau \rightarrow \pm T/2$ is the following:

$$\bar{F}(\tau) \sim \bar{F}_\mp e^{\pm\omega_\mp(\tau-\tau_I)},$$
 (B.8)

with $\bar{F}_\pm = \mp\omega_\mp/F_\pm$. Using these solutions, the function $\psi(\tau)$ is given as follows,

$$\psi(\tau) = \frac{1}{2\omega_+} \left(\frac{F(\tau)}{F(-T/2)} - \frac{\bar{F}(\tau)}{\bar{F}(-T/2)} \right).$$
 (B.9)

which satisfies the required boundary conditions at $\tau = -T/2$.

Next we will evaluate the lowest eigenvalue λ ,

$$(-\partial_\tau^2 + V''(q))\bar{\psi}(\tau) = \lambda\bar{\psi}(\tau),$$
 (B.10)

with $\bar{\psi}(\pm T/2) = 0$. We can construct the eigenfunction $\bar{\psi}(\tau)$ as a perturbation series in λ as follows,

$$\begin{aligned} \bar{\psi}(\tau) &= \psi(\tau) + \lambda \int_{-T/2}^{+T/2} d\tau' G(\tau, \tau') \bar{\psi}(\tau') \\ &= \psi(\tau) + \lambda \int_{-T/2}^{+T/2} d\tau' G(\tau, \tau') \psi(\tau') + O(\lambda^2), \end{aligned}$$
 (B.11)

where the function $\psi(\tau)$ given by Eq.(B.9) is used so that the boundary condition $\bar{\psi}(-T/2) = 0$ is satisfied. The Green function $G(\tau, \tau')$ is defined by,

$$G(\tau, \tau') = \frac{1}{W} (F(\tau)\bar{F}(\tau') - F(\tau')\bar{F}(\tau))\theta(\tau - \tau').$$
 (B.12)

and satisfies the following,

$$(-\partial_\tau^2 + V''(q))G(\tau, \tau') = \delta(\tau - \tau').$$
 (B.13)

The boundary condition $\bar{\psi}(T/2) = 0$ determines the eigenvalue λ . Straightforward calculation shows that the product of the second term of the Green function (B.12) and the $F(\tau')$ term in $\psi(\tau')$ makes the dominant contribution to $\bar{\psi}(T/2)$. Therefore we find that

$$\psi\left(\frac{T}{2}\right) \simeq \frac{\lambda}{W} \frac{\bar{F}(T/2)}{2\omega_+ F(-T/2)} \int_{-T/2}^{T/2} d\tau' F^2(\tau').$$
 (B.14)

Combining the results obtained so far, we find that

$$\frac{\det'(-\partial_\tau^2 + V'')}{\det(-\partial_\tau^2 + \omega_+^2)} \simeq \frac{e^{(\omega_- - \omega_+)(T/2 - \tau_I)}}{2\omega_- F_+ F_-} \int_{-\infty}^{\infty} d\tau F^2(\tau).$$
 (B.15)

C The relation between the valley parameter and the separation of valley-instantons

As has been shown by the explicit numerical integration of the valley equations carried out in Section 2, the solution approaches to the well-separated pair of the (anti-)valley-instantons as the parameter λ in the equation approaches zero from below. In this appendix we will clarify the relation between λ and the separation R . For the sake of simplicity we will confine ourselves to the case of the $I\bar{I}$ valley. Obtaining a similar result for the $\bar{I}I$ valley is a simple matter.

Assuming that λ is small enough that the solution consists of a well-separated pair of valley-instanton and anti-valley-instanton, we can locate the valley-instanton at $\tau = 0$ and the anti-valley-instanton at $\tau = R$. At the symmetric point $\tau_0 (= R/2)$, the time derivatives of the configuration vanish simultaneously; $\dot{F}(\tau_0) = \dot{q}(\tau_0) = 0$. In the asymptotic region to the far left of the valley-instanton, $\tau < 0$ and $|\tau| \gg 1/\omega_+$, the solution is well described by linearizing the valley equations (2.31)-(2.32). By requiring that it becomes a vacuum at q_+ as $\tau \rightarrow -\infty$, the solution is described by two parameters F_+ and Q_- ,

$$F \simeq F_+ e^{\kappa_+ \tau} \quad (C.1)$$

$$q - q_+ \simeq \left(Q_+ - \frac{F_+}{\lambda} \right) e^{\omega_+ \tau} + \frac{F_+}{\lambda} e^{\kappa_+ \tau}, \quad (C.2)$$

where $\kappa_\pm \equiv \sqrt{\omega_\pm - \lambda}$. Of two degrees of freedom in F_+ and Q_+ , one is related to the overall translation and the other should be fixed so that \dot{q} and \dot{F} are zero at τ_0 . We already know the asymptotic form of the valley-instanton as Eqs. (2.59)-(2.60). Thus

$$Q_+ \rightarrow \frac{1}{g}, \quad F_+ \rightarrow -6\epsilon g \quad (C.3)$$

at the limit of $\lambda \rightarrow 0$.

Similarly the solution is well described by linearized equations around τ_0 , for the configuration is almost a vacuum at q_- . Since $\dot{F}(\tau_0) = \dot{q}(\tau_0) = 0$, we can conclude the $I\bar{I}$ valley behaves as

$$F \simeq F_- e^{-\kappa_- \tau} + F_- e^{\kappa_- (\tau - 2\tau_0)} \quad (C.4)$$

$$\begin{aligned} q - q_- \simeq & \left(Q_- - \frac{F_-}{\lambda} \right) e^{-\omega_- \tau} + \frac{F_-}{\lambda} e^{-\kappa_- \tau} \\ & + \left(Q_- - \frac{F_-}{\lambda} \right) e^{\omega_- (\tau - 2\tau_0)} + \frac{F_-}{\lambda} e^{\kappa_- (\tau - 2\tau_0)}. \end{aligned} \quad (C.5)$$

When $\lambda \rightarrow -0$, τ_0 goes to the positive infinity and

$$Q_- \rightarrow -\frac{1}{g}, \quad F_- \rightarrow -6\epsilon g, \quad (C.6)$$

obtained again by comparing (C.4) and (C.5) with the asymptotic forms for positive τ in (2.59) and (2.60).

We use the conservation of H_V (2.35) to relate λ to τ_0 . At $\tau = -\infty$ H_V is equal to $-V(q_+)$, while at τ_0

$$H_V \simeq -V(q_-) - \frac{1}{2}\omega_-^2 [q(\tau_0) - q_-]^2 + \frac{1}{\lambda}\omega_-^2 F(\tau_0) [q(\tau_0) - q_-] - \frac{1}{2\lambda}F(\tau_0)^2. \quad (\text{C.7})$$

Equating the two expressions for H_V and using (C.4) and (C.5) to relate $F(\tau_0)$ and $q(\tau_0)$ to F_- , Q_- , and τ_0 , we obtain

$$\lambda = -\frac{2}{V(q_+) - V(q_-)} \left[2\omega_-^2 F_- Q_- + F_-^2 (\omega_- \tau_0 - 1) \right] e^{-2\omega_- \tau_0}. \quad (\text{C.8})$$

Although F_- and Q_- may have an $O(\lambda)$ correction, they are exponentially small compared to the values in (C.6) and are negligible. Thus we obtain

$$\lambda = - \left[24\omega_-^2 + 36\epsilon g^2 (\omega_- R - 2) \right] e^{-\omega_- R}. \quad (\text{C.9})$$

The valley parameter λ decreases simply as $e^{-\omega_- R}$ at $\epsilon = 0$, while it has an exotic dependence $\omega_- R e^{-\omega_- R}$ at non-zero ϵ .

D WKB evaluation

In this appendix, we will re-derive the result (4.15) by the WKB approximation. The system we will consider obeys the Schrödinger equation

$$\left[-\frac{1}{2} \frac{d^2}{dq^2} + V(q) \right] \Phi(q) = E\Phi(q). \quad (\text{D.1})$$

Around the upper minimum q_+ of the potential, this becomes

$$\left[-\frac{1}{2} \frac{d^2}{dq^2} + \frac{1}{2}q^2 \right] \Phi(q) = E\Phi(q), \quad (\text{D.2})$$

and a solution which vanishes at $q \rightarrow -\infty$ is

$$\Phi(q) = AD_\nu(-\sqrt{2}q), \quad (\text{D.3})$$

where $E = \nu + \frac{1}{2}$ and A is a constant. The function D_ν is the parabolic cylinder function [37]. And around the lower minimum q_- of the potential, the Schrödinger equation becomes

$$\left[-\frac{1}{2} \frac{d^2}{dq^2} + \frac{1}{2} \left(q - \frac{1}{g} \right)^2 - \epsilon \right] \Phi(q) = E\Phi(q), \quad (\text{D.4})$$

and a solution which vanishes at $q \rightarrow \infty$ is

$$\Phi(q) = \tilde{A} D_{\nu+\epsilon}(\sqrt{2}(q - 1/g)), \quad (\text{D.5})$$

where \tilde{A} is a constant. We must now connect these solutions with that in the forbidden region.

In the forbidden region, the usual semi-classical expression for the wave function is available:

$$\Phi(q) = \frac{C_1}{k(q)^{1/2}} \exp \left[- \int_{q_1}^q k(x) dx \right] + \frac{C_2}{k(q)^{1/2}} \exp \left[\int_{q_1}^q k(x) dx \right], \quad (\text{D.6})$$

where

$$k(q) = \sqrt{q^2(1 - gq)^2 - 2\epsilon gq - 2E}. \quad (\text{D.7})$$

and q_i ($i = 1, 2$) are the tunneling points $V(q_i) = E$. C_i ($i = 1, 2$) are constant. When $\epsilon g^2 \ll 1$, these are given by

$$gq_1 = \epsilon g^2 + \sqrt{2Eg^2 + (\epsilon g^2)^2}, \quad (\text{D.8})$$

$$gq_2 = 1 + \epsilon g^2 - \sqrt{2(E + \epsilon)g^2 + (\epsilon g^2)^2}. \quad (\text{D.9})$$

The integral in the wave function can be evaluated by expanding about g^2 :

$$\begin{aligned} \int_{q_1}^q k(x) dx &= \frac{1}{g^2} \int_{gq_1}^{gq} [w^2(1 - w)^2 - 2\epsilon g^2 w - 2g^2 E]^{1/2} dw \\ &= \frac{1}{g^2} \int_{gq_1}^{gq} w(1 - w) dw - \int_{z_1}^z \frac{\epsilon w + E}{w(1 - w)} dw + \dots \\ &= \frac{1}{g^2} \left[\frac{1}{2} w^2 - \frac{1}{3} w^3 - g^2 E \ln \left(\frac{w}{1 - w} \right) + g^2 \epsilon \ln(1 - w) \right]_{gq_1}^{gq} + \dots \end{aligned} \quad (\text{D.10})$$

In the region near the upper minimum, it becomes

$$\begin{aligned} \int_{q_1}^q k(x) dx &= \left[\frac{1}{2} q^2 - \frac{1}{3} gq^3 - E \ln \left(\frac{gq}{1 - gq} \right) + \epsilon \ln(1 - gq) \right] \\ &\quad - \left[\frac{1}{2} \left(\epsilon g + \sqrt{2E + \epsilon^2 g^3} \right)^2 - \frac{1}{3} g \left(\epsilon g + \sqrt{2E + \epsilon^2 g^3} \right)^3 \right. \\ &\quad \left. - E \ln \left(\frac{\epsilon g^2 + \sqrt{2Eg^2 + (\epsilon g^2)^2}}{1 - (\epsilon g^2 + \sqrt{2Eg^2 + (\epsilon g^2)^2})} \right) \right. \\ &\quad \left. + \epsilon \ln \left(1 - \left(\epsilon g^2 + \sqrt{2Eg^2 + (\epsilon g^2)^2} \right) \right) \right] \\ &= \left[\frac{1}{2} x^2 - E \ln(gq) - E - E \ln(\sqrt{2E}g) \right] + \dots \end{aligned} \quad (\text{D.11})$$

In the final expression, we have neglected the terms which vanish as $g \rightarrow 0$, so the wave function becomes

$$\begin{aligned}\Phi(q) &= C_1 q^{-1/2} \exp\left(-\frac{1}{2}q^2 + E \ln\left(\frac{q}{\sqrt{2E}}\right) + E\right) \\ &+ C_2 q^{-1/2} \exp\left(\frac{1}{2}q^2 - E \ln\left(\frac{q}{\sqrt{2E}}\right) - E\right) + \dots \\ &= C_1 e^{-q^2/2+E} (2E)^{-E/2} q^\nu + C_2 e^{q^2/2-E} (2E)^{E/2} q^{-\nu} + \dots.\end{aligned}\tag{D.12}$$

We are here using $k(q) = q + \dots$. This wave function must be connected with the one given by Eq.(D.3). As the wave function (D.3) has the following asymptotic form for $q \gg 1$:

$$\Phi(q) = A \left[e^{-q^2/2} (-\sqrt{2}q)^\nu - \frac{\sqrt{2\pi}}{\Gamma(-\nu)} e^{\pm\nu\pi i} e^{-q^2/2} (-\sqrt{2}q)^{-\nu-1} + \dots \right], \tag{D.13}$$

so we obtain the following matching condition

$$\frac{\sqrt{2\pi}}{\Gamma(-\nu)} e^{\pm\nu\pi i} 2^{-\nu-1/2} = \frac{C_2}{C_1} e^{-(2\nu+1)} (2\nu+1)^{-(\nu+1/2)}. \tag{D.14}$$

In a similar way, by connecting the wave function (D.6) with the one given by (D.5) near the lower minimum of the potential, we obtain another matching condition:

$$\frac{\sqrt{2\pi}}{\Gamma(-\nu-\epsilon)} e^{\pm(\nu+\epsilon)\pi i} 2^{-(\nu+1/2+\epsilon)} = \frac{C_1}{C_2} e^{-1/3g^2} (2\nu+1)^{-(\nu+1/2)} g^{-(4\nu+2+2\epsilon)}. \tag{D.15}$$

Finally, if we eliminate the undetermined ration of the coefficients C_1/C_2 in the matching conditions, the master equation (4.15) for the non-perturbative corrections of the energies is reproduced:

$$\alpha^2 \Gamma\left(-E + \frac{1}{2}\right) \Gamma\left(-E + \frac{1}{2} - \epsilon\right) \left(-\frac{2}{g^2}\right)^{2E+\epsilon} = 1, \tag{D.16}$$

where

$$\alpha = \frac{e^{-1/6g^2}}{g\pi^{1/2}}. \tag{D.17}$$

References

- [1] C. Callan, R. Dashen, and D. Gross, *Phys. Rev.* **D17** (1978) 2717.
- [2] E. Brézin, J. C. Le Guillou, and J. Zinn-Justin, *Phys. Rev.* **D15** (1977) 1558.
- [3] E. Brézin, G. Parisi, and J. Zinn-Justin, *Phys. Rev.* **D16** (1977) 408.
- [4] For a review, see “*Large-Order Behaviour of Perturbation Theory*”, ed. by J. C. Le Guillou and J. Zinn-Justin, (North-Holland, 1990), and references cited therein.
- [5] E. B. Bogomolny, *Phys. Lett.* **B91** (1980) 431.
- [6] I. I. Balitsky and A.V. Yung, *Phys. Lett.* **B168** (1986) 13.
- [7] H. Aoyama and H. Kikuchi, *Nucl. Phys.* **B369** (1992) 219.
- [8] T. Harano and M. Sato, hep-ph/9703457.
- [9] H. Aoyama, H. Kikuchi, T. Harano, M. Sato, and S. Wada, *Phys. Rev. Lett.* **79** (1997) 4052.
- [10] H. Aoyama, H. Kikuchi, T. Harano, I. Okouchi, M. Sato, S. Wada, *Prog. Theor. Phys. Supplement* **127** (1997) 1.
- [11] H. Aoyama, H. Kikuchi, I. Okouchi, M. Sato, and S. Wada, *Phys. Lett.* **B424** (1998) 93.
- [12] S. Coleman, in “*The Whys of Subnuclear Physics*”, (Plenum Publishing Co., New York, 1979).
- [13] A. Hosoya and K. Kikkawa, *Nucl. Phys.* **B101** (1975) 271.
- [14] J. Zinn-Justin, *Nucl. Phys.* **B192** (1981) 125; *Nucl. Phys.* **B218** (1983) 333.
- [15] G. 't Hooft, in “*The Whys of Subnuclear Physics*”, (Plenum Publishing Co., New York, 1979).
- [16] H. Kikuchi, *Phys. Rev.* **D45** (1991) 1240.
- [17] S. V. Faleev and P. G. Silvestrov, *Phys. Lett.* **A197** (1995) 372.
- [18] J. I. Verbaarschot, P. West, and Tai Tsun Wu, *Phys. Rev.* **D42** (1990) 1276.
- [19] J. I. Verbaarschot and P. West, *Phys. Rev.* **D43** (1991) 2718.

- [20] J. Zinn-Justin, *J. Math. Phys.* **25** (1984) 549.
- [21] E. Witten, *Nucl. Phys.* **B185** (1981) 513.
- [22] A. V. Turbiner, *Commun. Math. Phys.* **118** (1988) 513.
- [23] I. I. Balitsky and A.V. Yung, *Nucl. Phys.* **B274** (1986) 475.
- [24] V. A. Novikov, M. A. Shifman, A. I. Vainshtein and V. I. Zakharov, *Nucl. Phys.* **B229** (1983) 381.
- [25] G. Parisi, *Phys. Lett.* **68B** (1977) 361.
- [26] G. 't Hooft, *Phys. Rev. Lett.* **37** (1976) 8; *Phys. Rev.* **D14** (1976) 3422; *ibid (E)* **D18** (1978) 2199.
- [27] For a review, see V. A. Rubakov and M. E. Shaposhnikov, hep-ph/9603208.
- [28] H. Aoyama and H. Goldberg, *Phys. Lett.* **B188** (1987) 506.
- [29] A. Ringwald, *Nucl. Phys.* **B330** (1990) 1.
- [30] C. Espinosa, *Nucl. Phys.* **B343** (1990) 310.
- [31] M. Porrati, *Nucl. Phys.* **B347** (1990) 371.
- [32] V. V. Khoze and A. Ringwald, *Nucl. Phys.* **B355** (1991) 351.
- [33] H. Aoyama, T. Harano, M. Sato and S. Wada, *Mod. Phys. Lett.* **A11** (1996) 43; *Nucl. Phys.* **B466** (1996) 127.
- [34] M. Sato, talk at the International Symposium on “*Lepton- and Baryon-number Violation*”, Trento, Italy, April 1998.
- [35] S. H. Shenker, in “*Cargese 1990, Proceedings, Random surfaces and quantum gravity*”, (Plenum Publishing Co., New York, 1991).
- [36] J. Polchinski, *Phys. Rev. Lett.* **75** (1995) 4724.
- [37] I. S. Gradshteyn and I. M. Ryzhik, “*Tables of Integrals, Series, and Products*”, fifth edition (Academic Press).